STATE UNIVERSITY OF WESTERN PARANÁ (UNIOESTE)
CAMPUS OF FOZ DO IGUAÇU
GRADUATE PROGRAM IN
ELECTRICAL ENGINEERING AND COMPUTER

MASTER'S THESIS

HYBRID METHOD FOR THE RECONFIGURATION OF ELECTRIC POWER DISTRIBUTION SYSTEMS WITH DISTRIBUTED GENERATION ALLOCATION

ANDERSON FREIMAN

FOZ DO IGUAÇU
2026

Anderson Freiman

HYBRID METHOD FOR THE RECONFIGURATION OF ELECTRIC POWER DISTRIBUTION SYSTEMS WITH DISTRIBUTED GENERATION ALLOCATION

Master thesis presented to the Graduate Program in Electrical and Computing Engineering of Universidade Estadual do Oeste do Paraná as a requisite to obtain the title Master in Electrical and Computing Engineering. Field of research: Electrical and Computing Systems.

Supervisor: Prof. Dr. Ricardo L. Barros de Freitas
Co-supervisor: Prof. Dr. Vagner Cândido de Sousa

Foz do Iguaçu
2026

Ficha de identificação da obra elaborada através do Formulário de Geração Automática do Sistema de Bibliotecas da Unioeste.

Freiman, Anderson
   Hybrid method for the reconfiguration of electric power distribution systems with distributed generation allocation / Anderson Freiman; orientador Prof. Dr. Ricardo Luiz Barros de Freitas; coorientador Prof. Dr. Vagner Cândido de Sousa. -- Foz do Iguaçu, 2026.
   102 p.

   Dissertação (Mestrado Acadêmico Campus de Foz do Iguaçu) -- Universidade Estadual do Oeste do Paraná, Centro de Engenharias e Ciências Exatas, Programa de Pós-Graduação em Engenharia Elétrica e Computação, 2026.

   1. Electric Power Distribution System Reconfiguration. 2. Distributed Generation Allocation. 3. Multi-start. 4. Variable Neighborhood Descent. I. Freitas, Prof. Dr. Ricardo Luiz Barros de, orient. II. Sousa, Prof. Dr. Vagner Cândido de, coorient. III. Título.

HYBRID METHOD FOR THE RECONFIGURATION OF ELECTRIC POWER DISTRIBUTION SYSTEMS WITH DISTRIBUTED GENERATION ALLOCATION

Anderson Freiman

This Master Thesis was presented to the Graduate Program in Electrical and Computing Engineering and accepted by the Examination Committee with the following members:

Prof. Dr. **Ricardo Luiz Barros de Freitas** - (Supervisor)
Universidade Estadual do Oeste do Paraná - UNIOESTE

Prof. Dr. **Vagner Cândido de Sousa** - (Co-supervisor)
Universidade Estadual Paulista "Júlio de Mesquita Filho" - UNESP

Prof. Dr. **Renato Bobsin Machado**
Universidade Estadual do Oeste do Paraná - UNIOESTE

Prof. Dr. **Helton Fernando Scherer**
Universidade Federal da Integração Latina-Americana - UNILA

Final oral defense: August 6, 2026.

Abstract

The Brazilian electrical system faces significant challenges related to high technical losses in the distribution segment, which directly impact the efficiency and sustainability of the sector. Given the continuous growth in demand and the modernization of the consumption profile, electric Power Distribution System Reconfiguration (DSR) emerges as a strategy to reduce active power losses in the sector. By optimizing the existing infrastructure, DSR allows for the postponement of system expansion, providing operational relief without diminishing the importance of long-term investments in new assets. Another solution for minimizing losses is the introduction of Distributed Generators (DG). However, literature often treats reconfiguration and DG allocation as isolated problems, which represents a gap in coordinated network planning. This work aims to develop a hybrid method for EDSR that minimizes active losses and improves the voltage profile by integrating strategic DG allocation. The proposed methodological approach utilizes a sequence of heuristic and metaheuristic techniques, starting with a modified PRIM algorithm for generating radial topologies. The Multi-start method is employed to ensure the maximum number of initial solutions, followed by a Genetic Algorithm (GA) for population refinement, and finally, Variable Neighborhood Descent (VND) as a local search stage. Once the best topology is defined, DG allocation is performed at the buses with the most critical voltage levels. Tested on 84-, 136-, and 415-bus systems (the latter being a modification of the 417-bus system) the results demonstrate that the hybrid method achieved active loss reductions of up to 65.86%, 65.27%, and 65.76% in the tested systems, respectively. The integration of DG following reconfiguration enhances voltage profile improvement and relieves substation loading, confirming that coordinated action between topology and distributed resources is superior to isolated reconfiguration.

Keywords: Electric Power Distribution System Reconfiguration, Distributed Generation Allocation, Multi-start, Genetic Algorithm, Variable Neighborhood Descent.

Resumo

O sistema elétrico brasileiro enfrenta desafios significativos relacionados às elevadas perdas técnicas no segmento de distribuição, que impactam diretamente a eficiência e a sustentabilidade do setor. Diante do crescimento contínuo da demanda e da modernização do perfil de consumo, a Reconfiguração de Sistemas de Distribuição de Energia Elétrica (RSDEE) surge como uma estratégia para reduzir as perdas ativas no setor. Ao otimizar a infraestrutura existente, a RSDEE permite postergar a expansão do sistema, oferecendo fôlego operacional sem anular a relevância dos investimentos em novos ativos a longo prazo. Outra solução para a minimização das perdas é a introdução de Geradores Distribuídos (GD). Contudo, a literatura muitas vezes trata a reconfiguração e a alocação de GD como problemas isolados, o que representa uma lacuna para o planejamento coordenado da rede. Este trabalho tem como objetivo desenvolver um método híbrido para a RSDEE que minimize as perdas ativas e melhore o perfil de tensão, integrando a alocação estratégica de GD. A abordagem metodológica proposta utiliza uma sequência de técnicas heurísticas e meta-heurísticas iniciadas pelo algoritmo de PRIM modificado para a geração de topologias radiais. O método *Multi-start* é empregado para garantir o maior número possível soluções iniciais, seguido por um Algoritmo Genético (AG) para o refinamento da população e, por fim, a Busca em Vizinhança Descendente (*Variable Neighborhood Descent* - VND) como etapa de busca local. Após a definição da melhor topologia, realiza-se a alocação de GD nas barras com os níveis de tensão mais críticos. Testados nos sistema de 84, 136 e 415 barras, este último uma modificação do sistema de 417 barras, os resultados demonstram que o método híbrido promoveu reduções de até 65,86%, 65,27% e 65,76% nas perdas ativas nos sistemas testados, respectivamente. A integração da GD após a reconfiguração potencializa a melhoria do perfil de tensão e alivia o carregamento da subestação, confirmando que a ação coordenada entre topologia e recursos distribuídos é superior à reconfiguração isolada.

Palavras-chave: Reconfiguração de Sistemas de Distribuição de Energia Elétrica, Alocação de Geração Distribuída, *Multi-start*, Algoritmo Genético, Busca em Vizinhança Descendente.

I dedicate this work to my mother, Marleide Freiman,
thank you for all the love and support.

Acknowledgments

First and foremost, I would like to express my deepest gratitude to my mother, Marleide Freiman, who dedicated herself entirely to raising me and always believed in my dreams. Thank you for a lifetime of care, love, and affection; your unconditional support and unwavering faith in my potential were the pillars that brought me to this point. I also extend my gratitude to my entire family for providing a strong foundation and continuous encouragement.

To my supervisor, Prof. Dr. Ricardo Luis Barros de Freitas, I express my sincere gratitude for his generosity in teaching, his patience, and his invaluable guidance, which served as an essential compass throughout this journey. His availability and understanding were fundamental to the successful completion of this work.

To my co-supervisor, Prof. Dr. Vagner Cândido de Sousa, I express my sincere gratitude for his technical support and dedication to the review of this work. His corrections and suggestions were fundamental contributions to the editing and refinement of this dissertation.

To my fellow graduate program colleagues, I express my gratitude for the insightful conversations, the friendships formed, the camaraderie, and the mutual encouragement, which made this journey much lighter and truly enriching.

Finally, I would like to thank the Graduate Program in Electrical Engineering and Computer (PGEEC) for the opportunity to pursue this Master's degree, extending my gratitude to the faculty members and the academic administrative staff for all their hard work and the indispensable institutional support provided to conclude this milestone.

"In the vastness of space and the immensity of time,
it is a joy to share a planet and an epoch with you."
Carl Sagan

Contents

List of Figures **12**

List of Tables **13**

List of Symbols **14**

List of Acronyms and Abbreviations **16**

1 Introduction **17**

1.1 Objective 18

1.1.1 Specific Objectives 18

1.2 Justification 19

1.3 Contributions 19

1.4 Limitations 20

1.5 Dissertation Structure 20

2 Systematic Literature Review **22**

2.1 Reconfiguration without the Use of Distributed Generation 22

2.2 Reconfiguration Using Distributed Generation 24

3 Methodological Definitions **26**

3.1 Definitions 26

3.1.1 Distribution System Reconfiguration 26

3.1.2 Modified Prim's algorithm 27

3.1.3 Renumering 31

3.1.4 Multi-start 32

3.1.5 Maximum/Minimum Distance 33

3.1.6 Genetic Algorithm – GA 34

3.1.7 Variable Neighborhood Descent - VND 36

3.2 Mathematical Formulations 36

3.2.1 Objective Function and Constraints 37

3.2.2 Power Flow 38

3.2.3 Equations for DG Allocation 40

4 Methodological Procedures **43**

4.1 Electric Power Systems Tested 43

4.2 Modified Prim's Algorithm for Generating Radial Solutions 46

4.3 Renumbering of the Generated Radial Topologies 46

4.4 Power Flow — Backward/Forward Sweep Method 47

4.5 Radial Solution Diversity Generation — Multi-Start Method 48

4.6 Generating Quality Solutions — Maximum/Minimum Distance Method 49

4.7 Implementation of the Genetic Algorithm 50

4.8 Implementation of Variable Neighborhood Descent 51

4.9 Distributed Generation Allocation 52

4.9.1 Allocation of 1, 2, and 3 DG 52

4.9.2 Maximum DG Allocation 53

4.9.3 Block Diagram for the Proposed Methodology 54

5 Results and Discussions **56**

5.1 Results 56

5.1.1 84-Bus System 57

5.1.2 136-Bus System 60

5.1.3 415-Bus System 63

5.2 Discussions 66

5.2.1 84-Bus System 67

5.2.2 136-Bus System 68

5.2.3 415-Bus System 69

5.2.4 Comparative Analysis Among Systems 71

5.2.5 Comparative Analysis Among Methods 72

6 Conclusion **75**

6.1 Future Work 76

Bibliography **77**

A Data of the Tested Systems **80**

A.1 84-Bus System 80

A.2 136-Bus System 83

A.3 415-Bus System 88

List of Figures

Figure 3.1: 14-bus system 27
Figure 3.2: 14-bus system modified for use as an example. 28
Figure 3.3: 14-bus meshed system with the original weights used as an example. . . . 28
Figure 3.4: volution of the modified Prim's algorithm for the 14-bus system. 30
Figure 3.5: Radial solution for the 14-bus system. 31
Figure 3.6: Layer division for renumbering. 31
Figure 3.7: New numbering for the 14-bus system. 32
Figure 3.8: Weight variation. **(a)** Original input; **(b)** Random variation. 33
Figure 3.9: Procedure for adding a solution to the Maximum/Minimum Distance set. . 34
Figure 3.10: Gene exchange process between parents in the GA. 35
Figure 3.11: Evolution of the VND Method 36
Figure 3.12: Example of a branch in the electrical power system. 38
Figure 4.1: 84-bus System 43
Figure 4.2: 136-bus System 44
Figure 4.3: 415-bus System. 45
Figure 4.4: Block diagram illustrating the steps for the proposed methodology. . . . 54
Figure 5.1: Voltage profile for the 84-bus system. 58
Figure 5.2: Comparison of voltage profile without DG and with allocation of up to 3 DG. 59
Figure 5.3: Comparison of the voltage profile for the 84-bus system without DG (using VND), with 3 DG allocation, and with maximum DG allocation. 60
Figure 5.4: Voltage profile for the 136-bus system. 61
Figure 5.5: Voltage profile without DG and with allocation of up to 3 DG in the 136-bus system. 62
Figure 5.6: Comparison of the voltage profile for the 136-bus system without DG (using VND), with 3 DG allocation, and with maximum DG allocation. 63
Figure 5.7: Voltage profile for the 415-bus system. 64
Figure 5.8: Voltage profile without DG and with allocation of up to 3 DG in the 415-bus system. 65
Figure 5.9: Voltage profile comparison for the 415-bus system without DG (using VND), with 3 DG allocation, and with maximum DG. 66

List of Tables

Table 5.1: Number of results obtained for the 84-bus system. 57
Table 5.2: Results achieved for the 84-bus system. 58
Table 5.3: Results for the 84-bus system with and without DG allocation. 59
Table 5.4: Results for the 84-bus system with maximum DG allocation. 60
Table 5.5: Number of results obtained for the 136-bus system. 61
Table 5.6: Results achieved for the 136-bus system. 61
Table 5.7: Results for the 136-bus system with and without DG allocation. 62
Table 5.8: Results for the 136-bus system with maximum DG allocation. 63
Table 5.9: Number of results obtained for the 415-bus system. 64
Table 5.10: Results achieved for the 415-bus system. 64
Table 5.11: Results for the 415-bus system with and without DG allocation. 65
Table 5.12: Results for the 415-bus system without DG, with 3 DG, and with maximum DG allocation. 66
Table 5.13: Comparison of power losses obtained for the three tested systems. 71
Table 5.14: Comparison of power losses obtained for the 84-bus system. 72
Table 5.15: Comparison of power losses obtained for the 136-bus system. 73
Table 5.16: Comparison of power losses obtained for the 415-bus system. 74
Table A.1: 84-Bus System Data 80
Table A.2: 136-Bus System Data 83
Table A.3: 415-Bus System Data 88

List of Symbols

x_{ab}	Switching variable of the branch connecting buses a and b
N	Set of branches in the distribution system
ab	Branch belonging to set N
B	Set of buses in the distribution system
a	Bus belonging to set B
b	Bus belonging to set B
n_{ab}	Total number of branches in the system
n_b	Total number of buses in the system
$V_{\max}$	Maximum allowable voltage magnitude
$V_{\min}$	Minimum allowable voltage magnitude
V_a	Voltage magnitude at bus a
V_{ra}	Real component of the voltage at bus a
V_{ia}	Imaginary component of the voltage at bus a
V_{rb}	Real component of the voltage at bus b
V_{ib}	Imaginary component of the voltage at bus b
I_{rb}	Real component of the current at bus b
I_{ib}	Imaginary component of the current at bus b
I_{rab}	Real component of the current in branch ab
I_{iab}	Imaginary component of the current in branch ab
I_{rbn}	Real components of currents in branches connected to bus b, excluding branch ab
I_{ibn}	Imaginary components of currents in branches connected to bus b, excluding branch ab
P_{total}	Total active power losses of the electrical system
P_{ab}	Active power loss in branch ab
P_b	Net active power injection at bus b
$P_{\text{DG},a}$	Active power generated by the DG unit at bus a
$P_{\text{Load},a}$	Active power demand (load) at bus a
$P_{\max,\text{DG}}$	Maximum active power capacity allocated for DG
Q_b	Net reactive power injection at bus b (capacitive power minus inductive power)
$Q_{\text{DG},a}$	Reactive power generated by the DG unit at bus a

$Q_{\text{Load},a}$	Reactive power demand (load) at bus a
S_{ab}	Apparent power flow through branch ab
$S_{\max,ab}$	Maximum rated apparent power capacity of branch ab
R_{ab}	Resistance of branch ab
X_{ab}	Reactance of branch ab
G_{ab}	Conductance of branch ab (real part of the branch admittance between buses a and b)
B_{ab}	Susceptance of branch ab (imaginary part of the branch admittance between buses a and b)
G_{aa}	Sum of all conductances connected to bus a
B_{aa}	Sum of all susceptances connected to bus a, including shunt elements
g_{ab}	Line conductance between buses a and b
b_{ab}	Line susceptance between buses a and b
b_{sh}	Shunt susceptance
θ_a	Voltage phase angle at bus a
θ_b	Voltage phase angle at bus b
$\sum_{b\in B}$	Summation over all buses in set B connected to bus a
$\mathbf{Y}_{\text{bus}}$	Bus admittance matrix
f	System frequency
C	Line capacitance
a^*	Selected bus for DG allocation
$\min_{a\in B}\{V_a\}$	Minimum voltage magnitude V_a identified after reconfiguration
kW	Kilowatt
kVA	Kilovolt-ampere
kVAR	Kilovolt-ampere reactive
kV	Kilovolt
s	Seconds

List of Acronyms and Abbreviations

ANEEL	*Agência Nacional de Energia Elétrica*
BRKGA	Biased Random-Key Genetic Algorithm
BSS	Best Solution Set
DG	Distributed Generation
DSR	Distribution System Reconfiguration
EEHO	Enhanced Elephant Herding Optimization
EPDS	Electric Power Distribution System
GA	Genetic Algorithm
GAFS	Genetic Algorithm Feasible Solutions
GA QSS	Genetic Algorithm Quality Solution Set
IEEE	Institute of Electrical and Electronics Engineers
MILP	Mixed-Integer Linear Programming
PRIM	Prim's Algorithm
p.u.	per-unit
QSS	Quality Solution Set
SA	Simulated Annealing
VND	Variable Neighborhood Descent
VNDFS	Variable Neighborhood Descent Feasible Solutions
VNS	Variable Neighborhood Search

Chapter 1

Introduction

The conventional Brazilian power system encompasses large power generation plants that are generally located far from major load centers; power transmission lines to transport the generated energy from the plants to these major load centers; distribution systems to deliver electricity to end consumers; and, finally, the consumers themselves. his extensive system must be capable of supplying consumers with high-quality electricity in a sustainable manner and at the lowest possible cost, while complying with the parameters established by regulatory and supervisory authorities (Cardona, 2016).

The Electric Power Distribution System (EPDS) distributes electrical energy from distribution substations to end consumers, such as residential, commercial, and industrial clients. It consists of two main parts: the primary and secondary distribution systems. The primary distribution system distributes energy at medium voltage from the substation to distribution transformers, typically at voltages between 1 and 36.2 kV. This section of the circuit is composed of lines or branches that transport power between the distribution substation and the medium-voltage transformers or buses, the latter being the points where system loads are connected. The secondary distribution system, on the other hand, performs the final distribution of electrical energy between the medium-voltage transformers and the utility's captive consumers (loads) at voltages below 1 kV. This system comprises low-voltage distribution lines and energy meters. (Montemezzo, 2016).

In Brazil, the sector with the highest energy losses is the EPDS. It is estimated that approximately 14% of all generated electricity is lost in EPDS. Of this total, 7.36% corresponds to technical losses, which are inherent to the physical processes associated with power transmission and distribution, such as conductor heating (Joule effect), transformer losses, losses due to imperfect connections, phase imbalance, and capacitance. The remaining 6.64% corresponds to non-technical losses, resulting from energy fraud and theft, measurement inaccuracies, and other challenges related to the operation, maintenance, and control of the system (Aneel, 2026). Considering that acceptable technical losses range from 3% to 6%, it is evident that EPDS require greater attention to mitigate energy-loss-related problems in the Brazilian electric power sector.

Given the high losses occurring in the distribution sector, one solution adopted to minimize them is the Distribution System Reconfiguration (DSR). It consists of altering the system topology by opening or closing sectionalizing and tie switches at strategic points to optimize the path taken by electrical energy from the substation to the consumer. This procedure is commonly used for fault isolation, load balancing between feeders, voltage level improvement, and the minimization of power losses in distribution systems. (Ferreira, 2022).

The DSR problem is treated as a mixed-integer non-linear combinatorial optimization problem, requiring tools such as classical optimization, heuristics, metaheuristics, and hybrid algorithms to solve it. These techniques are employed to explore new topological configurations and to further investigate regions of the search space that have already shown promising results. (Pereira Junior, 2024).

Another factor that helps reduce losses and improve the voltage profile in the EPDS is the allocation of Distributed Generation (DG). DG generates a small amount of electrical energy close to the load center, which helps decrease power losses in the branches by alleviating the power supply from the substation, in addition to raising the bus voltage profile to help increase stability and improve power quality. (Chouhan & Thakur, 2023).

1.1 Objective

To develop a hybrid algorithm for DSR and DG allocation, aiming to identify solutions that minimize active power losses and improve the voltage profile. To achieve this objective, the following specific objectives were established.

1.1.1 Specific Objectives

- Create radial solutions using the Modified Prim's algorithm, as well as analyze and classify the generated solutions through power flow calculations to determine active power losses;
- Obtain a set of feasible and diversified radial solutions using the Multi-start method;
- Perform the crossover of feasible radial solutions using the Genetic Algorithm (GA) to improve solution quality and expand the search space;
- Investigate the neighborhood of the GA solutions using the Variable Neighborhood Descent (VND) method to provide local improvement;
- Allocate distributed generators in the reconfigured solutions to reduce active power losses and improve the voltage profile.

1.2 Justification

In the past, the Brazilian electricity consumer profile was characterized by having few electrical and electronic appliances at home, typically basic items such as refrigerators, televisions, electric showers, and a few other devices. Currently, this reality is completely different; a single residence can house a wide variety of electrical and electronic equipment, including televisions, air conditioners, microwaves, freezers, computers, electric vehicles, and even power generation systems, such as photovoltaic generation systems, alongside many other devices that have become indispensable, especially given the emerging technologies being integrated into the power system.

This evolution in consumption patterns highlights a central point: the demand for electrical energy continues to grow steadily, and distribution systems must adapt to ensure a continuous, efficient, safe, and sustainable supply. The growing electricity demand alongside DG, combined with the need for a sustainable power supply, has encouraged several studies focused on the modernization of EPDSs.

In this context, DSR emerges as a more economical solution, as it eliminates the need for the construction and installation of new equipment. DSR makes use of the equipment already installed and operating in the network, modifying only its topology. Reconfiguring the distribution network topology allows the system to operate more optimally, reducing losses and improving voltage levels without requiring substantial expenditures on the installation and construction of new generation infrastructure.

Another promising factor for improving power supply quality is the integration of distributed generation energy sources along with reconfiguration, helping to further minimize losses by reducing the need for all power to originate from the substation, while also improving the system's voltage profile when installed at buses with lower voltage levels.

The use of heuristic and metaheuristic tools for DSR is advantageous as they are faster compared to classical approaches. Although the latter guarantee optimal solutions, their processing time can be excessively long, particularly in systems with a high number of buses. Combining heuristic and metaheuristic tools for loss reduction with DG allocation makes it possible to obtain system topologies with significantly lower losses.

1.3 Contributions

The main contributions of this work to the literature are:

1. Integration of DSR with DG allocation in a unified methodology: studies such as Possagnolo (2015) and Pereira Junior (2024) address reconfiguration exclusively without con-

sidering DG allocation. The present work combines both stages, reconfiguration via the sequence modified Prim → Multi-start → Scatter Search → GA → Scatter Search → VND → Scatter Search and, subsequently, DG allocation at the minimum voltage bus, allowing simultaneous optimization of network topology and the location of distributed resources;

2. Inclusion of VND as a local refinement stage: the work of Pereira Junior (2024) uses Prim → GA, without a structured local search stage. The addition of VND allows for the exploration of the solution neighborhood provided by the GA, obtaining higher-quality solutions;

3. Multi-scenario analysis of DG allocation: this work systematically evaluates scenarios with 1, 2, 3, and the maximum number of DG allocated per system, quantifying the incremental gain of each additional DG. This analysis provides insights for planning decisions regarding the number of units to install.

1.4 Limitations

The methodology proposed in this work presents some limitations:

- The approach is deterministic regarding load and generation (without uncertainty modeling);
- Single-objective focus (minimization of active power losses), without considering other criteria such as reliability or investment costs in DG and infrastructure;
- DG allocation is always performed at the minimum voltage bus found; therefore, distributed generators may not be optimally connected;
- DG allocation was modeled using static installation decisions under steady-state conditions.

1.5 Dissertation Structure

The dissertation is structured as follows:

- Chapter 1: introduction to the dissertation, objectives, justification, contributions, and limitations;
- Chapter 2: systematic literature review on the topic addressed in this work;
- Chapter 3: methodological definitions and mathematical formulation used;
- Chapter 4: methodological procedures used to develop the proposed algorithm's codes;

- Chapter 5: results obtained and discussions comparing the methods used with each other and with the literature;
- Chapter 6: conclusions regarding the developed algorithm and future work.

Chapter 2

Systematic Literature Review

DSR is a widely debated topic in academia, with many authors proposing various methods to optimize electricity distribution. This chapter provides a literature review and presents the methods applied to DSR both with and without distributed generation, as well as surveying the state of the art in DSR.

2.1 Reconfiguration without the Use of Distributed Generation

Ferreira (2022) developed a hybrid solution for the DSR problem aiming to reduce active losses, combining the Biased Random-Key Genetic Algorithm (BRKGA) with Simulated Annealing (SA). In the BRKGA, two encoding schemes were tested, one based on Kruskal's algorithm and the other on co-tree, and elitist reinitialization routines were implemented to accelerate convergence. Additionally, a hybrid scheme (BRKGA/SA) was proposed. In tests conducted on 14- to 136-bus networks, the BRKGA with a co-tree decoder and elitist reinitialization yielded the best solutions in shorter computational times, while the hybrid method outperformed conventional approaches in terms of result quality.

The methodology proposed by Ferreira (2022) combines two distinct optimization methods in an attempt to obtain better solutions than either method could achieve separately. This idea is expanded in the present work by incorporating a third method, neighborhood search, along with a scatter search method after each reconfiguration stage to explore new solutions that can further reduce electrical losses in the tested systems.

In Pereira, Barbosa & Vasconcelos (2023), a combination of branch-exchange heuristics and evolutionary metaheuristics was proposed to solve the DSR problem. The method consists of coupling the branch-exchange heuristic to an iterative loop inspired by the generation process of an evolutionary algorithm to reduce the search space. This approach was applied to 33-, 70-, 84-, and 136-bus systems. The algorithm achieved better results than those in the literature using only the original configuration as the initial solution..

By proposing an algorithm that combines heuristics and metaheuristics, Pereira et al. (2023) attempts to reduce search time by directing the proposed methodology to search only for

solutions that already present lower losses, starting from a single initial solution. This concept is reused in this work; however, the developed algorithm searches for solutions providing lower losses by using a set of diverse solutions as a starting point. These solutions are both high-quality and significantly distinct from one another, ensuring that the search space is explored as broadly as possible..

In Greina, Karnib, Gaubert, Bertout, Grolleau & Larraillet (2023), a new Mixed-Integer Linear Programming (MILP) model was proposed for the DSR problem, primarily aiming at voltage balancing across buses as well as loss reduction. Two MILP models are presented: one termed $MILP_{loss}$, where losses are included in the power flow equations, and another termed $MILP_{no-loss}$, where losses are not included. Both models were tested on the standard 33-bus system and on a modified version where two DGs were added, considering a maximum voltage variation limit of 10%. Both models demonstrated consistency with the literature regarding both voltage profile and loss reduction.

The classical approach presented by Greina et al. (2023) served to show that this type of procedure still leaves considerable room for evolution, particularly in how classical methods are implemented for DSR, with the potential to offer optimal solutions in reduced computational time.

In Pereira Junior (2024), a hybrid methodology for DSR was proposed, integrating Prim's Algorithm, Multi-Start search strategies, and subsequent refinement through a GA. Tested on 136- and 415-bus networks (a modification of the 417-bus system), the approach proved effective in broadly scanning the solution space, identifying radial topologies capable of reducing electrical losses by up to 16.48%. Furthermore, the method stood out for its robustness, flexibility, and low computational cost, avoiding local minima traps.

In Nizer, Freitas, Rocha, Scherer, Perreira Junior & Freitas (2024), a hybrid procedure combining heuristics and metaheuristics was presented for DSR, focusing on the minimization of active power losses. Initially, Prim's Algorithm was used to generate candidate radial configurations. Next, the Multi-Start method was applied to generate multiple distinct feasible solutions, and Scatter Search was employed to filter the most promising topologies. Finally, a GA iteratively refines the selected topologies. Experiments demonstrated reductions in losses and showed that the procedure maintains a good balance between solution quality and processing time, even in higher-complexity systems.

The works proposed by Pereira Junior (2024) and Nizer et al. (2024) start from a set of diverse solutions provided by the Multi-start method and improved by the GA, an approach that served as the foundation for this study. The proposed methodology takes this concept further by incorporating the VND method to explore the neighborhood of the solutions produced by the GA. The work of Pereira Junior (2024) also served as a benchmark for comparing the results obtained using the proposed methodology with those available in the literature.

2.2 Reconfiguration Using Distributed Generation

In Marodin & Freitas (2020), an approach was proposed that integrates DSR with DG allocation, aiming to minimize active power losses. To this end, the suggested method used a combination of heuristic algorithms, such as Prim's and VND, and metaheuristic algorithms, such as the Multi-Start algorithm. The methodology applies Prim's and Multi-Start to generate several feasible radial solutions, followed by a scatter search technique applied to the solutions originating from Multi-Start to obtain a set of diverse solutions. Finally, it applies VND along with DG allocation to identify the best radial topology and the buses for connecting the DG. This methodology stands out for reducing active power losses and optimizing system operation, demonstrating effectiveness in tests conducted across systems with different numbers of buses.

The structure of this work is built upon the study by Marodin & Freitas (2020), from which the initial diversification strategy (Multi-Start and scatter search) and local refinement via VND were adapted, with the inclusion of the GA. However, the main difference lies in the final stage of DG insertion: while Marodin & Freitas (2020) initiates allocation at the minimum voltage bus and performs an exhaustive search across all buses for optimal connection, the proposed approach simplifies this process. Following three optimization phases in network reconfiguration, DG connection is carried out directly at the buses with the lowest voltage levels, without the need for searching for an optimal location.

In Bueno (2021), a methodology was proposed to optimize the operation of distribution systems through network reconfiguration and the simultaneous allocation of distributed generators, aiming to minimize loss costs. To solve this problem of high combinatorial complexity, the Variable Neighborhood Search (VNS) algorithm was used to determine network topology and generator placement, integrated with a Fibonacci Search method to define the optimal power dispatch for the DG. Tested on standard systems (33-, 69-, and 84-bus), the approach reduced losses and improved voltage levels, even under different load levels, while considering long-term economic viability.

The strategy of exhaustively exploring the neighborhoods of promising solutions proposed by Bueno (2021) using VNS also served as a reference for this work, confirming that local refinement around favorable topologies is efficient for reaching high-quality local optima. However, the approach adopted here simplifies this search: the exploration of new radial topologies for DSR is restricted to the Variable Neighborhood Descent (VND) algorithm, and the selection of nodes for DG connection is direct, prioritizing solely the buses with the lowest voltage levels.

In Chouhan & Thakur (2023), the problem of optimal allocation and sizing of DG in radial distribution systems was addressed, aiming to minimize voltage drops and energy losses. To resolve this issue, the authors proposed the use of the Enhanced Elephant Herding Optimization (EEHO) technique, an improved version of a metaheuristic inspired by the social behavior of

elephant herds. Through simulations on 33- and 69-bus systems, the study demonstrated that the proposed EEHO method outperforms traditional algorithms, providing loss reductions of up to 67% and a significant stabilization of voltage profiles.

In the work of Quang, Quoc & Minh (2023), a GA based on natural genetics and selection mechanisms was proposed for DSR considering DG allocation. The GA begins with a set of initial solutions, after which successive populations of solutions are generated through genome reproduction, crossover, and mutation (radial solutions). The GA was applied to the reconfiguration of the IEEE 33-bus system, both with and without DG integration. When integrated with DGs, the method yields superior results, achieving lower losses and an improved voltage profile.

In Pandey, Singh, Shantenu, Harsh & Choudhary (2026), DSR integrated with DG allocation was proposed. For network reconfiguration, an improved Grey Wolf Optimization algorithm was used, based on the hunting behavior of wolves, which is divided into three stages: chasing good solutions, encircling optimal solutions, and attacking global optimal solutions. Simultaneously, a sensitivity analysis is applied to identify the most suitable buses for DG allocation. The proposed method was applied to the IEEE 33-bus system and demonstrated superior results compared to other methods in the literature, achieving loss reductions of up to 72.28%."

Collectively, these works illustrate different methodological avenues for the DSR problem with DG allocation: while Quang et al. (2023) relies on a classical Genetic Algorithm, Chouhan & Thakur (2023) and Pandey et al. (2026) leverage enhanced versions of swarm/animal behavior metaheuristics (EEHO and Grey Wolf Optimizer). Pandey et al. (2026) takes a step further by using a deterministic technique (sensitivity analysis) prior to optimization, thereby reducing the search space for DG allocation. All these studies reflect the growing trend toward enhancing the operation of distribution networks in the face of the massive integration of distributed energy resources.

Chapter 3

Methodological Definitions

This chapter presents the definitions of the procedures and methods used, along with the mathematical formulation employed to construct the reconfiguration algorithm.

3.1 Definitions

The definitions of distribution system reconfiguration and the methods used in the distribution system reconfiguration algorithm are presented below.

3.1.1 Distribution System Reconfiguration

The EPDS is constructed in a meshed topology, meaning it forms loops, such that more than one path connects any two given buses. However, a radial topology, devoid of loops and with only a single path connecting any two buses in the circuit, is adopted for EPDS control because it is simpler and more cost-effective from the perspectives of operation, planning, modeling, and protection. Being constructed in a meshed fashion, the EDS offers flexibility to assume different topologies through DSR, enabling the reduction of branch losses and the improvement of bus voltage levels (Bueno, 2021).

DSR is a technique that consists in changing the status of the system switches (sectionalizing and tie switches) to obtain a topology with lower losses, improving the bus voltage profile and reducing line (branch) loading (Andrade & Ferreira, 2018).

The objective of DSR is to identify the best configuration for the distribution system while maintaining a radial topology and complying with voltage limits established by regulatory standards. DSR is primarily performed to minimize active power losses in the system, improve voltage levels, maintain system reliability, and enable preventive maintenance. Switching operations are used to maintain control over the network and ensure that it operates in accordance with high standards of electric power supply quality (Souza & Romero, 2013).

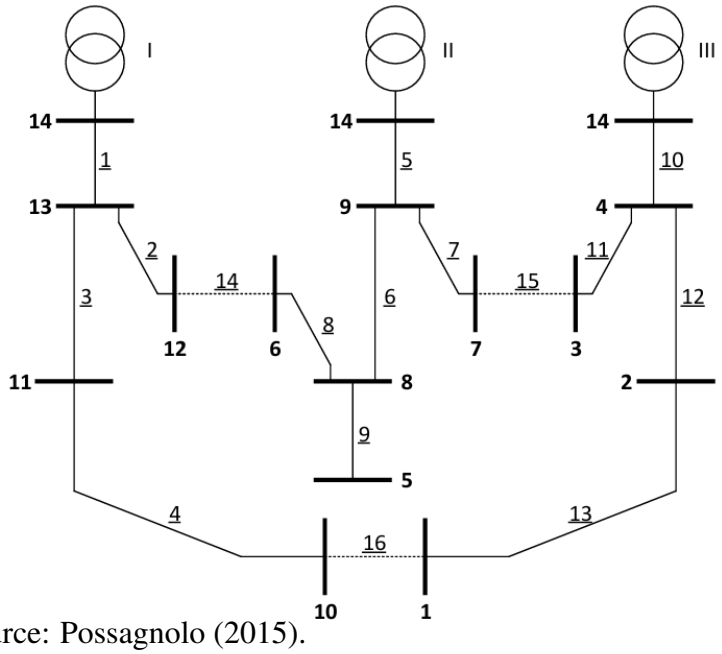
DSR is not an easy problem to solve and is considered a combinatorial optimization problem. The difficulty in solving it arises from the large number of possible configurations that the system can assume, which further increases in complexity as the size of the system grows. Since each sectionalizing or tie switch can have two states, either open or closed, the number of possible configurations is 2^n, where n is the number of switches in the system (Andrade & Ferreira, 2018).

3.1.2 Modified Prim's algorithm

Some combinatorial optimization problems can be formulated using a specific type of graph known as a tree. A tree guarantees complete connectivity among all nodes; that is, it is connected while eliminating any redundancy in the paths and avoiding cycles. In practical terms, this means that there is exactly one possible path connecting any two nodes (buses) (Wilhelm, 2015).

Since a tree satisfies the requirement of having a single path connecting all nodes, it is expected that it can be solved quite efficiently, including through greedy algorithms. There are several classical algorithms that enable the rapid construction of a tree, among them Prim's algorithm (Goldbarg & Luna, 2005).

Figure 3.1 illustrates the 14-bus system that will be used as an example to demonstrate the methods employed in this work.

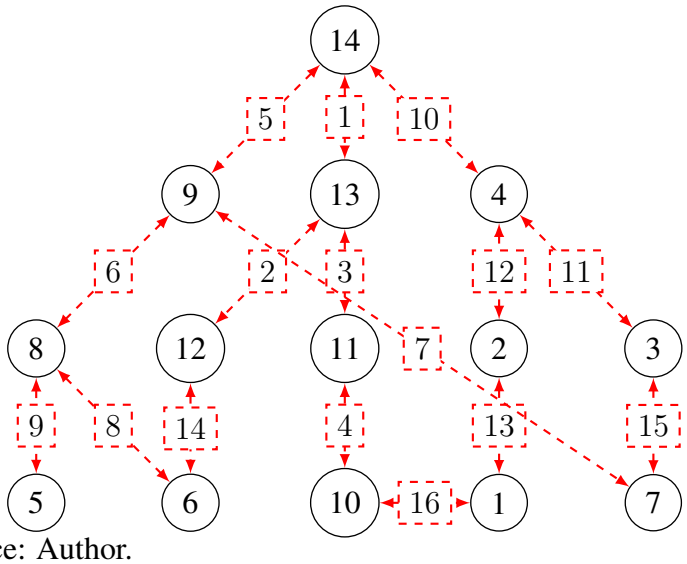


Source: Possagnolo (2015).

Figure 3.1: 14-bus system

However, to facilitate the illustration of the examples, Figure 3.2 and its variations will

be used, with circles representing the buses and dashed squares with arrows representing the branches.

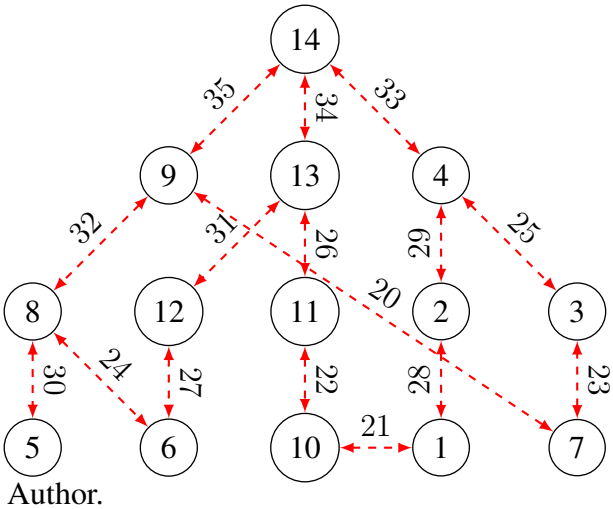


Source: Author.

Figure 3.2: 14-bus system modified for use as an example.

The classical Prim's algorithm constructs a minimum spanning tree by successively selecting the lowest-weight edges (branches) that connect the nodes (buses) (Prim, 1957). In this work, however, an adaptation of this process is adopted to construct a maximum spanning tree, prioritizing the highest available branch weights. The creation of the maximum spanning tree aims to maximize transmitted apparent power—that is, forcing power flow through paths that potentially cause the highest electrical losses.

Figure 3.3 illustrates the meshed topology for a 14-bus system with the weights of the connecting edges (branches) between the buses.



Source: Author.

Figure 3.3: 14-bus meshed system with the original weights used as an example.

The modified Prim's algorithm operates similarly to the classical Prim's algorithm. It begins by selecting a reference node and, from this node, seeks to identify the highest-weight path for constructing the maximum spanning tree, passing through all nodes of the graph (Pereira Junior, 2024).

In order to state the principles for solving the basic problem, it is necessary to introduce a few terms (Prim, 1957):

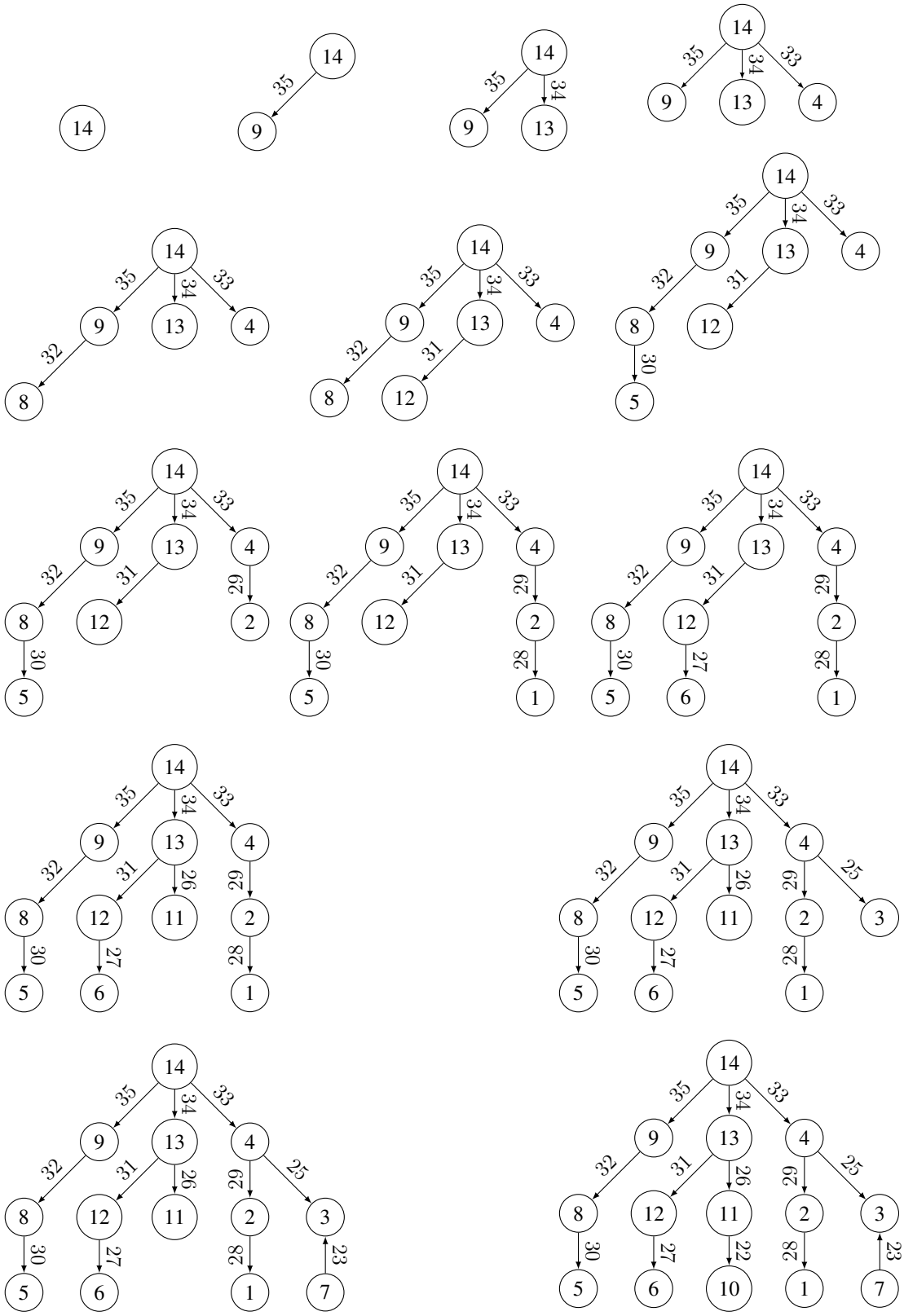
- Isolated node: a node to which, at a given phase of construction, no connections have yet been made.
- Fragment: a subset of nodes connected by direct links between members of the subset.
- Distance from a node to a fragment: for the traditional Prim's algorithm, it is the minimum of the distances to the individual nodes comprising the fragment; however, for the modified Prim's algorithm, it is the maximum of these distances instead of the minimum.
- Isolated fragment: a fragment to which, at a given phase of construction, no external connections have been made.
- Neighbor (of a node or fragment): for the modified Prim's algorithm, it is a node whose distance to another specified node (or fragment) is at least as large as that to any other node.

The two fundamental construction principles (P1 and P2) can be stated as (Prim, 1957):

- Principle 1: Any isolated node can be connected to a neighbor.
- Principle 2: Any isolated fragment can be connected to a neighbor through the longest available link.

An efficient algorithm consists of applying P1 only once to initiate a fragment from a node and then iteratively applying P2 to extend this fragment. At each iteration, a table F containing the distances from the connected fragment to the terminals that have not yet been connected is maintained. The largest entry is selected, the corresponding link is added to the solution, and the table F is updated by comparing the current distances with those of the newly added terminal. This procedure avoids cycle checks and requires access to only two rows of data at a time (Prim, 1957).

Figure 3.4 presents the evolution of modified Prim's algorithm and the construction of the radial topology for the 14-bus system.

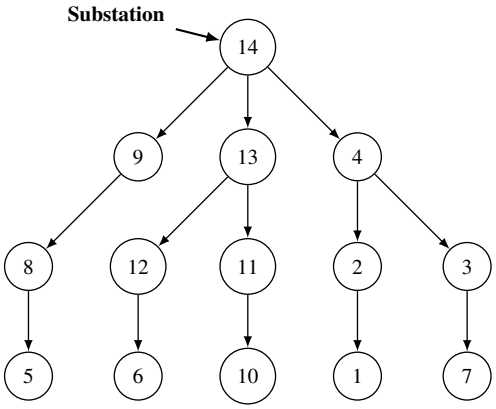


Source: Author.

Figure 3.4: volution of the modified Prim's algorithm for the 14-bus system.

3.1.3 Renumering

Renumbering is necessary to facilitate the implementation of the sweep-based power flow algorithm. This procedure reorders the identifiers of the buses and branches in ascending order, making it easier to track the direction of the power flow calculations. The renumbering process is performed by selecting a reference bus, generally the substation bus, as illustrated in Figure 3.5 for the 14-bus system used as an example (Figure 3.3). Starting from this initial point, the buses are renumbered by replacing the original system identifiers with new identifiers according to a new order (Fioravanti Junior, 2014).

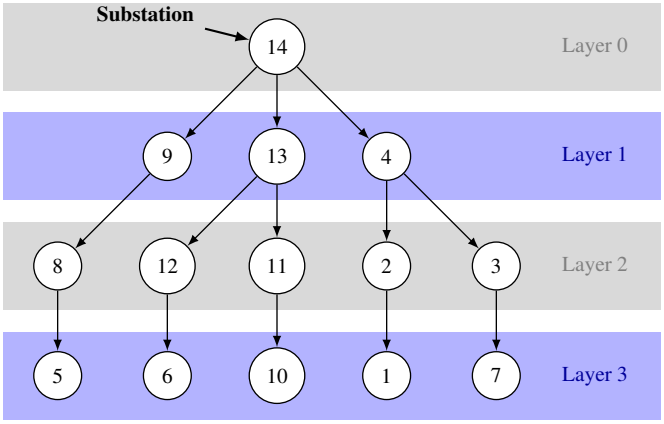


Source: Author.

Figure 3.5: Radial solution for the 14-bus system.

The process adopts a layer-by-layer sweep strategy: it starts with the branches directly connected to the substation and moves progressively to subsequent layers. All elements within the same layer are renumbered before the algorithm advances to the next layer, ensuring a logical and sequential ordering of the network (Cardona, 2016).

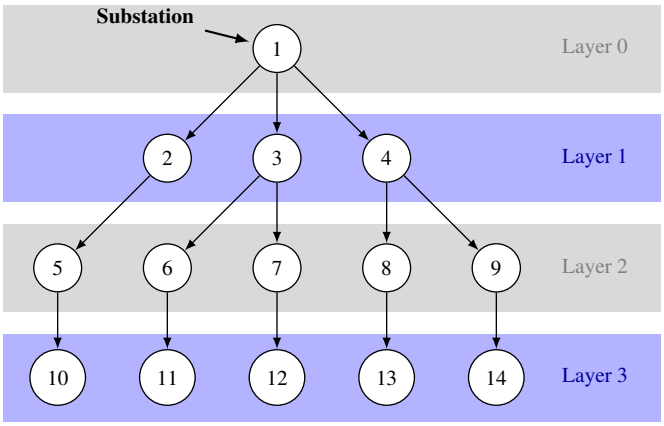
Figure 3.6 illustrates the layer-by-layer division for renumbering.



Source: Author.

Figure 3.6: Layer division for renumbering.

Figure 3.7 illustrates the new numbering for the 14-bus system after renumbering.



Source: Author.

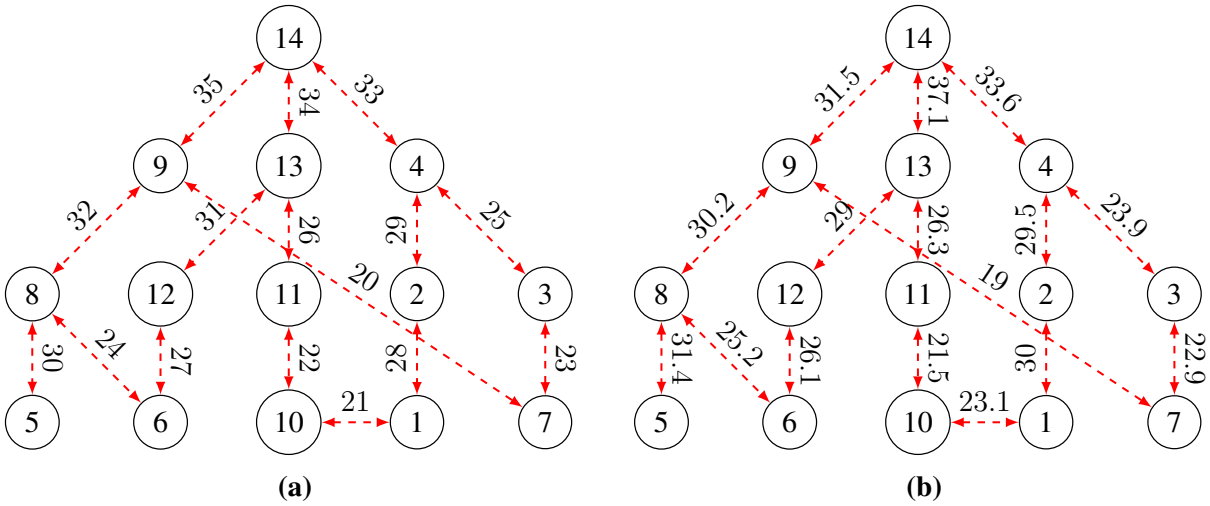
Figure 3.7: New numbering for the 14-bus system.

3.1.4 Multi-start

The Multi-start method is a procedure used in optimization problems to generate multiple solutions. Multi-start is based on exploring multiple starting points to identify high-quality solutions. Its operation involves repeatedly running a constructive algorithm from different initial configurations. In each iteration, starting from a new initial point, a new solution is created. The objective is to explore the diversity of the search space to increase the chances of finding better solutions (Pereira Junior, 2024).

The Multi-start method is divided into two stages: the first stage consists of generating random solutions, while the second stage involves classifying and/or improving the generated solutions. In this way, each iteration produces a local solution, and the best among all generated solutions becomes the incumbent, that is, the best solution found by the algorithm. The solutions created in the first stage are generated by a constructive algorithm, such as the Prim's algorithm. The second stage may range from a simple strategy, such as sorting the generated solutions in ascending order, to the use of a complex metaheuristic, which may or may not improve the solution (Cardona, 2016).

Figure 3.8 illustrates the random variation of branch weights that serve as input for Multi-start.



Source: Author.

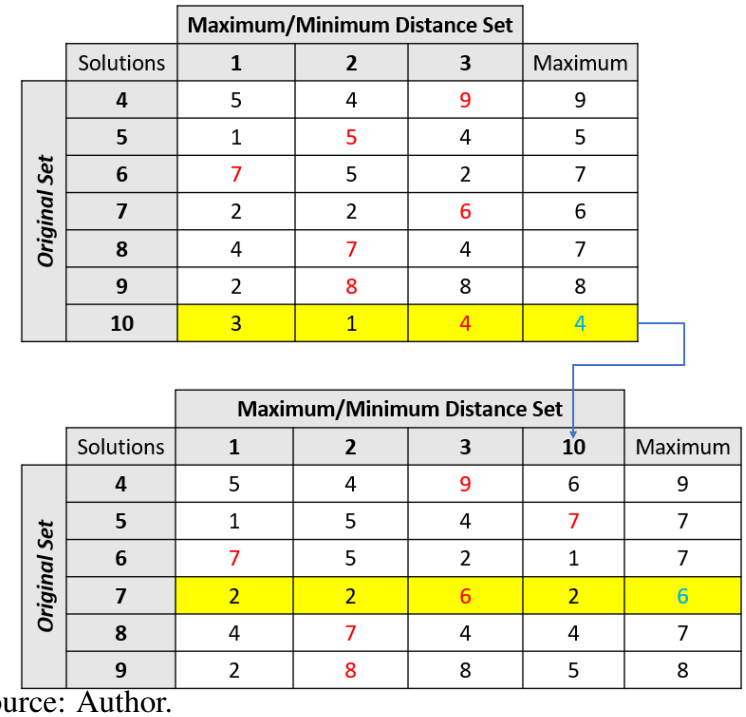
Figure 3.8: Weight variation. **(a)** Original input; **(b)** Random variation.

3.1.5 Maximum/Minimum Distance

The Maximum/Minimum Distance method aims to form a set of solutions that are significantly different from one another through a scatter search process, in order to prevent subsequent methods from becoming trapped in local optima (Pereira Junior, 2024).

Half of this set is populated with the best solutions obtained from the execution of another algorithm, such as Multi-start. The second half of the set is populated through an iterative process that aims to include solutions exhibiting the greatest possible difference with respect to the solutions already present (Freitas, Perreira Jr, Freitas, Sousa, Rocha, Scherer & Marodin, 2026).

Figure 3.9 illustrates the construction of this set. The process is exemplified starting from a stage in which the Maximum/Minimum Distance set already contains some of the best solutions (1, 2, and 3). To select the next solution from the original set (4 to 10), the difference in open branches between each candidate and the already selected solutions is calculated, storing the largest distance found for each candidate in the "Maximum" column. Next, the smallest value in this column is identified (in the first case, the value 4 corresponding to solution 10), which determines the radial topology to be transferred from the original set to the Maximum/Minimum Distance set. This iterative process is repeated until the Maximum/Minimum Distance set reaches the predefined number of radial solutions.



Source: Author.

Figure 3.9: Procedure for adding a solution to the Maximum/Minimum Distance set.

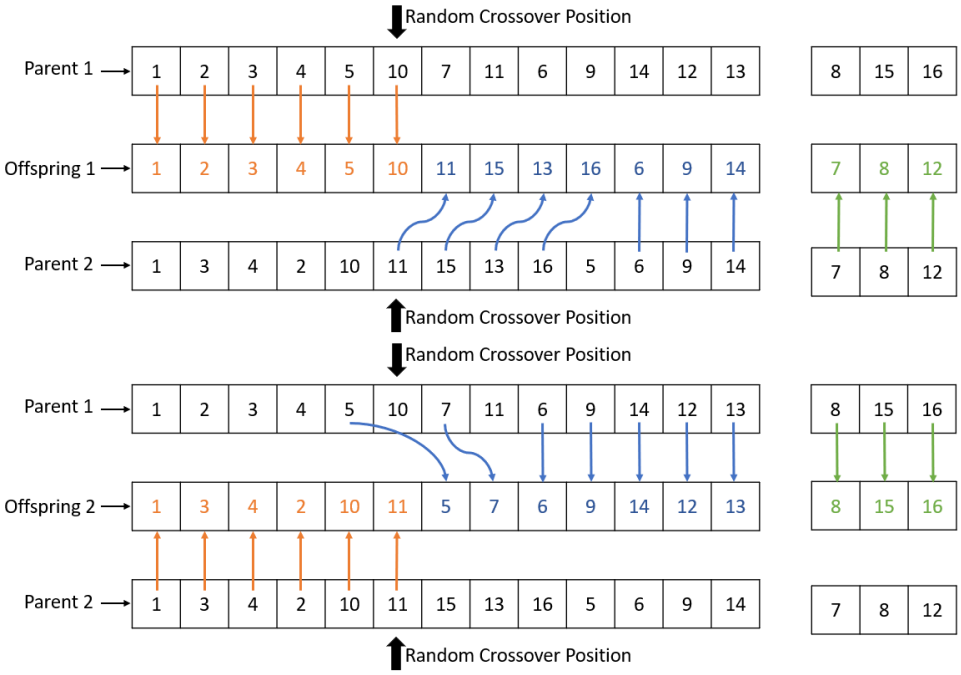
The way in which the set for the Maximum/Minimum Distance method is constructed aims to reduce a set of feasible radial solutions obtained from another method while preserving the diversity and quality of the solutions found. This strategy seeks to achieve a broader search space (Pereira Junior, 2024).

3.1.6 Genetic Algorithm – GA

GA operate by simulating the evolution of biological organisms, such that populations with superior characteristics are refined across successive generations through selection, crossover, and mutation mechanisms. In this process, the evolution of solutions is guided by the fitness of each individual, prioritizing those that best satisfy the problem's objectives and constraints to produce offspring. A basic GA consists of four main stages (Almeida & Nagan, 2010):

- Evaluation and selection: individuals (parents) considered to be good are propagated so that they can be further improved and generate offspring with better characteristics;
- Random selection: random selection of the permutation position of the parents;
- Reproduction: genes from the chromosomes of the parent individuals are exchanged to form new offspring;
- Mutation: the offspring are subjected (optionally or mandatorily) to small changes in order to provide potential improvements.

Figure 3.10 illustrates the reproduction (crossover) stage starting from two feasible radial solutions for the 14-bus system, represented as the "Parent 1" and "Parent 2" individuals. Each individual carries the network mapping: the primary vector indicates the closed branches that ensure energization and radial topology, while the secondary vector indicates the branches kept open. Once the random crossover position (cut point) is defined, two new offspring are generated through the exchange of genetic material: "Offspring 1" inherits the first section from the Parent and complements the network with genes from the Parent 2, whereas "Offspring 2" receives the initial segment from the Parent 2 and is completed with connections from the Parent 1. This rearrangement allows the exploration of new viable topologies by combining promising characteristics from both original solutions.



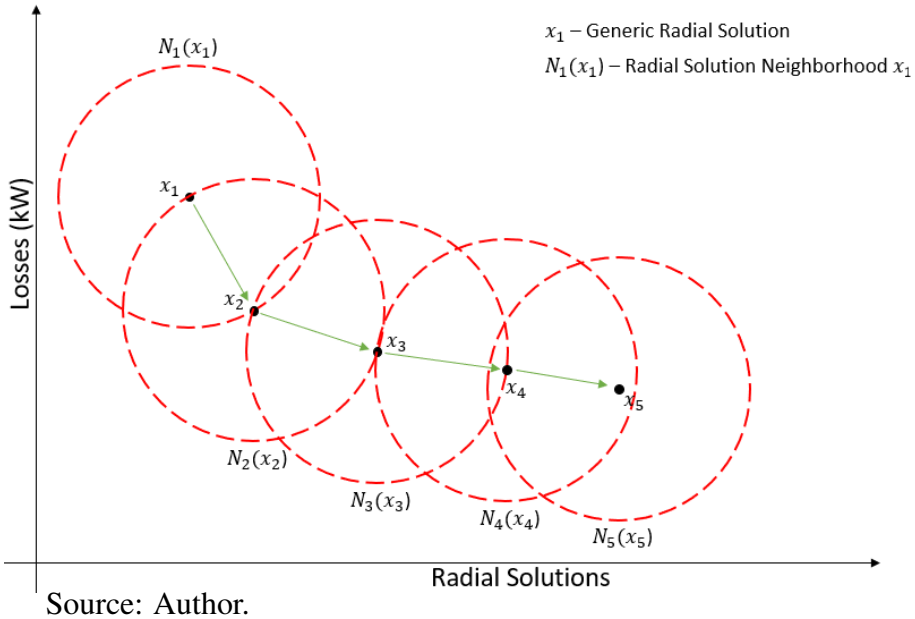
Source: Author.

Figure 3.10: Gene exchange process between parents in the GA.

The operational dynamics of the GA occur through successive cycles of evaluation, selection, and reproduction. Better-performing individuals have a higher probability of being selected as parents, transmitting their genes to future generations through crossover, which combines characteristics from different solutions, and mutation, which introduces random variations to maintain diversity and prevent the system from becoming stagnant. This iterative process, governed by probabilistic transitions, allows the population to continuously evolve and adapt, converging toward solutions that optimally satisfy the objectives and constraints of the proposed problem (Goldbarg & Luna, 2005).

3.1.7 Variable Neighborhood Descent - VND

VND (Figure 3.11) is a variation of VNS. The basic VNS algorithm for solving the problem is a metaheuristic based on the systematic change of neighborhood structures to escape local optima in combinatorial optimization problems.(Mladenovic & Hansen, 1997).



Source: Author.

Figure 3.11: Evolution of the VND Method

In each step, the VND algorithm performs local searches within the neighborhood of a given point. If no improvement is achieved, the neighborhood of the point changes to cover a larger region of the search space. Thus, instead of stopping the search at the point where no improvement was found, the VND algorithm moves to another neighborhood structure where a better solution might be obtained. This process continues until a solution is found that yields no improvement in any of the neighborhood structures (Possagnolo, 2015).

3.2 Mathematical Formulations

This section presents the equations used for the Objective Function and its constraints, the power flow calculation via the Backward/Forward Sweep method, and the allocation of distributed generators.

3.2.1 Objective Function and Constraints

The objective of DSR is to minimize system losses, which are given by the following Equation (3.1):

$$\min Pd_{totais} = \sum_{ab \in N} x_{ab} \cdot Pd_{ab} \tag{3.1}$$

Equation 3.1 is subject to the constraints defined by Equations 3.2, 3.3, and 3.4:

$$x_{ab} \in \{0, 1\} \tag{3.2}$$

$$\sum_{ab \in N} n_{ab} = n_b - 1 \tag{3.3}$$

$$V_{min} \leq V_a \leq V_{max} \tag{3.4}$$

Where:

- $\min Pd_{totais}$ is the minimization of the total losses in the EPDS;
- N is the set of branches in the distribution system;
- ab is an arbitrary branch belonging to the set N;
- Pd_{ab} represents the power losses in branch ab;
- x_{ab} represents the switching variable of the branch between buses a and b, where (0) represents an open state and (1) represents a closed state;
- n_{ab} is the number of branches in the system;
- n_b is the number of buses in the system;
- V_{min} is the minimum allowable voltage at bus a, set to 0.93 p.u., and V_{max} is the maximum allowable voltage at bus a, set to 1.05 p.u. Both values were defined according to the requirements established by regulatory authorities to ensure the quality of the supplied electricity;
- V_a is the voltage at bus a, given by Equation (3.5):

$$V_a = V_{ra} + jV_{ia} \tag{3.5}$$

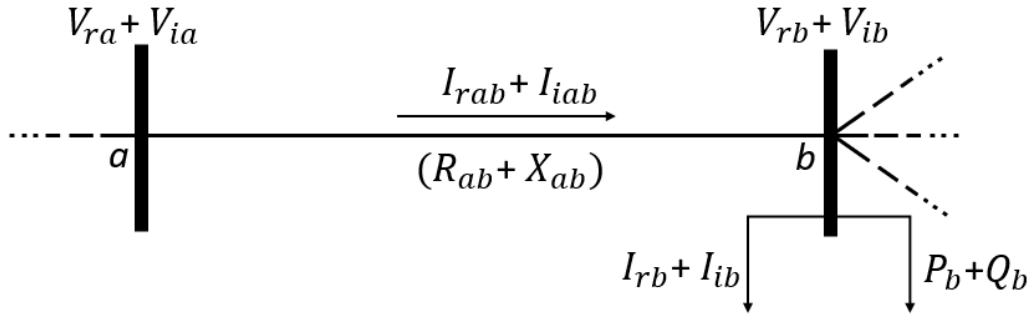
Where:

- V_{ra} is the real component of the voltage at bus a;
- jV_{ia} is the imaginary component of the voltage at bus a.

Equation 3.2 indicates which branches are closed and participate in the radial solution, as well as which ones are open. Equation 3.3 ensures that the number of branches is sufficient to connect all buses while preventing loop formation. Together, Equations 3.2 and 3.3 guarantee the radiality of the system. Equation 3.4 defines the voltage constraints for each bus in the electrical system and ensures that voltages remain within the specified limits, preventing overvoltage or undervoltage issues.

3.2.2 Power Flow

Figure 3.12 illustrates an example of electrical circuit branches in the power distribution system with their respective buses and branch components, including the variables used for the power flow calculation.



Source: Author.

Figure 3.12: Example of a branch in the electrical power system.

The real and imaginary components of the bus voltages for the power flow calculation are given by Equations 3.6 and 3.7:

$$V_{rb} = V_{ra} - R_{ab} \cdot I_{rab} + X_{ab} \cdot I_{iab} \tag{3.6}$$

$$V_{i_b} = V_{ia} - R_{ab} \cdot I_{iab} - X_{ab} \cdot I_{rab} \tag{3.7}$$

Where:

- V_{rb} is the real component of the voltage at bus b;
- V_{ib} is the imaginary component of the voltage at bus b;
- I_{rab} is the real component of the current in branch ab;
- I_{iab} is the imaginary component of the current in branch ab;
- R_{ab} is the resistance of branch ab;
- X_{ab} is the reactance of branch ab;

- a and b represent buses in the EPDS;

The bus currents are calculated using Equations 3.8 and 3.9.

$$I_{rb} = \frac{P_b \cdot V_{rb} + Q_b \cdot V_{ib}}{V_{rb}^2 + V_{ib}^2} \tag{3.8}$$

$$I_{ib} = \frac{P_b \cdot V_{ib} - Q_b \cdot V_{rb}}{V_{rb}^2 + V_{ib}^2} \tag{3.9}$$

Where:

- I_{rb} is the real component of the current at bus b;
- I_{ib} is the imaginary component of the current at bus b;
- P_b is the active power at bus b;
- Q_b is the reactive power at bus b, given by the sum of capacitive power minus inductive power.

The branch currents are calculated using Equations 3.10 and 3.11.

$$I_{rab} = I_{rb} + \sum_{n \neq a} I_{rbn} \tag{3.10}$$

$$I_{iab} = I_{ib} + \sum_{n \neq a} I_{ibn} \tag{3.11}$$

Where:

- I_{rab} is the real component of the current in branch ab;
- I_{iab} is the imaginary component of the current in branch ab;
- I_{rbn} represents the real components of the currents in branches connected to bus b, excluding branch ab;
- I_{ibn} represents the imaginary components of the currents in branches connected to bus b, excluding branch ab.

The branch power losses are calculated using Equation 3.12.

$$Pd_{ab} = R_{ab} \cdot (I_{rab}^2 + I_{iab}^2) \tag{3.12}$$

Where:

- Pd_{ab} represents the power losses in branch ab.

The total system power losses are given by Equation 3.13.

$$Pd_{totais} = \sum_{ab \in N} Pd_{ab} \tag{3.13}$$

Where:

- Pd_{total} represents the total power losses of the system.

3.2.3 Equations for DG Allocation

For each bus $a \in B$, where a denotes an arbitrary bus and B is the set of buses in the EDS, the power balance must be satisfied according to Equations 3.14 and 3.15.

$$P_{DG,a} - P_{Load,a} = V_a \sum_{b \in B} V_b (G_{ab} \cos(\theta_a - \theta_b) + B_{ab} \sin(\theta_a - \theta_b)) \tag{3.14}$$

$$Q_{DG,a} - Q_{Load,a} = V_a \sum_{b \in B} V_b (G_{ab} \sin(\theta_a - \theta_b) - B_{ab} \cos(\theta_a - \theta_b)) \tag{3.15}$$

Where:

- $P_{DG,a}$ is the active power generated by the DG at bus a;
- $P_{Load,a}$ is the active power consumed by the load (demand) at bus a;
- $Q_{DG,a}$ is the reactive power generated by the DG at bus a;
- $Q_{Load,a}$ is the reactive power consumed by the load (demand) at bus a;
- θ_a is the voltage phase angle at bus a;
- θ_b is the voltage phase angle at bus b;
- $\sum_{b \in B}$ represents the summation over all buses in set B connected to bus a;
- G_{ab} is the conductance of branch ab, representing the real part of the branch admittance between buses a and b;
- B_{ab} is the susceptance of branch ab, representing the imaginary part of the branch admittance between buses a and b;
- B is the set of buses in the EPDS.

Where G_{ab} and B_{ab} are computed from the bus admittance matrix Y_{bus}, given by Equation 3.16.

$$Y_{bus} = \begin{pmatrix} g_{11} + jb_{11} & g_{12} + jb_{12} & \cdots & g_{1b} + jb_{1b} \\ g_{21} + jb_{21} & g_{22} + jb_{22} & \cdots & g_{2b} + jb_{2b} \\ \vdots & \vdots & \ddots & \vdots \\ g_{a1} + jb_{a1} & g_{a2} + jb_{a2} & \cdots & g_{ab} + jb_{ab} \end{pmatrix} \tag{3.16}$$

Such that:

$$g_{ab} + jb_{ab} = \frac{1}{R_{ab} + jX_{ab}} \tag{3.17}$$

Where:

- g_{ab} is the real part of the admittance (conductance) between buses a and b;
- b_{ab} is the imaginary part of the admittance (susceptance) between buses a and b.

Thus, the conductance (G_{ab}) and susceptance (B_{ab}) can be calculated using Equations 3.18 and 3.19 for the elements on the main diagonal, that is, when a equals b.

$$G_{aa} = \sum g_{ab} \tag{3.18}$$

$$B_{aa} = \sum b_{ab} + \sum \frac{b_{sh}}{2} \tag{3.19}$$

Where:

- G_{aa} is the sum of all conductances connected to bus a;
- B_{aa} is the sum of all susceptances connected to bus a, including shunt elements;
- b_{sh} is the shunt susceptance given by the equation $2\pi \cdot f \cdot C$, where f denotes the grid frequency and C represents the line capacitance.

And by Equations 3.20 and 3.21 for the off-diagonal elements, that is, when a and b are distinct.

$$G_{ab} = -g_{ab} \tag{3.20}$$

$$B_{ab} = -b_{ab} \tag{3.21}$$

Equation for Candidate Bus Selection for DG Allocation

The selection of the bus to receive the DG allocation is performed using Equation 3.22.

$$a^* = \min_{a \in B}\{V_a\} \tag{3.22}$$

Where:

- a^* is the candidate bus selected to receive the DG allocation;
- $\min_{a \in B}\{V_a\}$ is the minimum voltage identified following system reconfiguration.

However, the DG integration will only occur if the power limits specified by Equations 3.23 and 3.24 are satisfied.

$$0 \leq P_{DG,a} \leq P_{max,DG} \tag{3.23}$$

$$S_{ab} \leq S_{max,ab} \tag{3.24}$$

Where:

- $P_{max,DG}$ is the maximum active power capacity that can be allocated to DG;
- S_{ab} is the apparent power flow along branch ab;
- $S_{max,ab}$ is the maximum apparent power capacity supported by branch ab.

The implementation of the methods and equations presented in this chapter is demonstrated in the following chapter (Chapter 4 - Methodological Procedures).

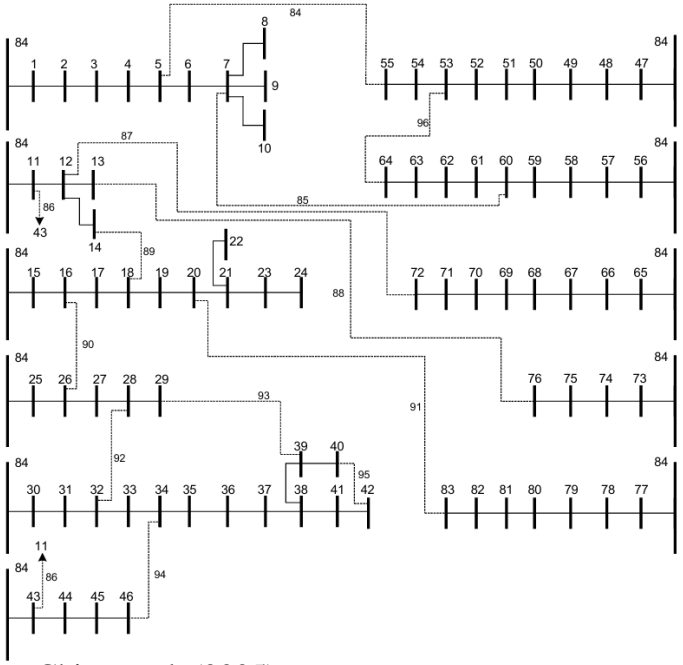
Chapter 4

Methodological Procedures

This section presents the test systems utilized to evaluate the algorithm, the methodology employed to build the algorithm developed for DSR aimed at active power loss reduction and bus voltage profile improvement, and the techniques used for DG allocation at the system buses following reconfiguration.

4.1 Electric Power Systems Tested

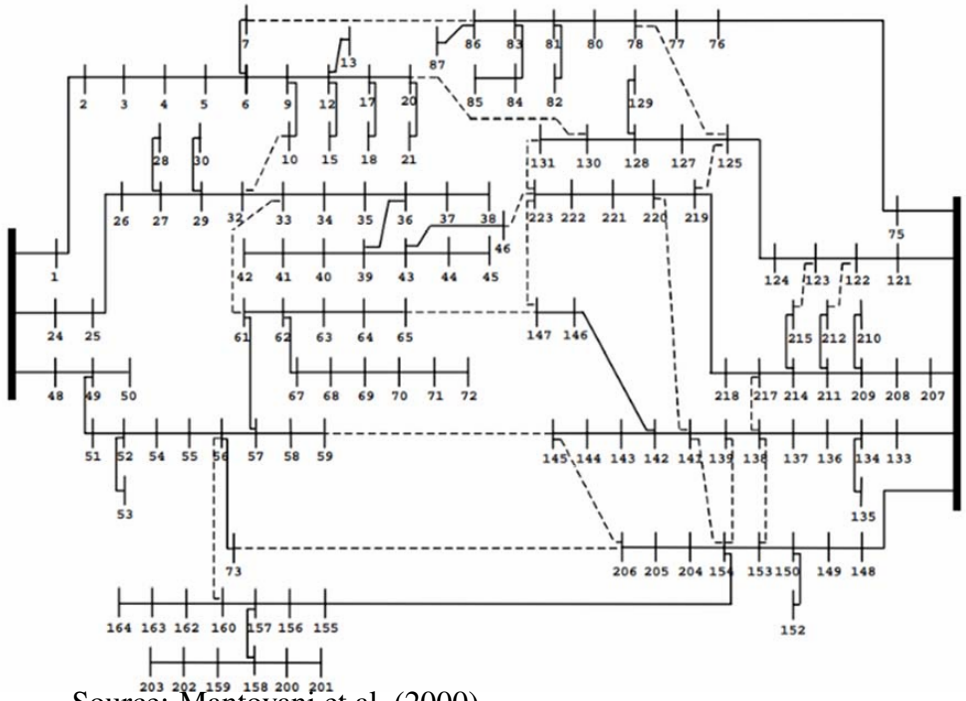
The electrical data of the distribution systems used to test the developed algorithm were obtained from the literature and are characterized by the number of buses: the 84-bus system (Figure 4.1), presented in Chiou, Chang & Su (2005); the 136-bus system (Figure 4.2), presented in Mantovani, Casari & Romero (2000); and the 415-bus system (Figure 4.3), which is a modified version of the 417-bus system presented in Bernal-Agustin (1998).



Source: Chiou et al. (2005).

Figure 4.1: 84-bus System

The 84-bus system (Figure 4.1) features a substation voltage of 1.0 p.u. (11.4 kV base voltage), 83 load buses with total peak active and reactive power demands of 28,351 kW and 20,700 kVAr, respectively, a base power of 100,000 kVA, and 96 branches. Detailed data for the 84-bus system can be found in Appendix A, Section A.1.



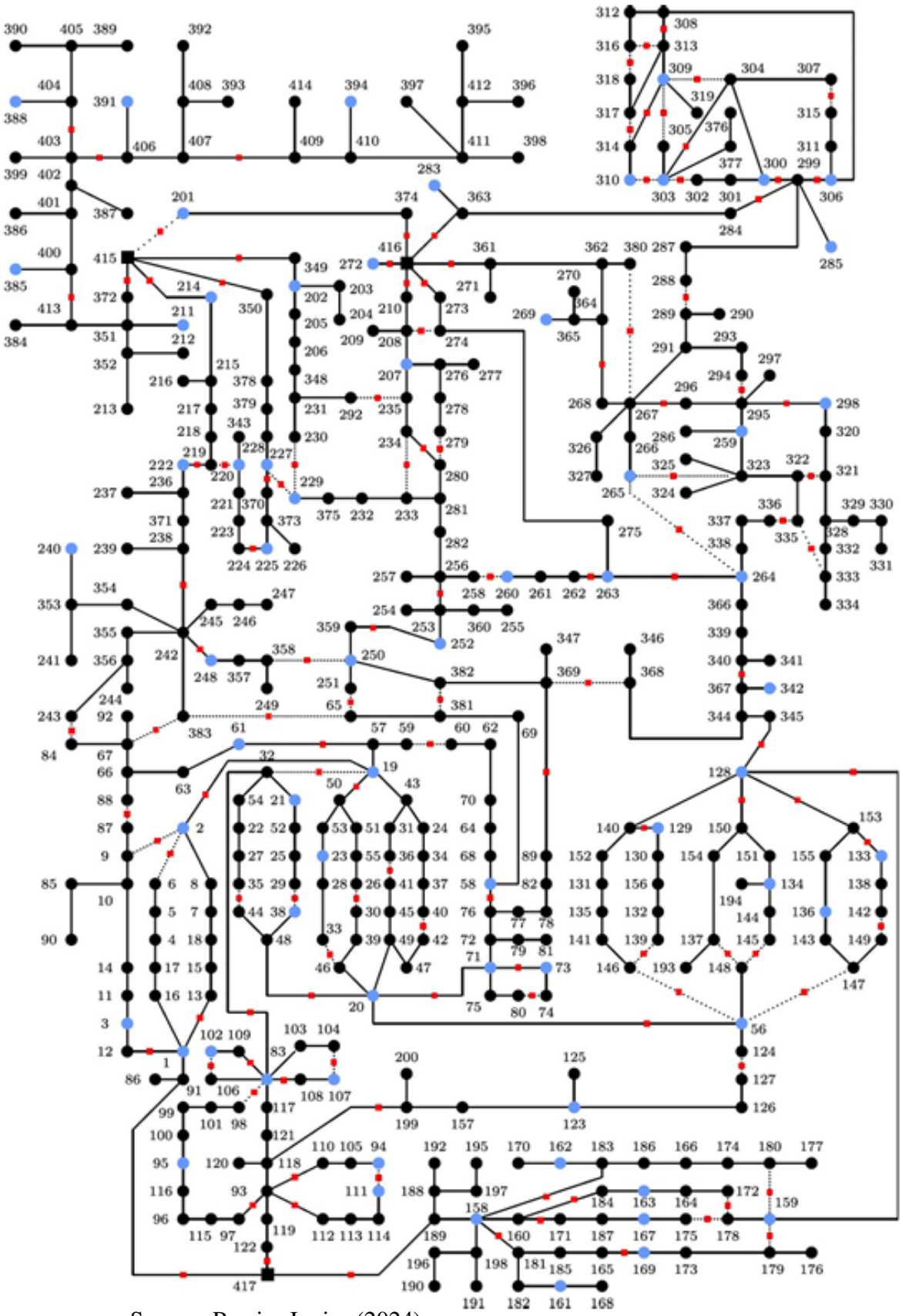
Source: Mantovani et al. (2000).

Figure 4.2: 136-bus System

The 136-bus system (Figure 4.2) features a substation voltage of 1.0 p.u. (13.8 kV base voltage), 135 load buses with total peak active and reactive power demands of 18,313.8090 kW and 7,932.5335 kVAr, respectively, a base power of 100,000 kVA, and 156 branches. Detailed data for the 136-bus system can be found in Appendix A, Section A.2.

The 415-bus system (Figure 4.3) is a modified version of the 417-bus network, featuring a substation voltage of 1.0 p.u. (10.0 kV base voltage), 414 load buses with total peak active and reactive power demands of 27,372.40 kW and 13,237.00 kVAr, respectively, a base power of 100,000 kVA, and 473 branches. Detailed data for the 415-bus system can be found in Appendix A, Section A.3.

These data also specify the minimum and maximum allowable voltage limits for each bus (0.93 p.u. and 1.05 p.u., respectively); the convergence tolerance for the power flow calculation, set to 10^{-8}; and the sending-end and receiving-end buses of each branch, along with their respective resistance, reactance, and apparent power rating.



Source: Pereira Junior (2024).

Figure 4.3: 415-bus System.

4.2 Modified Prim's Algorithm for Generating Radial Solutions

The radial topology was obtained from the meshed system data using the modified Prim's algorithm detailed in Subsection 3.1.2. This approach constructs a maximum spanning tree by iteratively adding the branch with the highest weight to the tree, where this weight is a symbolic value assigned to the branch based on its apparent power flow.

The assignment of branch weights follows an ascending scale: the branch with the lowest apparent power receives the smallest weight (initial value), which was set to 20 for this study (the use of this value is detailed in Section 4.5); for each subsequent branch with a higher apparent power, one unit is added to the preceding weight. Consequently, the branch with the highest apparent power will have the largest weight.

Initially, the modified Prim's algorithm loads two vectors and one matrix: a vector containing the active buses, initially populated only with the substation bus; a vector containing the inactive buses, which includes all system buses except the substation bus; and a matrix containing the data of the original meshed system. After the data are loaded, the algorithm preprocesses the data and creates new vectors to optimize program execution.

The construction of the radial topology starts at the substation and proceeds toward the most distant bus. At each iteration, the connection is established through the available branch with the highest weight that links a bus already connected to the tree (considered an active bus) to a bus not yet connected to the tree (considered an inactive bus).

In the iterative stage of the algorithm, the branch with the highest available weight that connects a bus in the "active bus vector" to a bus in the "inactive bus vector" is identified. The buses connected to this branch are then analyzed to determine whether the branch should be included or discarded. After analyzing all available branches, the branch with the highest weight is selected, activating the inactive bus to which it is connected. This process continues until all buses in the system are active. As output, the algorithm provides a matrix containing the radial solution and another matrix containing the open branches.

4.3 Renumbering of the Generated Radial Topologies

This step aims to facilitate the implementation of the power flow calculation. Renumbering is a method that updates the identification numbers of all buses and branches in the generated radial system, arranging them in ascending order from the substation (renumbered as 1) to the most distant bus.

To execute the renumbering procedure, a copy of the radial solution generated by the modified Prim's algorithm is created. This step is performed to preserve the original topology

data of the generated radial system without altering it.

In this copy, the bus identifiers are modified by multiplying the original bus identifier by a sufficiently large number. In the developed algorithm, a factor of 1000 was used for this purpose. The original identifier of the same bus is then added to the resulting value. This procedure facilitates the comparison between renumbered and non-renumbered buses.

Subsequently, the substation bus is identified and renumbered as 1. This enables the algorithm to determine whether a given bus has been renumbered, as renumbered indices will never exceed their scaled original values. This index correlation is stored in a data structure designated as the "map," allowing the renumbered radial topology to be mapped back to its original identifiers.

The renumbering process originates at the substation bus and expands outward to the most distant bus. To accomplish this, the "sending-end" and "receiving-end" buses of each branch are evaluated. If either of these buses has already been renumbered, the remaining bus is assigned the next sequential integer, following the updated numbering scheme.

Branch renumbering is performed based on the updated bus indices. The new branch identifier is set equal to the receiving-end bus index minus one, likewise following the direction of branches from the substation outward to the branch connected to the most distant bus.

4.4 Power Flow — Backward/Forward Sweep Method

The Backward/Forward Sweep method is an iterative technique used for calculating power flow in distribution systems, enabling the determination of bus voltages and currents, as well as branch currents and power losses.

The process begins with the propagation of voltages, progressing from the substation bus toward the terminal buses. Concurrently, node currents are calculated during this forward stage (Forward sweep). Bus voltages are calculated using Equations (3.6) and (3.7), while bus currents are determined using Equations (3.8) and (3.9).

During the voltage calculation, if any bus exhibits a voltage magnitude outside the permissible limits (between 0.93 p.u. and 1.05 p.u.), the system configuration is deemed infeasible. In such cases, the power flow calculation is aborted, and the candidate radial topology is discarded. Equation (3.4) is used to enforce these voltage magnitude limits.

Following the determination of bus voltages and currents, the subsequent step consists of calculating branch currents along with power losses. This is performed in the reverse direction, from the network extremities (branches connected to the most distant buses) toward the branches connected to the substation (Backward sweep). Branch currents are calculated using Equations (3.10) and (3.11).

The current flowing through each branch is given by the sum of the load current at the node immediately downstream of the branch and the currents of all other branches connected to that same node. During this process, active power losses for each branch are also computed using Equation (3.12).

At the end of each iteration, the total active power losses of the system are calculated using Equation (3.13), followed by the error calculation to verify whether convergence has been achieved.

The iterative power flow solution process terminates when the system converges below a predefined error tolerance, which was set to 10^{-8} in this study. This error metric is evaluated as the difference in total active power losses between the current iteration and the previous iteration

4.5 Radial Solution Diversity Generation — Multi-Start Method

The Multi-Start metaheuristic relies on randomly perturbing the weights assigned to the branches of the initial meshed network. As described in Section 4.2, the weight is defined relative to the apparent power flowing through the branches, starting at 20 and increasing in unit increments of 1 until a weight is assigned to every branch.

The initial value of 20 was established due to its impact on the weight variations at each iteration. Thus, when applying the stochastic variations, changes in the branches with lower apparent power become more controlled and remain closer to the base value, resulting in more contained changes. In contrast, branches with higher power levels exhibit greater dispersion, which expands the algorithm's search space and favors the exploration of new topologies.

For each candidate radial solution generation attempt, the branch weights are randomly perturbed within a predefined margin of $\pm 32\%$. These stochastic variations were executed over 10,000 attempts to construct new radial topologies.

The choice of a $\pm 32\%$ margin for weight variation was determined empirically following tests with several candidate values. While variations below 25% produced minimal diversity among the generated radial solutions, resulting in a high frequency of duplicate topologies, variations exceeding 50% yielded a high proportion of infeasible configurations. Consequently, a value of 32% was selected, as it provided the optimal balance between solution diversity and the yield of feasible candidate topologies.

These perturbations ensure that the modified Prim's algorithm generates diverse radial network configurations from the same original meshed system. To achieve this, the baseline weight of each branch is adjusted by adding a random variation bounded within the range of $\pm 32\%$.

Following the generation of a new radial topology using the modified Prim's algorithm, a

uniqueness check was performed to determine whether the candidate solution was identical to an existing configuration. If determined to be unique, node and branch renumbering was executed, followed by the power flow calculation to ensure that the resulting network configuration satisfies the established voltage limits. This analysis leads to three potential outcomes:

1. The generated radial solution is identical to a previously existing configuration.
2. The generated radial solution is unique (distinct from previously generated configurations) but fails to converge to the predetermined error tolerance due to voltage constraint violations.
3. The generated radial solution is unique and successfully converges to the predetermined error tolerance while satisfying all voltage limits.

To manage the feasible solutions generated by the Multi-Start method, a Best Solution Set (BSS) was defined and populated as follows: if Scenario 1 occurred, the candidate radial topology was recorded as a duplicate and excluded from the BSS; if Scenario 2 occurred, the radial configuration was classified as infeasible and discarded; and if Scenario 3 occurred, the solution produced by the Multi-Start approach was categorized as feasible and added to the BSS.

Upon completing all 10,000 generation attempts for new radial solutions, the candidate topologies stored in the BSS were sorted in ascending order according to their active power losses, positioning the solution with the lowest loss generated by the Multi-Start method at the first index. The BSS subsequently served as the input dataset for applying the Maximum/Minimum Distance criterion.

4.6 Generating Quality Solutions — Maximum/Minimum Distance Method

The Maximum/Minimum Distance method operates as a scatter search algorithm. The objective of this method is to generate a reduced subset of solutions relative to the initial BSS obtained from the Multi-Start approach, while maintaining both the quality of the top-performing solutions found and the structural diversity provided by the Multi-Start phase.

The method begins by constructing an auxiliary set designated as the Quality Solution Set (QSS). Half of the QSS is populated with the top-performing solutions obtained from the Multi-Start execution, stored in the BSS, which correspond to the radial topologies exhibiting the lowest power losses. In this study, the QSS was dimensioned to hold 20 solutions; initially, it was composed of the 10 best feasible radial configurations extracted from the BSS. These selected configurations were subsequently removed from the BSS to prevent duplicate selection.

The second half of the QSS was populated through an iterative process in which solutions exhibiting the greatest possible difference from the radial solutions already included in the QSS are selected. To perform this selection, the set of open branches of the identified radial solutions is used.

First, a comparison was performed to evaluate the difference between the open branches of the solutions in the QSS and those in the BSS. Each BSS solution was compared against all solutions in the QSS to select those with the highest number of differing open branches, which were then stored in a list named "maximum".

Subsequently, the minimum value in the "maximum" list was selected to identify which radial solution from the BSS would be included in the QSS. This solution was also removed from the BSS to prevent duplication. This process was repeated until the QSS reached the predefined number of solutions. The QSS then served as the initial population for the GA.

4.7 Implementation of the Genetic Algorithm

The Genetic Algorithm seeks to find new ways of connecting the buses in the distribution system by combining two feasible radial topologies, referred to as "parent 1" and "parent 2", into a new feasible radial topology, called "offspring". This combination is performed by altering the chromosomes (connected branches) of the "parents" to attempt to generate new "offspring".

The initial population of 20 individuals, originating from the QSS, was combined pairwise among all individuals in this population, generating 380 possible combinations of offspring.

The process begins with the selection of two individuals (radial solutions) from the QSS to serve as "parents". Then, a random crossover point was selected within the structure of the solution chosen as the "parent 1". The new radial topology ("offspring 1") inherits all branches (chromosomes) from the "parent 1" up to that position. To complete the structure and ensure that the network has $N_{\text{buses}} - 1$ branches, the algorithm retrieves the remaining branches from the "parent 2".

If the branches (chromosomes) from the "parent 2" are not sufficient to guarantee a radial topology connecting all buses, the algorithm utilizes the open branches (tie switches) from the "parent 2" itself to repair the topology and prevent isolated buses.

This process is repeated, allowing a new "offspring 2" to inherit all branches (chromosomes) from the "parent 2" up to the randomly selected position, which are then completed by the branches from the "parent 1".

At the end of this process, the radial solution initially selected as the "parent 1" is retained, and a new individual is selected as the "parent 2". The process is repeated again for these new "parents" to create new offspring.

After the creation of a new "offspring", the generated radial topology was subjected to a power flow calculation to verify whether all of its buses fall within the voltage limits, which can result in three distinct possibilities, just as in the Multi-start method:

1. The generated radial solution is identical to an existing solution.
2. The generated radial solution is different from an existing solution and fails to converge within the predetermined error tolerance due to voltage limit violations.
3. The generated radial solution is different from an existing solution and converges within the predetermined error tolerance while respecting all voltage limits.

To organize the solutions generated by the GA, similarly to the Multi-start method, a set named Genetic Algorithm Feasible Solutions (GAFS) was created to store all generated feasible radial solutions, sorted in ascending order from the lowest active power loss found in the power flow up to the highest loss. This set was populated as follows: if Situation 1 was verified, the "offspring" was counted as feasible but considered a duplicate and not added to the population generated by the GA; if Situation 2 occurred, the created "offspring" was counted as infeasible and discarded; and if Situation 3 occurred, the "offspring" was classified as feasible and added to the population created by the GA. The GAFS set served as input for the VND method.

4.8 Implementation of Variable Neighborhood Descent

The VND algorithm seeks to perform local refinement on the solutions found by the Genetic Algorithm. The objective is to 'fine-tune' each received radial topology by testing minor modifications to its branches to verify whether it is possible to further reduce power losses.

This process begins as follows: the algorithm selects a radial solution (originating from the GA) and attempts to create a 'neighbor'. To create this neighbor, the VND closes a branch that was previously open. From the moment this new branch is connected, the network ceases to be radial and forms a loop (a closed power path).

To restore the radiality condition, the algorithm identifies all branches that make up this loop and systematically opens one of the other branches belonging to the same loop (excluding the one that was just closed). This yields a new radial topology, very similar to the original one, but with an altered connection.

After creating this new 'neighbor', the algorithm performs a power flow calculation aimed at validating two criteria:

- Stability: verify whether all buses remain within the allowable voltage limits;

- Improvement: verify whether the power loss of this new neighbor is lower than the loss of the solution it is attempting to improve.

If the neighbor exhibits a lower power loss and stable voltages, it becomes the new best solution. At this point, the algorithm discards previous progress and restarts the neighborhood search from this new configuration, attempting to exhaust all possibilities for improvement.

The process terminates when the algorithm tests all available open branches and fails to find any exchange that reduces power losses. To store the solutions generated by the VND, a set named Variable Neighborhood Descent Feasible Solutions (VNDFS) was created. This set served as the input for the DG allocation methods.

4.9 Distributed Generation Allocation

Two strategies were used for DG allocation: one to allocate a fixed number of DG, for this work, allocation scenarios for 1, 2, and 3 DG were determined, and another to allocate as many DG as possible until power losses could no longer be reduced.

4.9.1 Allocation of 1, 2, and 3 DG

The allocation of 1, 2, and 3 DG aims to identify the optimal locations in the network for inserting small generators (such as solar panels), with the objective of reducing system losses and maintaining voltage stability. The method operates as a localized reinforcement process for the solutions that have already undergone the VND stage.

The process operates as follows: the algorithm analyzes a radial topology and identifies the bus with the lowest voltage, determining that it is the optimal position for placing a DG.

The DG insertion is performed through an incremental power adjustment:

- A generator was created at the selected bus with zero active power;
- The algorithm incrementally increases the power of this generator (in small steps);
- At each step increase, a power flow calculation is executed to verify whether the network losses are decreasing;
- Termination Criterion: If an increase in power causes the power losses to rise instead of drop, or if the maximum capacity limit of the generator is reached, the algorithm stops increasing the power and fixes ("locks") the generator at that optimal value.

By repeating this cycle (identifying the bus with the lowest voltage and installing a new

DG) for a set number of iterations,specifically 1, 2, and 3 or until all network buses have voltages near 1.0 p.u..

Finally, each solution is re-evaluated and stored in an ordered list in ascending sequence: from the radial topology exhibiting the lowest total loss to the one with the highest loss. Thus, in addition to obtaining a loss-reducing topology, the method ensures that the generators are placed at the locations where they achieve the maximum energy savings.

4.9.2 Maximum DG Allocation

The maximum DG allocation method employs a Binary Search to optimize the systems by placing generators at the most critical points in the network. Beyond determining DG locations, it utilizes a technique to define the amount of active power each generator must inject to minimize power losses as much as possible.

The process operates as follows: an examination of the network is performed to locate the bus with the lowest voltage (the node with the lowest voltage magnitude), designating this bus as the installation site for a new DG.

The main distinction of this version lies in the Binary Search for optimal power, in which an interval between zero and the maximum allowable power is defined, testing the midpoint of this interval and evaluating the behavior of the network power losses:

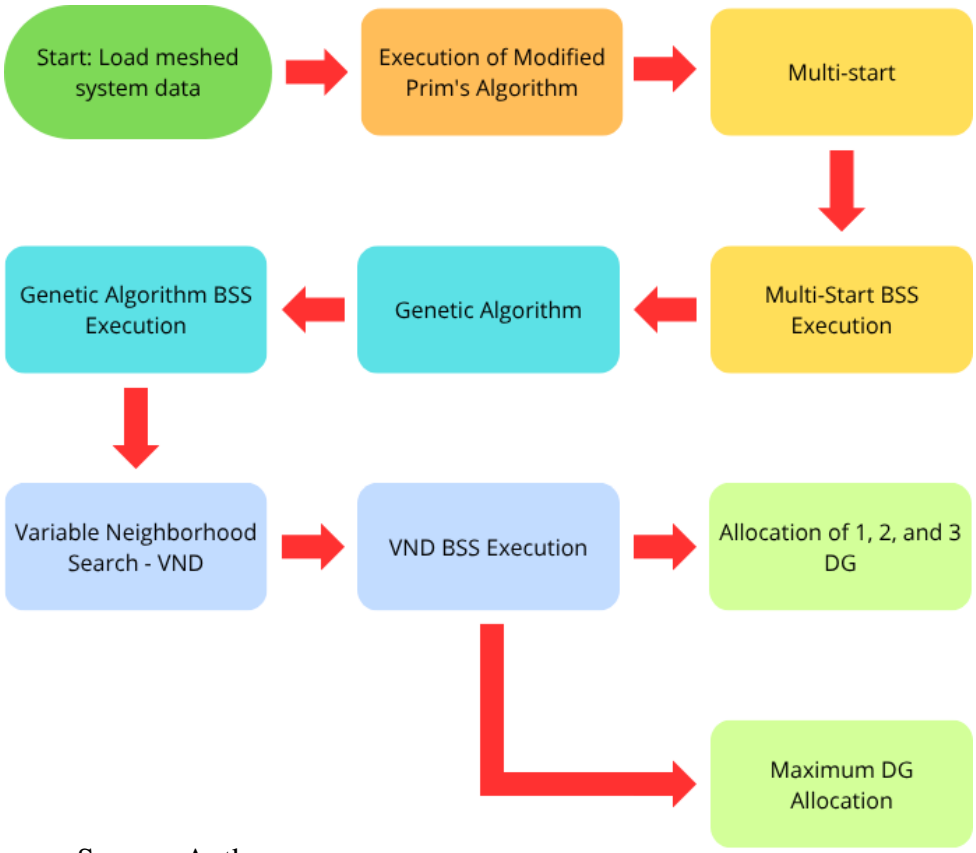
- If the loss decreases, the method infers that the optimal power lies in the upper half;
- If the loss increases or the power flow fails to converge, it searches in the lower half;
- Refinement: this interval-halving test is repeated n times, specifically 30 times in the developed algorithm.

After fixing the optimal power for that generator, the algorithm validates whether a real benefit was achieved. If, even with the binary search, the new power loss is not lower than the previous one, the method removes the DG, considering that it provided no improvement to the system.

At the end of all iterations, the solutions are stored in a list and organized in an ascending *ranking*, from the lowest active power loss found to the highest. The final result is a doubly optimized system: first in topology (via GA and VND) and then in local power support (via maximum DG allocation).

4.9.3 Block Diagram for the Proposed Methodology

Fig. 4.4 illustrates the block diagram outlining the steps performed by the proposed algorithm to achieve the optimized solutions, indicating the execution sequence of each proposed method.



Source: Author.

Figure 4.4: Block diagram illustrating the steps for the proposed methodology.

The algorithm begins by loading the meshed system data from three files: the first containing the bus active and reactive power demands, the second containing the branch parameters (sending and receiving buses, impedance, and apparent power rating), and the third specifying the general system settings (substation bus, nominal voltage, base voltage and base power, convergence tolerance, and the acceptable minimum and maximum bus voltage limits). After loading the data, the algorithm prepares it by arranging it into matrices—one for the bus demands and another for the branches of the meshed network, appending the branch index and branch weight to the latter.

Following pre-processing, the modified Prim's algorithm is executed for the first time using the original branch weights, serving as a baseline for comparison. Subsequently, the Multi-start metaheuristic is applied to generate an initial set of feasible and diverse radial topologies. Scatter search is then applied for the first time to this set using the Maximum/Minimum Distance method to reduce the number of candidate solutions without compromising population

diversity, establishing the Quality Solution Set (QSS) of the Multi-Start algorithm

The next method applied is the Genetic Algorithm (GA) to explore new regions of the search space through the crossover and reproduction of individuals from the QSS obtained from the Multi-start metaheuristic. As in the previous phase, the resulting set of solutions from the GA is subjected once again to scatter search (Maximum/Minimum Distance) in order to select a reduced group that preserves both topological diversity and solution quality (Genetic Algorithm Quality Solution Set - GA QSS)

Finally, the Variable Neighborhood Descent (VND) algorithm is applied to the solutions from the GA QSS. This stage performs small perturbations on the radial structures by manipulating open branches, systematically exploring the neighborhood of promising candidate solutions. Upon completion of the VND method, its set of feasible solutions is filtered once again via scatter search using the Maximum/Minimum Distance method, analogous to the Multi-start and GA phases, thereby reducing the number of solutions while maintaining diversity and quality.

Following the reconfiguration stage (Multi-start, GA, and VND, along with their respective scatter search phases), the algorithm transitions to the DG allocation stage, where two procedures are employed to integrate distributed generators into the distribution network: the first performs the placement of a fixed number of DG, while the second executes maximum DG penetration to achieve the greatest possible reduction in active power losses.

Chapter 5

Results and Discussions

This chapter presents the results of the tests conducted on the 84-, 136-, and 415-bus systems presented in Section 4.1, along with a discussion of the obtained results in comparison with those available in the literature.

The source code, input datasets, and best obtained results are available via Mendeley Data DOI: 10.17632/mp5nntd36h.1 (Freiman, 2026).

The results were obtained using an Acer Nitro ANV15-51 laptop equipped with an Intel(R) Core(TM) i9-13900H 13th Gen processor (2.60 GHz), an NVIDIA GeForce RTX 4060 Laptop GPU (8 GB) paired with integrated Intel(R) UHD Graphics (128 MB), 500 GB of storage, and running the Windows 11 Pro operating system.

5.1 Results

This section presents the results obtained by the proposed algorithm for electrical distribution network reconfiguration aimed at reducing line active power losses and improving the bus voltage profile across the tested systems. The results found for each system are divided into three subsections:

1. Methods performing network reconfiguration only, without DG allocation;
2. Distributed Generation (DG) allocation, placing 1, 2, and 3 generators;
3. Maximum DG allocation, integrating the maximum possible number of generators to minimize power losses.

For all tested systems, the algorithm was executed for 10,000 (ten thousand) radial topology generation attempts in the Multi-start method with a weight variation of $\pm 32\%$, as this weight range yielded the best results.

A BSS was created with the feasible radial solutions generated by the Multi-start method, arranged in ascending order.

A QSS comprising 20 solutions was then created from the candidate topologies stored in the MSS to serve as the initial population for the GA.

The GA generated a total of 380 offspring across all conducted tests. The feasible, non-redundant offspring were compiled to form the set designated as GAFS. Subsequently, the GAFS underwent the scatter search filtering process (using the Maximum/Minimum Distance method), yielding the GA Quality Solution Set (GA QSS), which likewise comprised 20 solutions.

In the VND phase, the QSS obtained from the GA was used as input. Additionally, the set designated as VNDFS was created to store the feasible, non-redundant solutions generated by the VND.

The results obtained by the proposed algorithm for each test system are presented below.

5.1.1 84-Bus System

The 84-bus system consists of 83 load buses, in addition to the substation buses, which are modeled as a single slack bus,and 96 branches, yielding approximately 1.5×10^6 radial candidate topologies (Chiou, Chang & Su, 1990). To obtain the presented results, the proposed algorithm required an execution time of 216.759 seconds (approximately 3 minutes and 36 seconds).

Method Without DG Allocation

Table 5.1 illustrates the breakdown for the 84-bus system in terms of feasible solutions that satisfied the problem's voltage limit constraints, infeasible solutions that violated the voltage limit constraints, and duplicate solutions, which are identified as identical to previously found topologies and recorded as repeated.

Table 5.1: Number of results obtained for the 84-bus system.

Method	*Feasible*	*Infeasible*	*Repeated*	*Total Solutions*
First Modified Prim	1	-	-	1
Multi-start	9462	64	474	10000
GA	57	315	8	380
VND	303	0	274	577

Source: Author.

Table 5.2 illustrates the results achieved for the initial Modified Prim algorithm (initial

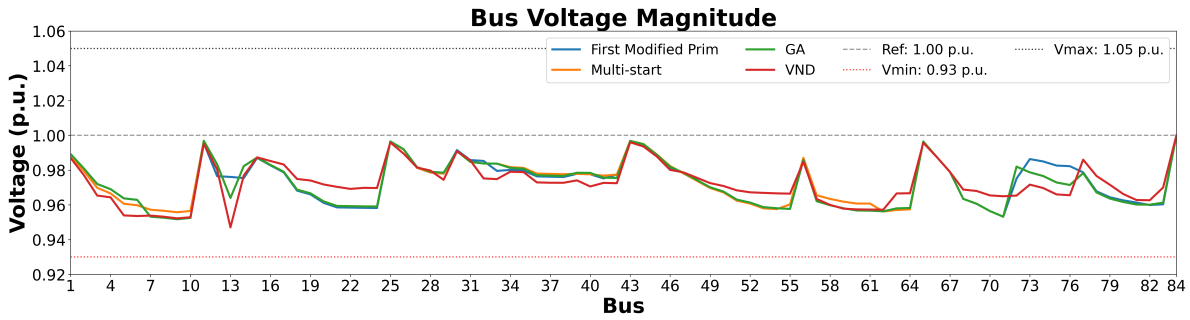
configuration) along with the best results obtained by the Multi-start, GA, and VND methods, compared against several benchmark results reported in the literature.

Table 5.2: Results achieved for the 84-bus system.

Method	*Minimum Voltage* (p.u.)	*Losses* (kW)	*Reduction Relative to First Modified Prim* (%)	*Time* (s)
First Modified Prim	0.9518	471.72	-	0.002
Multi-start	0.9532	469.88	0.39	28.073
GA	0.9518	470.21	0.32	0.212
VND	0.9497	470.21	0.32	1.748
Possagnolo (2015)	0.9517	469.88	-	0.006
Pereira Junior (2024)	-	469.72	-	-
Chiou et al. (1990)	0.9716	466.10	-	-

Source: Author.

Figure 5.1 illustrates the bus voltage profile for the 84-bus system following electrical Distribution System Reconfiguration (DSR) without DG allocation (depicting values for the initial Modified Prim algorithm alongside the best results from the Multi-start, GA, and VND methods).



Source: Author.

Figure 5.1: Voltage profile for the 84-bus system.

Allocation of 1, 2, and 3 DG

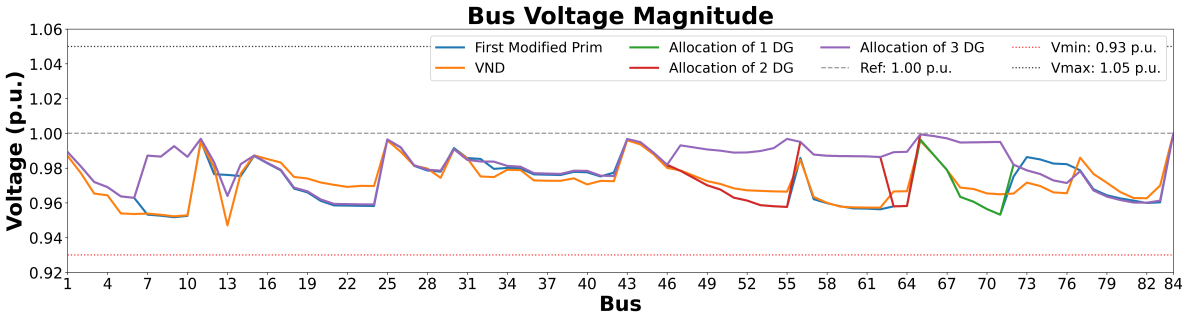
For comparison of the results, Table 5.3 illustrates the initial result and the best result achieved with reconfiguration (using VND) alongside the methods for 1, 2, and 3 DG allocation.

Table 5.3: Results for the 84-bus system with and without DG allocation.

Method	*Minimum Voltage* (p.u.)	*Losses* (kW)	*Buses with DG*	*Reduction relative to PRIM* (%)	*Time* (s)
First Modified Prim	0.9518	471.72	-	-	0.002
VND	0.9497	470.21	-	0.32	1.748
1 DG	0.9532	419.83	9	11.00	14.461
2 DG	0.9577	361.75	70; 9	23.31	18.424
3 DG	0.9591	323.15	9; 71; 55	31.50	23.353

Source: Author.

Figure 5.2 illustrates the voltage profile for the 84-bus system, comparing the initial result, the best result achieved solely through reconfiguration (using VND), and the outcomes from the method for 1, 2, and 3 DG allocation following DSR.



Source: Author.

Figure 5.2: Comparison of voltage profile without DG and with allocation of up to 3 DG.

Maximum DG Allocation

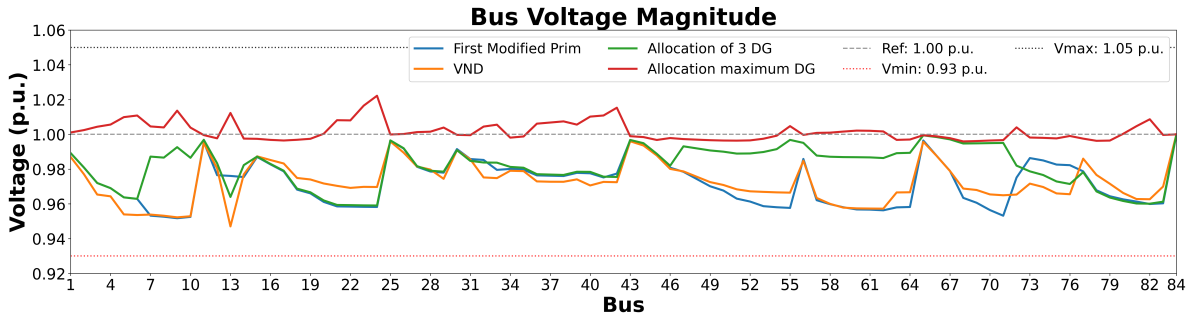
Table 5.4 illustrates the initial result and the best result achieved without DG allocation (using VND), the method for 3 DG allocation, and the method with maximum DG allocation aimed at minimizing losses.

Table 5.4: Results for the 84-bus system with maximum DG allocation.

Method	*Minimum Voltage* (p.u.)	*Losses* (kW)	*Buses with DG*	*Reduction relative to PRIM* (%)	*Time* (s)
First Modified Prim	0.9518	471.72	-	-	0.002
VND	0.9497	470.21	-	0.32	1.748
3 DG	0.9591	323.15	9; 71; 55	31.45	23.353
Maximum DG (qty=16)	0.9959	161.01	81; 72; 62; 9; 29; 6; 80; 39; 14; 24; 76; 19; 34; 31; 55; 18	65.87	130.022

Source: Author.

The voltage profile for the initial result and the best results achieved with reconfiguration (VND), 3 DG allocation, and maximum DG allocation is illustrated in Figure 5.3.



Source: Author.

Figure 5.3: Comparison of the voltage profile for the 84-bus system without DG (using VND), with 3 DG allocation, and with maximum DG allocation.

5.1.2 136-Bus System

The 136-bus system comprises 135 load buses, in addition to the substation buses which are considered as a single bus, and 156 branches, allowing the creation of approximately 10^9 radial solutions (Mantovani et al., 2000). To obtain the presented results, the algorithm required 205.57 seconds (approximately 3 min and 25 s).

Method Without DG Allocation

Table 5.5 illustrates the number of feasible solutions, infeasible solutions, and repeated solutions for the 136-bus system.

Table 5.5: Number of results obtained for the 136-bus system.

Method	*Feasible*	*Infeasible*	*Repeated*	*Total Solutions*
First Modified Prim	1	-	-	1
Multi-start	6292	16	3692	10000
GA	69	302	9	380
VND	522	0	159	681

Source: Author.

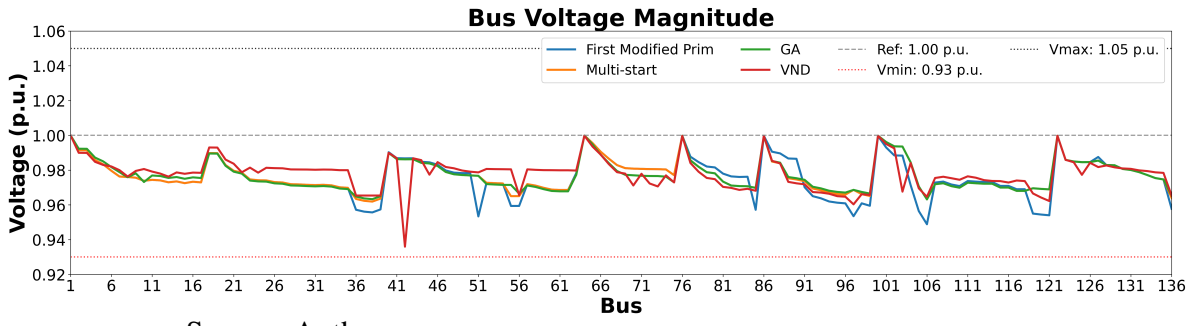
Table 5.6 illustrates the results obtained for the first Prim algorithm and the best results achieved with the Multi-start, GA, and VND methods in comparison with selected results found in the literature.

Table 5.6: Results achieved for the 136-bus system.

Method	*Minimum Voltage* (p.u.)	*Losses* (kW)	*Reduction Relative to PRIM* (%)	*Time* (s)
First Modified Prim	0.9488	293.00	-	0.003
Multi-start	0.9619	285.23	2.65	36.088
GA	0.9631	284.37	2.95	0.357
VND	0.9359	284.37	2.95	4.154
Possagnolo (2015)	0.9426	280.19	-	0.012
Pereira Junior (2024)	-	280.37	-	-
Mantovani et al. (2000)	-	286.18	-	-

Source: Author.

Figure 5.4 illustrates the voltage profile for the 136-bus system following DSR using the methods without DG allocation (values for the first modified Prim and best results for Multi-start, GA, and VND).



Source: Author.

Figure 5.4: Voltage profile for the 136-bus system.

Allocation of 1, 2, and 3 DG

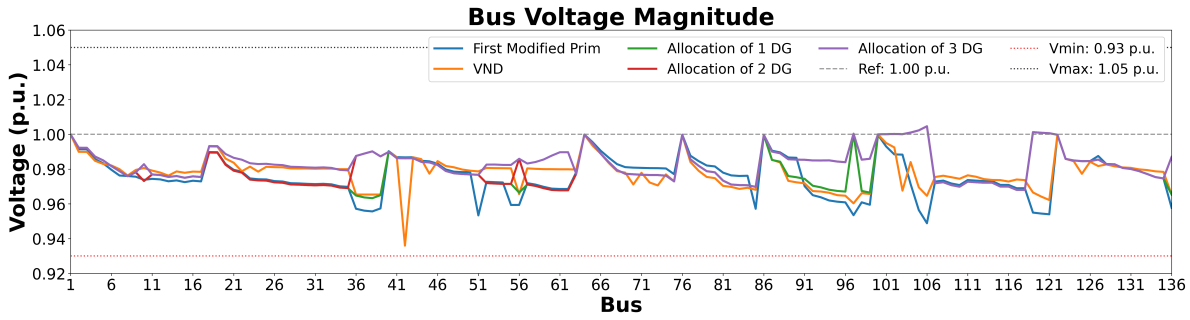
For comparison of the results, Table 5.7 illustrates the initial result and best result achieved with reconfiguration (using VND) and with allocation of 1, 2, and 3 DG after DSR.

Table 5.7: Results for the 136-bus system with and without DG allocation.

Method	*Minimum Voltage* (p.u.)	*Losses* (kW)	*Buses with DG*	*Reduction relative to PRIM* (%)	*Time* (s)
First Modified Prim	0.9488	293.00	-	-	0.003
VND	0.9359	284.37	-	2.95	4.154
1 DG	0.9633	222.06	106	24.21	19.892
2 DG	0.9678	197.96	106; 61	32.44	19.892
3 DG	0.9680	173.30	134; 17; 107	40.85	23.972

Source: Author.

Figure 5.5 illustrates the voltage profile for the 136-bus system, comparing the initial result and the best result achieved with reconfiguration (VND) and with the allocation of 1, 2, and 3 DG after DSR.



Source: Author.

Figure 5.5: Voltage profile without DG and with allocation of up to 3 DG in the 136-bus system.

Maximum DG Allocation

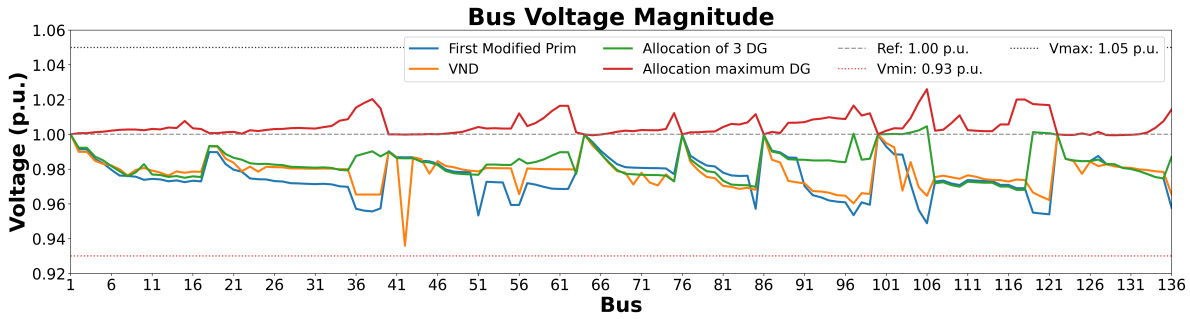
Table 5.8 illustrates the initial result and the best results achieved with reconfiguration (VND), 3 DG allocation, and the method with maximum DG allocation aimed at minimizing losses.

Table 5.8: Results for the 136-bus system with maximum DG allocation.

Method	*Minimum Voltage* (p.u.)	*Losses* (kW)	*Buses with DG*	*Reduction relative to PRIM* (%)	*Time* (s)
First Modified Prim	0.9488	293.00	-	-	0.003
VND	0.9359	284.37	-	2.95	4.154
3 DG	0.9680	173.30	134; 17; 107	40.85	23.972
Maximum DG (qty=19)	0.9995	101.77	106; 117; 61; 85; 75; 135; 15; 35; 90; 38; 51; 13; 125; 88; 63 127; 6; 45; 129	65.27	143.391

Source: Author.

The voltage profile for the best results achieved with the method without DG allocation (VND), 3 DG allocation, and the maximum DG allocation method is illustrated in Figure 5.6.



Source: Author.

Figure 5.6: Comparison of the voltage profile for the 136-bus system without DG (using VND), with 3 DG allocation, and with maximum DG allocation.

5.1.3 415-Bus System

The 415-bus system (a modified version of the 417-bus system) consists of 414 load buses, in addition to the substation buses which are treated as a single bus, and 473 branches, allowing the formation of radial configurations on the order of 10^{20} (Bernal-Agustin, 1998). To achieve the presented results, the algorithm required 636.854 seconds (approximately 10 min and 36 s).

Method Without DG Allocation

Table 5.9 illustrates the number of feasible, infeasible, and duplicate solutions for the 415-bus system.

Table 5.9: Number of results obtained for the 415-bus system.

Method	*Feasible*	*Infeasible*	*Duplicates*	*Total Solutions*
First Modified Prim	1	-	-	1
Multi-start	4423	0	5577	10000
GA	200	165	15	380
VND	5587	0	59	5646

Source: Author.

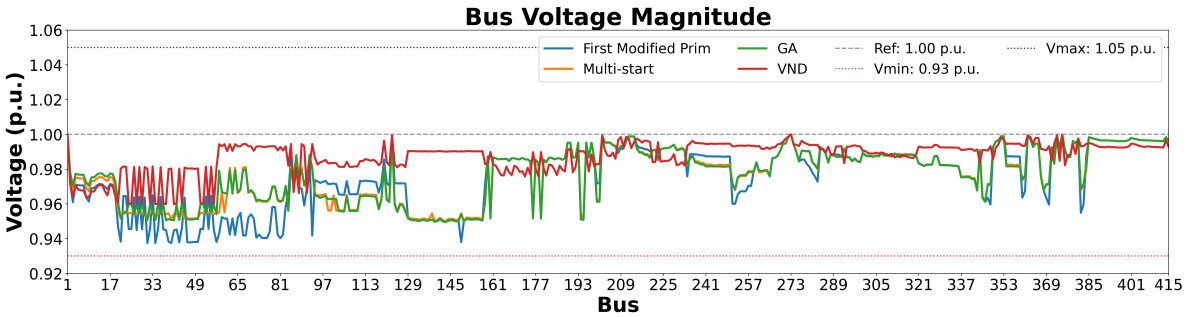
Table 5.10 illustrates the results achieved with the first Prim algorithm and the best results obtained with the Multi-start, GA, and VND methods in comparison with selected results found in the literature.

Table 5.10: Results achieved for the 415-bus system.

Method	*Minimum Voltage* (p.u.)	*Losses* (kW)	*Reduction Relative to PRIM* (%)	*Time* (s)
First Modified Prim	0.9374	662.51	-	0.009
Multi-start	0.9498	605.29	8.64	107.792
GA	0.9495	598.27	9.70	2.931
VND	0.9598	578.58	12.67	163.423
Possagnolo (2015)	0.9462	581.55	-	270.293
Pereira Junior (2024)	-	592.68	-	-
Bernal-Agustin (1998)	-	708.84	-	-

Source: Author.

Figure 5.7 illustrates the voltage profile of the 415-bus system after DSR for the methods without DG allocation (first modified Prim, Multi-start, GA, and VND).



Source: Author.

Figure 5.7: Voltage profile for the 415-bus system.

Allocation of 1, 2, and 3 DG

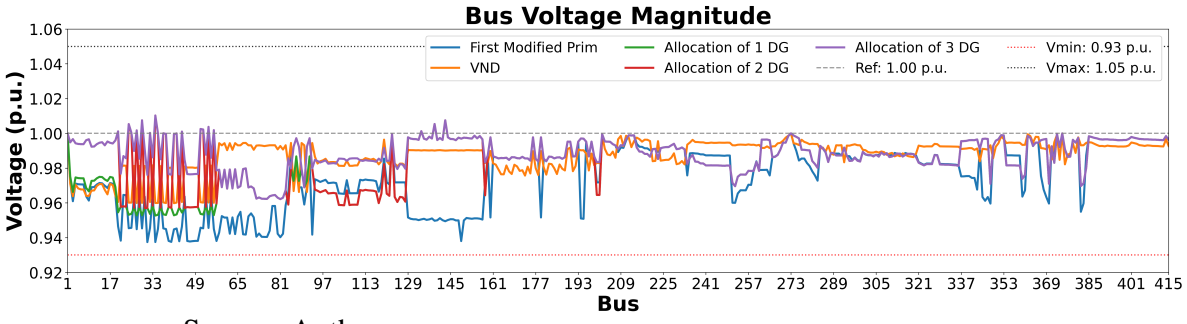
For comparison of the results, Table 5.11 illustrates the initial result and the best results achieved with the reconfiguration methods (VND) and with the method for 1, 2, and 3 DG allocation.

Table 5.11: Results for the 415-bus system with and without DG allocation.

Method	*Minimum Voltage* (p.u.)	*Losses* (kW)	*Buses with DG*	*Reduction relative to PRIM* (%)	*Time* (s)
First Modified Prim	0.9374	662.51	-	-	0.009
VND	0.9598	578.58	-	12.67	163.423
1 DG	0.9527	476.63	143	28.06	47.461
2 DG	0.9570	402.32	38; 143	39.27	59.870
3 DG	0.9621	298.15	38; 150; 27	55.00	73.384

Source: Author.

Figure 5.8 illustrates the voltage profile for the 415-bus system, comparing the initial result, the best result achieved with reconfiguration (VND), and the method for 1, 2, and 3 DG allocation after DSR.



Source: Author.

Figure 5.8: Voltage profile without DG and with allocation of up to 3 DG in the 415-bus system.

Maximum DG Allocation

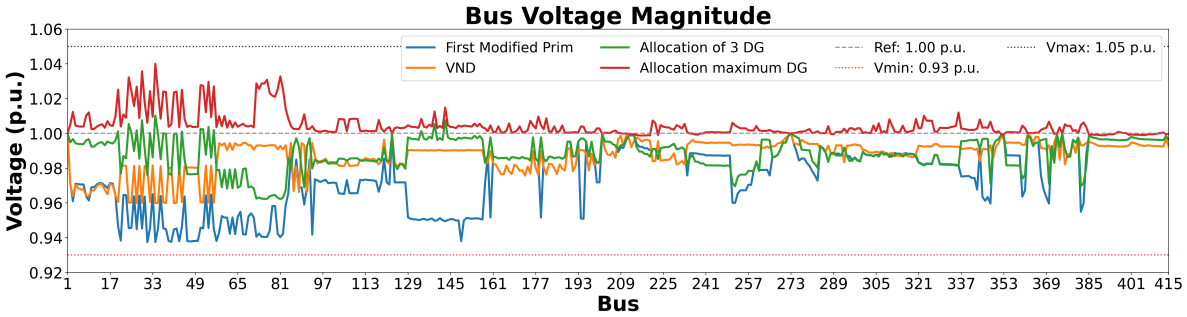
Table 5.12 illustrates the initial result, the best result achieved with reconfiguration methods (VND), the 3 DG allocation, and the method with maximum DG allocation aimed at minimizing power losses.

Table 5.12: Results for the 415-bus system without DG, with 3 DG, and with maximum DG allocation.

Method	*Minimum Voltage* (p.u.)	*Losses* (kW)	*Buses with DG*	*Reduction relative to PRIM* (%)	*Time* (s)
First Modified Prim	0.9374	662.51	-	-	0.009
VND	0.9598	578.58	-	12.67	163.423
3 DG	0.9621	298.15	38; 150; 27	55.00	73.384
Maximum DG (qty=20)	0.9987	220.25	38; 150; 27; 336; 64; 178; 17; 60; 99; 377; 344; 337; 279; 89; 231; 188; 335; 396; 319; 202	66.76	255.308

Source: Author.

The voltage profile for the initial result, the best result achieved with reconfiguration (VND method), the 3 DG allocation, and the maximum DG allocation aimed at minimizing losses is illustrated in Figure 5.9.



Source: Author.

Figure 5.9: Voltage profile comparison for the 415-bus system without DG (using VND), with 3 DG allocation, and with maximum DG.

5.2 Discussions

This section analyzes the results obtained for the 84-, 136-, and 415-bus systems, discussing the performance of each stage of the proposed methodology and comparing the results with the works of Possagnolo (2015) and Pereira Junior (2024), which constitute the closest references in terms of test systems and methodological approach.

5.2.1 84-Bus System

This subsection presents the discussion of the results obtained for the reconfiguration of the 84-bus system with and without DG allocation.

Reconfiguration Without DG Allocation

The results without DG allocation for the 84-bus system are presented in Table 5.2. The sequence first modified Prim → Multi-start → GA → VND produced progressive reductions in losses: from 471.72 kW (first modified Prim) to 469.86 kW (Multi-start), and 470.21 kW (GA and VND). Relative to the initial value (first modified Prim), the Multi-start method showed a reduction of 0.36%, while the GA and VND presented a reduction of 0.08%.

The GA and VND converged to the same loss value, which indicates that the solution provided by the GA to the VND already corresponded to a local optimum within the neighborhoods explored by the VND, leaving no margin for further improvement via local search in this system.

A factor that warrants attention is the minimum voltage obtained by the VND: 0.9497 p.u., which is lower than that obtained by the GA (0.9518 p.u.). Although the losses are identical, the topology found by the VND resulted in a slightly worse voltage profile. This stems from the fact that the objective function considers exclusively active power loss minimization, without an explicit constraint on minimum voltage. Distinct topologies can yield equivalent losses with different voltage distributions.

In comparison with the literature, Possagnolo (2015) obtained 469.88 kW with a minimum voltage of 0.9517 p.u., and Pereira Junior (2024) obtained 469.72 kW. The result of the proposed VND (470.21 kW) yielded a slightly lower performance than that of Possagnolo (2015), with a difference of 0.33 kW (0.07%), and 0.49 kW (0.10%) above that of Pereira Junior (2024). These differences are within the expected variability of metaheuristic algorithms. Chiou et al. (1990) reported 466.10 kW with a minimum voltage of 0.9716 p.u., a superior performance result that can be attributed to differences in the power flow modeling adopted in that work.

DG Allocation

The allocation of DG produced increasing and consistent loss reductions with the higher number of units: 11.00% with 1 DG (419.83 kW), 23.31% with 2 DG (361.75 kW), and 31.50% with 3 DG (323.15 kW), all relative to the initial result without DG (471.72 kW). The marginal

gain of each additional DG is decreasing: the first DG reduces losses by 51.89 kW, the second by 58.08 kW, and the third by 38.60 kW. This behavior is expected, as the initial units are allocated at buses with the highest impact on loss reduction, leaving lower-return locations for subsequent units.

With the maximum allocation of 16 DG, losses were reduced to 161.01 kW, representing a reduction of 65.87% (310.71 kW) relative to the initial result without DG. The minimum voltage improved from 0.9518 p.u. to 0.9959 p.u., an increase of 0.0441 p.u. The distribution of the DG across buses 81, 72, 62, 9, 29, 6, 80, 39, 14, 24, 76, 19, 34, 31, 55, and 18 indicates that the allocation algorithm dispersed the units along the feeder, which is consistent with the objective of loss reduction through distributed active power injection.

The incremental gain between 3 DG and the maximum of 16 DG is 162.14 kW (50.18%), achieved with the addition of 13 units. This result points to a significant diminishing return. From a planning perspective, this data is useful for evaluating the economic viability of installing additional units beyond the first three.

5.2.2 136-Bus System

This subsection presents the discussion of the results obtained for the reconfiguration of the 136-bus system with and without DG allocation.

Reconfiguration Without DG Allocation

In the 136-bus system, the methodological progression for the results without DG allocation resulted in the following losses: 293.00 kW (first modified Prim), 285.23 kW (Multi-start), 284.37 kW (GA), and 284.37 kW (VND). As observed in the 84-bus system, the GA and VND converged to the same value, indicating that the VND did not find any better solution starting from the solutions provided by the GA. However, the reduction from first modified Prim to Multi-start was significant (7.77 kW, 2.65%), demonstrating that the diversification of initial solutions generated by Multi-start has a relevant impact on this system, whereas the GA and VND presented a reduction of 2.95%. Meanwhile, the difference between Multi-start and GA was small (0.86 kW), indicating that the GA produced a marginal refinement relative to the solutions from Multi-start.

In comparison with the literature, the method proposed by Possagnolo (2015) reported 280.19 kW with a minimum voltage of 0.9426 p.u., that proposed by Pereira Junior (2024) reported 280.37 kW, and that proposed by Mantovani et al. (2000) reported 286.18 kW. The proposed VND obtained 285.07 kW, a value 1.47% higher than that of Possagnolo (2015), 1.41% higher than that of Pereira Junior (2024), and 4.15% lower than that of Mantovani et al.

(2000).

The difference between the proposed methodology and the works of Possagnolo (2015) and Pereira Junior (2024), although small in absolute terms (4.18 kW and 4.00 kW, respectively), is the most significant among the three systems analyzed. A possible explanation is that Possagnolo (2015) utilizes a variable neighborhood search employing multiple neighborhood structures and re-initialization criteria distinct from those adopted in this work, which may allow the method proposed by Possagnolo (2015) to escape local optima that the VND implemented here is unable to overcome.

It is important to emphasize that the result of Mantovani et al. (2000), obtained with a voltage drop criterion method, was higher than the value of the proposed VND (284.37 kW), indicating that the methodology developed in this work outperforms that older benchmark.

DG Allocation

The loss reductions with DG allocation were: 24.21% with 1 DG (222.06 kW), 32.44% with 2 DG (197.96 kW), and 40.85% with 3 DG (173.30 kW), relative to the initial result (first modified Prim) without DG (293.00 kW). The marginal gain between units is: 62.31 kW (1st DG), 24.10 kW (2nd DG), and 24.66 kW (3rd DG). The marginal loss reduction between the 2nd and 3rd DG is virtually constant, differing from the decreasing pattern observed in the 84-bus system, which suggests that in this system, the first three DG are allocated at locations with relatively homogeneous impacts.

With maximum DG allocation, totaling 19 DG, losses were reduced to 101.77 kW, representing a 65.27% reduction (191.23 kW) relative to the initial result (first modified Prim) without DG (293.00 kW). The minimum voltage increased from 0.9488 p.u. to 0.9995 p.u., an increase of 0.0507 p.u., which represents the largest variation in minimum voltage among the three systems. The incremental gain between 3 DG and the maximum of 19 DG is 71.53 kW (70.29%), achieved with 16 additional DG.

In the 136-bus system, the return from additional DG beyond the first three is proportionally greater than in the 84-bus system. This may be associated with the greater extension of the 136-bus system and the wider geographical dispersion of loads, which creates more opportunities for distributed injection with a significant impact on loss reduction.

5.2.3 415-Bus System

This subsection presents the discussion of the results obtained for the reconfiguration of the 415-bus system with and without DG allocation.

Reconfiguration Without DG Allocation

The 415-bus system is the largest tested system and exhibits the most significant results in absolute terms. The methodological progression was: 662.51 kW (first modified Prim), 605.29 kW (Multi-start), 598.27 kW (GA), and 578.58 kW (VND). Relative to the initial value (first modified Prim), the Multi-start method yielded an 8.64% reduction, whereas the GA achieved a 9.70% reduction and the VND achieved a 12.67% reduction. Unlike the other two systems, the VND produced a significant improvement relative to the GA: a reduction of 19.69 kW (3.40%).

This indicates that, in larger-scale systems, the local search space is richer, and the VND is capable of exploring neighborhoods that the GA cannot reach within the used number of generations. This result highlights the importance of the VND as a refinement step in large-scale systems.

The reduction from first modified Prim to Multi-start was 57.22 kW (8.64%), the most significant among the three systems. This reinforces that the diversification of initial solutions generated by Multi-start is particularly relevant in larger systems, where the quality of the initial solution has a greater impact on the final outcome.

In relation to the literature, Possagnolo (2015) reported losses of 581.55 kW with a minimum voltage of 0.9462 p.u., and Pereira Junior (2024) found losses of 592.68 kW. The proposed VND obtained losses of 578.58 kW and a minimum voltage of 0.9598 p.u., a result 0.51% lower than that of Possagnolo (2015) and 2.44% lower than that of Pereira Junior (2024).

The result obtained by the methodology proposed herein outperforms Pereira Junior (2024) by 14.10 kW, which is attributable to the VND refinement stage, absent in that work. The difference relative to Possagnolo (2015) (2.97 kW / 0.51%) is small. Bernal-Agustin (1998) reported losses of 708.84 kW, a substantially higher value, reflecting the limitations of older methods when applied to large-scale systems.

DG Allocation

The loss reductions with DG allocation were: 28.06% for 1 DG allocation (476.63 kW), 39.27% for 2 DG allocation (402.32 kW), and 55.00% for 3 DG allocation (298.15 kW), relative to the initial result without DG (662.51 kW). The marginal gains are: 101.95 kW (1st DG), 74.31 kW (2nd DG), and 104.17 kW (3rd DG).

With maximum DG allocation, totaling 20 DG, losses were reduced to 220.25 kW, representing a 66.76% reduction (442.26 kW) relative to the initial result without DG (662.51 kW), which is the largest percentage reduction among the three systems. The minimum voltage increased from 0.9598 p.u. (VND) to 0.9987 p.u. under maximum DG allocation.

The incremental gain between 3 DG and the maximum of 12 DG is 73.84 kW (19.83%), achieved with 9 additional DG. Compared to the 84-bus system (10.68% with 4 additional DG) and the 136-bus system (33.44% with 9 additional DG), the 415-bus system exhibits an intermediate return for additional DG beyond the first three.

5.2.4 Comparative Analysis Among Systems

Table 5.13 synthesizes the loss reduction results obtained by reconfiguration (VND) and maximum DG allocation for the three systems, in comparison with reference benchmarks from the literature.

Table 5.13: Comparison of power losses obtained for the three tested systems.

System	*Initial losses* (kW)	*Proposed VND* (kW)	*Possagnolo (2015)* (kW)	*Pereira Junior (2024)* (kW)	*Max. DG* (kW)	*Reduction w/ max. DG relative to PRIM* (%)
84-bus	471.72	470.21	469.88	469.72	161.01	65.87
136-bus	293.00	284.37	280.19	280.37	101.77	65.27
415-bus	662.51	578.58	581.55	592.68	220.25	66.76

Source: Author.

Three general observations emerge from this comparison:

1. For the reconfiguration stage without DG, the proposed VND produces results equivalent to those of Possagnolo (2015) and Pereira Junior (2024) in the 84-bus system, slightly lower in the 136-bus system, and superior to Pereira Junior (2024) in the 415-bus system. The most significant difference occurs in the 136-bus system, where the proposed VND is 1.47% lower than that of Possagnolo (2015).

2. The most relevant contribution of the present work lies not in the reconfiguration stage alone, but in its integration with DG allocation. The loss reductions under maximum DG allocation (65.87%, 65.27%, and 66.76% for the 84-, 136-, and 415-bus systems, respectively) are substantially superior to those achieved by standalone reconfiguration, demonstrating the synergy between the two strategies. None of the benchmark works (Possagnolo (2015) and Pereira Junior (2024)) address this combination.

3. The effect of DG allocation on the voltage profile is consistently positive in maximum allocation scenarios, with minimum voltages remaining above 0.97 p.u. across all three systems. However, in intermediate scenarios (1 to 3 DG), a reduction in minimum voltage relative to the VND without DG is observed in certain cases (notably in the 415-bus system with 1 and 2 DG). This indicates that partial DG integration can alter power flow in a manner that adversely affects the voltage profile at specific buses, an effect that must be closely monitored in practical applications.

5.2.5 Comparative Analysis Among Methods

Para fazer a analisa comparativa entre os métodos será utilizado o melhor resultado alcançado para cada sistema, ou seja, serão comparados o resultados alcançados com a alocação máxima de GD com todos os outros resultados.

84-Bus System

Table 5.14: Comparison of power losses obtained for the 84-bus system.

Method	*First Modified Prim*	*Multi-start*	*GA*	*VND*	*1 DG*	*2 DG*	*3 DG*	*Max. DG*
Losses (kW)	471.72	469.88	470.21	470.21	419.83	361.75	323.15	161.01
Reduction (%)	-	0.39	0.32	0.32	11.00	23.31	31.50	65.87

Source: Author.

The comparative analysis of the values in Table 5.14 for the 84-bus system reveals the following behavior in loss reduction:

- Reconfiguration phase (without DG): The initial losses (PRIM) are the highest recorded (471.72 kW). The application of Multi-start produces a subtle reduction to 469.88 kW (a drop of 1.84 kW). Subsequent refinement via GA and VND stabilizes losses at 470.21 kW, indicating that topological reconfiguration achieved a savings of 1.51 kW relative to the initial state;
- DG allocation phase: The introduction of the 1st DG induces a sharper decline, reducing losses to 419.83 kW (a reduction of 51.89 kW). The insertion of 2 and 3 DG yields deeper gains, removing an additional 58.08 kW and 38.60 kW from the grid, respectively (accumulating 109.97 kW and 148.57 kW total reductions relative to the reconfigured topology);

- Limit scenario: The losses achieved under maximum DG allocation (16 DG) drop to 161.01 kW, consolidating an overall reduction of 310.71 kW (or 65.87%) from the initial configuration.

136-Bus System

Table 5.15: Comparison of power losses obtained for the 136-bus system.

Method	*First Modified Prim*	*Multi-start*	*GA*	*VND*	*1 DG*	*2 DG*	*3 DG*	*Max. DG*
Losses (kW)	293.00	285.23	284.37	284.37	222.06	197.96	173.30	101.77
Reduction (%)	-	2.65	2.95	2.95	24.21	32.44	40.85	65.27

Source: Author.

The analysis of Table 5.15 for the 136-bus system reveals the following behavior in loss reduction:

- Reconfiguration phase (without DG): The initial losses under PRIM are the highest recorded (293.00 kW). The application of Multi-start yields an initial reduction to 285.23 kW (a drop of 7.77 kW). Subsequent refinement via GA and VND stabilizes losses at 284.37 kW, saving 8.63 kW relative to the initial topology;
- DG allocation phase: The introduction of the 1st DG induces a sharp decline, reducing losses to 222.06 kW (a drop of 62.31 kW relative to the reconfigured topology, or 70.94 kW relative to the initial state). The sequential insertion of 2 and 3 DG sustains significant gains, removing a total of 95.04 kW and 119.70 kW from the network, respectively, relative to the initial result;
- Limit scenario: The lowest loss benchmark is achieved under maximum DG allocation (19 DGs) at 101.77 kW, consolidating an overall reduction of 191.23 kW (or 65.27%) from the initial first modified Prim configuration.

415-Bus System

Table 5.16: Comparison of power losses obtained for the 415-bus system.

Method	*First Modified Prim*	*Multi-start*	*GA*	*VND*	*1 DG*	*2 DG*	*3 DG*	*Max. DG*
Losses (kW)	662.51	605.29	598.27	578.58	476.63	402.32	298.15	220.25
Reduction (%)	-	8.64	9.70	12.67	28.06	39.27	55.00	66.76

Source: Author.

The analysis of the values in Table 5.16 reveals the evolutionary impact of each method on loss reduction for the 415-bus system:

- Reconfiguration phase (without DG): The process begins with PRIM exhibiting the highest losses (662.51 kW). The application of Multi-start reduces this value to 605.29 kW (a drop of 57.22 kW), which is subsequently refined by the GA to 598.27 kW (a reduction of 64.24 kW relative to the initial state). The VND consolidates the optimal topology at 578.58 kW, saving a total of 83.93 kW solely by altering the grid topology;
- DG allocation phase: The introduction of the 1st distributed generator drives losses down to 476.63 kW (a steep reduction of 185.88 kW relative to the initial configuration). The sequential insertion of 2 and 3 DG sustains significant reductions of 260.19 kW and 364.36 kW, respectively, relative to the initial result;
- Limit scenario: The method reaches maximum loss suppression under maximum DG allocation (20 DG) at 220.25 kW, representing an overall decrease of 442.26 kW (or 66.76%) relative to the initial process baseline.

Chapter 6

Conclusion

In this work, a hybrid algorithm for Distribution System Reconfiguration (DSR) was developed and implemented with a focus on active power loss reduction. The approach combines metaheuristic methods, such as Multi-start and GA, with heuristic techniques, such as VND, subsequently integrating strategies for DG allocation at the most critical buses of the system. The proposed methodology aims to provide a unified tool for distribution system operation, enabling coordinated adjustments in network topology and allocation of electrical power generation resources.

The results achieved through DSR without DG allocation demonstrated that the sequence modified Prim's algorithm $\rightarrow$ Multi-start $\rightarrow$ Scatter Search $\rightarrow$ GA $\rightarrow$ Scatter Search $\rightarrow$ VND $\rightarrow$ Scatter Search exhibited a progressive reduction in active power losses. This confirmed that topology alteration alone serves as a cost-effective and efficient strategy for optimizing power flow.

The results achieved through DG allocation following DSR demonstrated a significant reduction in active power losses across the system. The allocation of up to 3 DG units produced incremental loss reductions. In maximum DG allocation scenarios, losses were reduced even further relative to the VND without DG, highlighting the role of local generation in relieving branch loading and providing voltage support directly at buses with the most severe voltage drops.

A comparison between the two strategies (reconfiguration without DG allocation and subsequent DG allocation) reveals that, although reconfiguration is a low-cost solution that leverages existing infrastructure, its integration with DG significantly enhances grid efficiency. While reconfiguration acts on the power transfer "pathway," DG acts at the generation "source" near the load centers. Multi-scenario analysis demonstrated that combining both techniques achieves loss levels and voltage profiles that would be unattainable through either approach applied in isolation.

The proposed hybrid methodology fulfilled the established objectives, proving to be a promising tool for the operation and control of modern distribution systems. The capability to process large-scale systems within low computational execution times reinforces the viability of applying heuristics and metaheuristics to complex combinatorial optimization problems.

This study contributes to the power sector by quantifying the efficiency gains that smart grid operation and decentralized generation can deliver to energy distribution.

6.1 Future Work

Future work extending this research may include:

- Expanding the neighborhood search depth in the VND to explore additional solution spaces;
- Implementing optimal DG placement and sizing algorithms instead of allocating units strictly at the lowest-voltage bus;
- Performing DSR considering time-varying daily load profiles rather than relying solely on peak load conditions;
- Developing a multi-objective optimization framework that accounts for technical losses, DG installation and capital costs, and system reliability metrics;
- Applying Artificial Intelligence (AI) and machine learning techniques to perform joint DSR and DG allocation.

Bibliography

Almeida, C. F. M. & Nagan, N. (2010). Aplicação de algoritmos genéticos e teoria dos conjuntos fuzzy no dimensionamento de sistemas de monitoramento para redes de transmissão de energia elétrica, *Revista Controle & Automação* **21**. Cited on page 34.

Andrade, B. A. R. & Ferreira, N. R. (2018). Simulated annealing and tabu search applied on network reconfiguration in distribution systems, *IEEE Xplore* . Cited 2 times on pages 26 and 27.

Aneel (2026). Relatório de perdas de energia, Aneel, Agência Nacional de Energia Elétrica. Acesso em: março/26.
URL: *https://portalrelatorios.aneel.gov.br/luznatarifa/perdasenergias!* Cited on page 17.

Bernal-Agustin, J. L. (1998). *Application of genetic algorithms to the optimal design of power distribution systems*, Tese doutorado, Universidade de Zaragoza, Zaragoza. Cited 4 times on pages 43, 63, 64, and 70.

Bueno, N. K. A. (2021). *Algoritmo vns para a reconfiguração de sistemas de distribuição de energia elétrica considerando a alocação simultânea de geradores distribuídos*, Dissertação de mestrado, Universidade Estadual Paulista, Ilha Solteira, SP. Cited 2 times on pages 24 and 26.

Cardona, N. P. (2016). *Reconfiguração do sistema de distribuição de energia elétrica utilizando uma metodologia multipartida*, Dissertação de mestrado, Universidade Estadual Paulista, Ilha Solteira, SP. Cited 3 times on pages 17, 31, and 32.

Chiou, J. P., Chang, C. F. & Su, C. T. (1990). Optimal network reconfigurations in distribution systems: part 1: a new formulation and a solution methodology, *IEEE Transactions on Power Delivery* **5**. Cited 3 times on pages 57, 58, and 67.

Chiou, J. P., Chang, C. F. & Su, C. T. (2005). Variable scaling hybrid differential evolution for solving network reconfiguration of distribution systems, *IEEE Transactions on Power Systems* **20**. Cited on page 43.

Chouhan, V. & Thakur, R. (2023). Optimization of dg with enhanced elephant herding optimization in distribution network, *ICCCIS 2023 - International Conference on Computing, Communication, and Intelligent Systems*, pp. 817–822. Cited 3 times on pages 18, 24, and 25.

Ferreira, O. J. N. (2022). *Algoritmo genético de chaves aleatórias viciadas e recozimento simulado aplicado ao problema da reconfiguração de redes de distribuição de energia elétrica considerando técnicas de realização e hibridização*, Dissertação de mestrado, Universidade Federal de Santa Catarina, Florianópolis, SC. Cited 2 times on pages 18 and 22.

Fioravanti Junior, C. (2014). *Reconfiguração de alimentadores em sistemas de distribuição usando uma metaheurística e espaço de busca reduzido*, Dissertação de mestrado, Universidade Estadual Paulista, Ilha Solteira, SP. Cited on page 31.

Freiman, A. (2026). Mhybrid method for the reconfiguration of electric power distribution systems with distributed generation allocation, *Mendeley Data* . Cited on page 56.

Freitas, R. L. B., Perreira Jr, W. G., Freitas, L. P. S., Sousa, V. C., Rocha, C. R. M., Scherer, H. F. & Marodin, R. C. (2026). Metaheuristic-based hybrid system for optimal reconfiguration of electrical grids leveraging distributed generation allocation, *Electrical Power Systems Research* **259**. Cited on page 33.

Goldbarg, M. C. & Luna, H. P. L. (eds) (2005). *Otimização combinatória e programação linear: modelos e algoritmos*, Elsevier, Rio de Janeiro. Cited 2 times on pages 27 and 35.

Greina, A., Karnib, N., Gaubert, J., Bertout, A., Grolleau, E. & Larraillet, D. (2023). A mixed integer linear programming model for the distribution network reconfiguration problem, *ICSC - 11th International Conference on Systems and Control*, Sousse, Tunísia. Cited on page 23.

Mantovani, J. R. S., Casari, F. & Romero, R. (2000). Reconfiguração de sistemas de distribuição radiais utilizando o critério de queda de tensão, *SBA Controle e Automação* **11**. Cited 6 times on pages 43, 44, 60, 61, 68, and 69.

Marodin, R. C. & Freitas, R. L. B. (2020). Aplicação de algoritmo prim com multi-start e busca local para minimização de perdas de sistema de distribuição, *V CONAPESC - Congresso Nacional de Pesquisa e Ensino em Ciências*, Digital Edition (Online). Cited on page 24.

Mladenovic, N. & Hansen, P. (1997). Variable neighborhood search, *Computers & Operations Research* **24**. Cited on page 36.

Montemezzo, J. F. (2016). *Influência dos parâmetros e modelos de linhas na solução do fluxo de carga de sistemas de distribuição de energia elétrica*, Dissertação de mestrado, Universidade Estadual do Oeste do Paraná, Foz do Iguaçu, PR. Cited on page 17.

Nizer, L. A., Freitas, L. P. S., Rocha, C. R. M., Scherer, H. F., Perreira Junior, W. G. & Freitas, R. L. B. (2024). Algoritmo híbrido aplicado para redução das perdas de operação nos sistemas de distribuição de energia elétrica, *Revista Contribuiciones a las Ciencias Sociales* **17**. Cited on page 23.

Pandey, A. D., Singh, N., Shantenu, P., Harsh, P. & Choudhary, N. K. (2026). Minimization of power loss in distribution networks through network reconfiguration with integrated distributed generation, *EPREC - 2026 International Conference on Electric Power and Renewable Energy*, Durg, India, pp. 1 – 6. Cited on page 25.

Pereira, E. C., Barbosa, C. H. N. R. & Vasconcelos, J. A. (2023). Distribution network reconfiguration using iterative branch exchange and clustering technique, *Energies* **16**. Cited on page 22.

Pereira Junior, W. G. (2024). *Otimização do fluxo de potência utilizando algoritmo prim e genético*, Dissertação de mestrado, Universidade Estadual do Oeste do Paraná, Foz do Iguaçu, PR. Cited 18 times on pages 18, 19, 20, 23, 29, 32, 33, 34, 45, 58, 61, 64, 66, 67, 68, 69, 70, and 71.

Possagnolo, L. H. F. M. (2015). *Reconfiguração de sistemas de distribuição operando em vários níveis de demanda através de uma meta-heurística de busca em vizinhança variável*, Dissertação de mestrado, Universidade Estadual Paulista, Ilha Solteira, SP. Cited 12 times on pages 19, 27, 36, 58, 61, 64, 66, 67, 68, 69, 70, and 71.

Prim, R. C. (1957). Shortest connection networks and some generalizations, *Bell System Tech-*

nical Journal **36**. Cited 2 times on pages 28 and 29.

Quang, P. P., Quoc, H. C. A. & Minh, Q. T. (2023). Distribution network reconfiguration using genetic algorithm considering load profile and the penetration of distributed generation, *Asia Meeting on Environment and Electrical Engineering* . Cited on page 25.

Souza, S. S. F. & Romero, R. (2013). Reconfiguração de sistemas de distribuição de energia elétrica utilizando o algoritmo imunológico artificial copt-ainet. Cited on page 26.

Wilhelm, V. E. (2015). Problema da Árvore geradora mínima, *Departamento de Engenharia de Produção - UFPR* . Cited on page 27.

Appendix A

Data of the Tested Systems

This appendix presents the bus and branch data for the distribution systems used to evaluate the algorithm developed in this study. The test networks comprise the 84-bus, 136-bus, and 415-bus systems, the latter being a modification of the standard 417-bus system.

A.1 84-Bus System

Substation bus: 84

Substation voltage: 1 p.u.

Base voltage: 11.4 kV

Base power: 100,000 kVA

Table A.1: 84-Bus System Data

Branch Data					**Bus Data**			
From	*To*	*Resistance* (Ω)	*Reactance* (Ω)	*Apparent Power* (kVA)	*Bus*	*Active Demand* (kW)	*Capacitive Demand* (kVAr)	*Inductive Demand* (kVAr)
16	17	0.0524	0.1076	4995.8728	1	0	0	0
17	18	0.1572	0.3228	4364.8729	2	100	50	0
11	12	0.3406	0.6944	4203.2090	3	300	200	0
47	84	0.2430	0.8280	3891.2978	4	350	250	0
47	48	0.0655	0.1345	3891.2978	5	220	100	0
48	49	0.0655	0.1345	3875.2124	6	1100	800	0
49	50	0.0393	0.0807	3859.1458	7	400	320	0
11	84	0.0786	0.1614	3844.9192	8	300	200	0
15	84	0.1134	0.3864	3758.9827	9	300	230	0
15	16	0.0524	0.1076	3758.9827	10	300	260	0
25	84	0.0567	0.1932	3747.3965	11	0.90	0	0

Table A.1: 84-Bus System Data (Continued)

Branch Data					**Bus Data**			
From	*To*	*Resistance* (Ω)	*Reactance* (Ω)	*Apparent Power* (kVA)	*Bus*	*Active Demand* (kW)	*Capacitive Demand* (kVAr)	*Inductive Demand* (kVAr)
25	26	0.1048	0.2152	3689.2650	12	1200	800	0
50	51	0.0786	0.1614	3593.7006	13	800	600	0
77	84	0.2511	0.8556	3592.0668	14	700	500	0
77	78	0.1296	0.4416	3592.0668	15	0	0	0
18	19	0.0393	0.0807	3553.4174	16	300	150	0
30	84	0.1965	0.3960	3526.1285	17	500	350	0
30	31	0.1310	0.2690	3526.1285	18	700	400	0
43	84	0.0486	0.1656	3385.8085	19	1200	1000	0
43	44	0.0393	0.0807	3019.1841	20	300	300	0
78	79	0.0486	0.1656	3016.3137	21	400	350	0
44	45	0.1310	0.2690	2977.5315	22	50	20	0
1	84	0.1944	0.6624	2883.9406	23	50	20	0
1	2	0.2096	0.4304	2883.9406	24	50	10	0
2	3	0.2358	0.4842	2745.8950	25	50	30	0
56	84	0.2268	0.7728	2623.7786	26	100	60	0
56	57	0.5371	1.1029	2623.7786	27	100	70	0
51	52	0.0393	0.0807	2577.3057	28	1800	1300	0
57	58	0.0524	0.1076	2529.4141	29	200	120	0
3	4	0.0917	0.1883	2356.9794	30	0	0	0
73	84	0.3240	1.1040	2301.7304	31	1800	1600	0
73	74	0.0324	0.1104	2301.7304	32	200	150	0
74	75	0.0567	0.1932	2297.6938	33	200	100	0
65	84	0.0486	0.1656	2249.1487	34	800	600	0
65	66	0.1703	0.3497	2249.1487	35	100	60	0
66	67	0.1215	0.4140	2177.7501	36	100	60	0
67	68	0.2187	0.7452	2164.2209	37	20	10	0
52	53	0.0786	0.1614	1991.8016	38	20	10	0
19	20	0.1703	0.3497	1989.6968	39	20	10	0
26	27	0.2489	0.5111	1974.3608	40	20	10	0
4	5	0.2096	0.4304	1918.6956	41	200	160	0
45	46	0.2358	0.4842	1899.0305	42	50	30	0
27	28	0.0486	0.1656	1836.9830	43	0	0	0
58	59	0.0405	0.1380	1791.5386	44	30	20	0
59	60	0.0393	0.0807	1788.5739	45	800	700	0
34	46	0.0262	0.0538	1634.5169	46	200	150	0

Table A.1: 84-Bus System Data (Continued)

Branch Data					**Bus Data**			
From	*To*	*Resistance* (Ω)	*Reactance* (Ω)	*Apparent Power* (kVA)	*Bus*	*Active Demand* (kW)	*Capacitive Demand* (kVAr)	*Inductive Demand* (kVAr)
5	6	0.0393	0.0807	1632.4874	47	0	0	0
68	69	0.0486	0.1656	1601.9883	48	0	0	0
69	70	0.0729	0.2484	1598.9888	49	0	0	0
16	26	0.0917	0.1883	1596.2419	50	200	160	0
70	71	0.0567	0.1932	1594.4954	51	800	600	0
7	60	0.1310	0.2690	1376.9520	52	500	300	0
12	72	0.3406	0.6994	1172.4528	53	500	350	0
31	32	0.1310	0.2690	1126.2673	54	500	300	0
71	72	0.0262	0.0528	915.5951	55	200	80	0
12	14	0.0786	0.1614	899.7665	56	0	0	0
20	83	0.0786	0.1614	893.5711	57	30	20	0
28	32	0.0524	0.1076	887.5468	58	600	420	0
75	76	0.0486	0.1656	761.3632	59	0	0	0
53	54	0.0524	0.1076	754.1594	60	20	10	0
20	21	0.2358	0.4842	681.9506	61	20	10	0
79	80	0.1310	0.2640	654.0549	62	200	130	0
53	64	0.0393	0.0807	623.6547	63	300	240	0
12	13	0.0262	0.0538	602.0557	64	300	200	0
28	29	0.1310	0.2690	469.8607	65	0	0	0
80	81	0.1310	0.2640	429.1470	66	50	30	0
13	76	0.4585	0.9415	421.9036	67	0	0	0
82	83	0.3144	0.6456	414.3260	68	400	360	0
34	35	0.0524	0.1076	400.0365	69	0	0	0
7	10	0.1048	0.2152	397.2804	70	0	0	0
60	61	0.0262	0.0538	385.8136	71	2000	1500	0
7	9	0.2358	0.4842	378.6010	72	200	150	0
11	43	0.1310	0.2690	370.6154	73	0	0	0
61	62	0.1048	0.2152	363.4054	74	0	0	0
7	8	0.1048	0.2152	360.7809	75	1200	950	0
81	82	0.0917	0.1883	315.3357	76	300	180	0
35	36	0.4978	1.0222	283.3027	77	0	0	0
6	7	0.0405	0.1380	275.1565	78	400	360	0
63	64	0.0243	0.0828	267.1426	79	2000	1300	0
29	39	0.0786	0.1614	236.7062	80	200	140	0
33	34	0.1703	0.3497	235.4787	81	500	360	0

Table A.1: 84-Bus System Data (Continued)

Branch Data					**Bus Data**			
From	*To*	*Resistance* (Ω)	*Reactance* (Ω)	*Apparent Power* (kVA)	*Bus*	*Active Demand* (kW)	*Capacitive Demand* (kVAr)	*Inductive Demand* (kVAr)
38	41	0.1965	0.4035	219.4362	82	100	30	0
54	55	0.1310	0.2690	174.9218	83	400	360	0
36	37	0.0393	0.0807	166.0948	84	0	0	0
37	38	0.0393	0.0807	143.8637	-	-	-	-
62	63	0.2358	0.4842	126.7493	-	-	-	-
39	40	0.2096	0.4304	116.8551	-	-	-	-
21	23	0.1965	0.4035	104.4350	-	-	-	-
38	39	0.0786	0.1614	97.9787	-	-	-	-
40	42	0.1965	0.4035	94.7592	-	-	-	-
5	55	0.1310	0.2690	89.5600	-	-	-	-
21	22	0.1572	0.3228	53.8581	-	-	-	-
23	24	0.1310	0.2690	50.9941	-	-	-	-
14	18	0.5371	1.0824	39.5467	-	-	-	-
41	42	0.2096	0.4304	37.2982	-	-	-	-
32	33	0.0262	0.0538	35.5310	-	-	-	-

A.2 136-Bus System

Substation bus: 136

Substation voltage: 1 p.u.

Base voltage: 13,8 kV

Base power: 100000 kVA

Table A.2: 136-Bus System Data

Branch Data					**Bus Data**			
From	*To*	*Resistance* (Ω)	*Reactance* (Ω)	*Apparent Power* (kVA)	*Bus*	*Active Demand* (kW)	*Capacitive Demand* (kVAr)	*Inductive Demand* (kVAr)
136	39	0.3321	0.7665	3448.7816	136	0.000	0.000	0.000
39	40	0.1182	0.2728	3409.9714	1	0.000	0.000	0.000
40	42	0.0019	0.0043	3388.0685	2	47.780	19.009	0.000

Table A.2: 136-Bus System Data (Continued)

Branch Data					**Bus Data**			
From	*To*	*Resistance* (Ω)	*Reactance* (Ω)	*Apparent Power* (kVA)	*Bus*	*Active Demand* (kW)	*Capacitive Demand* (kVAr)	*Inductive Demand* (kVAr)
42	43	0.0694	0.1602	3387.8518	3	42.551	16.929	0.000
43	45	0.0638	0.1472	3183.7603	4	87.022	34.622	0.000
45	46	0.1313	0.3032	2990.1456	5	311.310	123.855	0.000
136	17	0.3321	0.7665	2957.6296	6	148.869	59.228	0.000
17	18	0.0019	0.0043	2928.8311	7	238.672	94.956	0.000
18	19	0.2232	0.5154	2928.6688	8	62.299	24.786	0.000
19	20	0.1088	0.2512	2909.4323	9	124.598	49.571	0.000
136	85	0.0113	0.0260	2750.6182	10	140.175	55.768	0.000
85	86	0.4184	0.9658	2749.7910	11	116.813	46.474	0.000
136	1	0.3321	0.7665	2693.7880	12	249.203	99.145	0.000
1	2	0.0019	0.0043	2670.1361	13	291.447	115.952	0.000
2	3	0.2232	0.5154	2618.6362	14	303.720	120.835	0.000
20	22	0.1820	0.4201	2609.2959	15	215.396	85.695	0.000
3	4	0.0994	0.2295	2557.6662	16	198.586	79.007	0.000
46	47	0.0619	0.1429	2480.2854	17	0.000	0.000	0.000
4	5	0.1557	0.3595	2457.5658	18	0.000	0.000	0.000
136	99	0.0094	0.0217	2415.3619	19	0.000	0.000	0.000
99	100	0.1688	0.3898	2414.8238	20	30.127	14.729	0.000
100	101	0.1182	0.2728	2349.4313	21	230.972	112.920	0.000
22	24	0.0244	0.0563	2272.6673	22	60.256	29.458	0.000
101	103	0.4559	1.0524	2268.1311	23	230.972	112.920	0.000
136	63	0.0075	0.0173	2255.9271	24	120.507	58.915	0.000
63	64	0.2701	0.6236	2255.5554	25	0.000	0.000	0.000
5	6	0.1632	0.3768	2113.3386	26	56.981	27.857	0.000
136	121	0.0113	0.0260	2044.9969	27	364.665	178.281	0.000
121	122	0.6491	1.4984	2044.5314	28	0.000	0.000	0.000
24	25	0.0450	0.1039	1997.1043	29	124.647	60.939	0.000
64	65	0.3827	0.8835	1926.0081	30	56.981	27.857	0.000
122	123	0.0450	0.1039	1912.5613	31	0.000	0.000	0.000
136	75	0.0113	0.0260	1879.7815	32	85.473	41.787	0.000
75	76	0.7298	1.6846	1879.3961	33	0.000	0.000	0.000
125	127	0.0976	0.2252	1851.6019	34	396.735	193.960	0.000
65	66	0.3302	0.7622	1822.7703	35	0.000	0.000	0.000
131	132	0.1613	0.3724	1770.6648	36	181.152	88.563	0.000
123	125	0.0206	0.0476	1718.3717	37	242.172	118.395	0.000

Table A.2: 136-Bus System Data (Continued)

Branch Data					**Bus Data**			
From	*To*	*Resistance* (Ω)	*Reactance* (Ω)	*Apparent Power* (kVA)	*Bus*	*Active Demand* (kW)	*Capacitive Demand* (kVAr)	*Inductive Demand* (kVAr)
6	8	0.0568	0.0567	1555.2665	38	75.316	36.821	0.000
104	105	0.4577	1.0567	1534.3607	39	0.000	0.000	0.000
127	129	0.1388	0.3205	1524.1850	40	1.254	0.531	0.000
129	130	0.0432	0.0996	1523.2958	41	6.274	2.660	0.000
90	91	0.3321	0.7665	1498.9985	42	0.000	0.000	0.000
8	10	0.1088	0.1086	1492.5008	43	117.880	49.971	0.000
130	131	0.0919	0.2122	1482.8382	44	62.668	26.566	0.000
77	78	0.2082	0.4807	1420.7158	45	172.285	73.034	0.000
110	47	0.4970	0.6457	1386.2930	46	458.556	194.388	0.000
86	88	0.4390	1.0134	1385.1369	47	262.962	111.473	0.000
76	77	0.2251	0.5197	1365.3089	48	235.761	99.942	0.000
25	26	0.0188	0.0433	1333.0676	49	0.000	0.000	0.000
78	79	0.0469	0.1083	1312.2351	50	109.215	46.298	0.000
90	103	0.0769	0.1776	1293.5647	51	0.000	0.000	0.000
26	27	0.1182	0.1181	1269.3219	52	72.809	30.865	0.000
86	87	0.1050	0.1364	1236.4781	53	258.473	109.570	0.000
79	80	0.6195	0.6186	1113.5264	54	69.169	29.322	0.000
107	110	0.0455	0.0591	1052.0233	55	21.843	9.260	0.000
66	67	0.3283	0.7579	1041.9605	56	0.000	0.000	0.000
80	81	0.3405	0.3400	957.2432	57	20.527	8.702	0.000
103	104	0.6960	1.6067	948.5210	58	150.548	63.819	0.000
10	13	0.1182	0.1181	946.9472	59	220.687	93.552	0.000
67	68	0.1707	0.3941	926.7768	60	92.384	39.163	0.000
92	93	0.1332	0.3075	893.1330	61	0.000	0.000	0.000
51	52	0.0263	0.0606	882.9018	62	226.693	96.098	0.000
132	133	0.3783	0.3778	882.1509	63	0.000	0.000	0.000
88	89	0.0752	0.0258	879.0205	64	294.016	116.974	0.000
27	28	0.0237	0.0236	862.4056	65	83.015	33.028	0.000
91	104	0.1419	0.1417	808.2938	66	83.015	33.028	0.000
66	79	0.1294	0.2988	680.8726	67	103.770	41.285	0.000
25	51	0.0450	0.1039	668.7354	68	176.408	70.184	0.000
28	31	0.0568	0.0567	660.4457	69	83.015	33.028	0.000
68	70	0.0582	0.1343	646.4828	70	217.917	86.698	0.000
91	92	0.0844	0.1949	604.9666	71	23.294	9.267	0.000
79	131	0.0169	0.0390	588.5714	72	5.075	2.019	0.000

Table A.2: 136-Bus System Data (Continued)

Branch Data					**Bus Data**			
From	*To*	*Resistance* (Ω)	*Reactance* (Ω)	*Apparent Power* (kVA)	*Bus*	*Active Demand* (kW)	*Capacitive Demand* (kVAr)	*Inductive Demand* (kVAr)
81	83	0.1088	0.1086	567.8673	73	72.638	28.899	0.000
92	132	0.0769	0.1776	544.9433	74	405.990	161.524	0.000
93	97	0.1032	0.2382	542.3829	75	0.000	0.000	0.000
97	98	0.1351	0.3118	542.0298	76	100.182	42.468	0.000
31	32	0.0948	0.0499	537.5735	77	142.523	60.417	0.000
47	48	0.1144	0.2642	533.0469	78	96.042	40.713	0.000
52	56	0.1088	0.2512	527.6505	79	300.454	127.366	0.000
56	57	0.2559	0.1346	527.3448	80	141.238	59.873	0.000
133	134	0.3972	0.3966	512.7403	81	279.847	118.631	0.000
57	58	0.4170	0.2193	504.6053	82	87.312	37.013	0.000
107	108	0.5497	0.2891	499.8140	83	243.849	103.371	0.000
106	107	0.2135	0.2774	473.7188	84	247.750	105.025	0.000
35	36	0.3696	0.1944	471.8430	85	0.000	0.000	0.000
89	90	0.0769	0.1776	460.3350	86	89.878	38.101	0.000
32	33	0.4170	0.2193	442.2610	87	1137.280	482.108	0.000
33	34	0.1137	0.0598	441.7493	88	458.339	194.296	0.000
73	74	1.3235	0.4540	438.4247	89	385.197	163.290	0.000
38	135	0.0851	0.0850	437.3607	90	0.000	0.000	0.000
6	7	0.1144	0.2642	396.3589	91	79.608	33.747	0.000
126	76	0.1706	0.0897	388.9062	92	87.312	37.013	0.000
70	73	0.0675	0.1559	382.1589	93	0.000	0.000	0.000
135	98	0.2932	0.2928	375.8412	94	74.001	31.370	0.000
93	94	0.2932	0.2928	359.4791	95	232.050	98.369	0.000
35	38	0.0568	0.0567	354.0886	96	141.819	60.119	0.000
104	118	0.3227	0.7449	342.1951	97	0.000	0.000	0.000
58	59	0.5023	0.2642	340.4252	98	76.449	32.408	0.000
13	14	0.5023	0.2642	327.2096	99	0.000	0.000	0.000
13	15	0.0568	0.0567	313.3246	100	51.322	21.756	0.000
127	128	0.1182	0.2728	305.4625	101	59.874	25.381	0.000
47	62	0.1388	0.3205	284.6182	102	9.065	3.843	0.000
94	95	0.2175	0.2172	279.5840	103	2.092	0.887	0.000
52	53	0.0600	0.1386	279.5003	104	16.735	7.094	0.000
108	109	0.5402	0.2842	272.4642	105	1506.522	638.634	0.000
109	116	1.0993	0.5783	272.2111	106	313.023	132.694	0.000
36	37	0.2654	0.1396	269.6851	107	79.831	33.842	0.000

Table A.2: 136-Bus System Data (Continued)

Branch Data					**Bus Data**			
From	*To*	*Resistance* (Ω)	*Reactance* (Ω)	*Apparent Power* (kVA)	*Bus*	*Active Demand* (kW)	*Capacitive Demand* (kVAr)	*Inductive Demand* (kVAr)
10	12	0.9174	0.3147	268.5881	108	51.322	21.756	0.000
118	119	0.1463	0.3378	265.9996	109	0.000	0.000	0.000
20	21	0.7108	0.3739	257.3877	110	202.435	85.815	0.000
22	23	0.3033	0.1595	257.2222	111	60.823	25.784	0.000
90	129	0.0769	0.1776	256.8532	112	45.618	19.338	0.000
134	135	0.2932	0.2928	246.2168	113	0.000	0.000	0.000
48	51	0.0450	0.1039	241.0214	114	157.070	66.584	0.000
125	126	0.5307	0.2792	234.5631	115	0.000	0.000	0.000
119	120	0.1238	0.2858	231.0642	116	250.148	106.041	0.000
128	77	0.0525	0.1213	225.6855	117	0.000	0.000	0.000
15	16	0.2938	0.1545	213.8090	118	69.809	29.593	0.000
92	104	0.0769	0.1776	209.9250	119	32.072	13.596	0.000
96	120	0.2648	0.2644	203.1792	120	61.084	25.894	0.000
28	29	0.1895	0.0997	202.2305	121	0.000	0.000	0.000
108	114	0.7771	0.4088	170.7431	122	94.622	46.260	0.000
105	106	0.2030	0.2637	168.3875	123	49.858	24.375	0.000
15	83	0.1419	0.1417	167.7500	124	123.164	60.214	0.000
84	135	0.3317	0.1745	161.5762	125	78.350	38.304	0.000
83	84	0.5686	0.2991	158.4108	126	145.475	71.121	0.000
9	24	0.2654	0.1396	148.2786	127	21.369	10.447	0.000
7	73	0.1313	0.3032	143.5813	128	74.789	36.564	0.000
123	124	0.5264	0.1806	137.1513	129	227.926	111.431	0.000
31	35	0.0757	0.0756	129.9793	130	35.614	17.411	0.000
10	11	0.3980	0.2094	125.7575	131	249.295	121.877	0.000
55	98	0.1419	0.1417	118.2276	132	316.722	154.842	0.000
110	111	0.4739	0.2493	115.6632	133	333.817	163.199	0.000
59	60	0.3317	0.1745	100.3631	134	249.295	121.877	0.000
54	55	0.0206	0.0476	97.6890	135	0.000	0.000	0.000
81	82	0.5686	0.2991	94.8652	-	-	-	-
68	69	0.5591	0.2941	89.3716	-	-	-	-
50	96	0.1419	0.1417	71.6854	-	-	-	-
43	44	0.8150	0.4287	68.0895	-	-	-	-
29	30	0.3980	0.2094	63.4360	-	-	-	-
53	54	0.0300	0.0693	54.0548	-	-	-	-
62	120	0.0394	0.0909	50.0608	-	-	-	-

Table A.2: 136-Bus System Data (Continued)

Branch Data					**Bus Data**			
From	*To*	*Resistance* (Ω)	*Reactance* (Ω)	*Apparent Power* (kVA)	*Bus*	*Active Demand* (kW)	*Capacitive Demand* (kVAr)	*Inductive Demand* (kVAr)
111	112	0.8624	0.4536	49.5609	-	-	-	-
95	96	0.2648	0.2644	49.2410	-	-	-	-
48	49	0.2837	0.2833	49.1856	-	-	-	-
49	50	0.2837	0.2833	49.1803	-	-	-	-
8	9	0.5212	0.2742	42.7455	-	-	-	-
70	71	0.7013	0.3689	30.5358	-	-	-	-
101	102	2.2861	0.7841	9.8472	-	-	-	-
40	41	2.9629	1.0163	6.8154	-	-	-	-
71	72	1.0235	0.5384	5.4621	-	-	-	-
60	61	0.2085	0.1097	0.0000	-	-	-	-
112	113	0.5686	0.2991	0.0000	-	-	-	-
114	115	1.0804	0.5683	0.0000	-	-	-	-
116	117	0.4739	0.2493	0.0000	-	-	-	-

A.3 415-Bus System

Substation bus: 1

Substation voltage: 1 p.u.

Base voltage: 10.1 kV

Base power: 100,000 kVA

Table A.3: 415-Bus System Data

Branch Data					**Bus Data**			
From	*To*	*Resistance* (Ω)	*Reactance* (Ω)	*Apparent Power* (kVA)	*Bus*	*Active Demand* (kW)	*Capacitive Demand* (kVAr)	*Inductive Demand* (kVAr)
362	1	0.02415	0.02849	4754.35400	1	0.1	0.0	0.0
363	362	0.01887	0.01922	4682.02030	2	0.1	0.0	0.0
211	1	0.05629	0.03881	4556.11060	3	122.0	59.0	0.0
209	211	0.05592	0.03856	4476.91320	4	0.1	0.0	0.0
1	190	0.14154	0.14412	3992.80390	5	0.1	0.0	0.0

Table A.3: 415-Bus System Data (Continued)

Branch Data					Bus Data			
From	*To*	*Resistance* (Ω)	*Reactance* (Ω)	*Apparent Power* (kVA)	*Bus*	*Active Demand* (kW)	*Capacitive Demand* (kVAr)	*Inductive Demand* (kVAr)
208	209	0.03838	0.02646	3929.42860	6	114.0	55.0	0.0
159	190	0.23590	0.24020	3887.44690	7	51.0	25.0	0.0
365	363	0.04836	0.04924	3472.93890	8	83.0	40.0	0.0
123	1	0.01352	0.01595	3451.86800	9	0.1	0.0	0.0
269	365	0.07077	0.07206	3420.14880	10	122.0	59.0	0.0
120	123	0.29488	0.30025	3403.25240	11	122.0	59.0	0.0
120	94	0.25383	0.25846	3403.16630	12	77.0	37.0	0.0
268	269	0.05496	0.05597	3272.48480	13	0.1	0.0	0.0
1	274	0.11550	0.07963	2771.58170	14	68.0	33.0	0.0
275	276	0.11586	0.07988	2706.87750	15	71.0	34.0	0.0
274	275	0.08370	0.05771	2621.25470	16	0.1	0.0	0.0
276	264	0.11513	0.07938	2557.19630	17	0.1	0.0	0.0
1	92	0.38889	0.26813	2441.31570	18	77.0	37.0	0.0
92	2	0.34101	0.23512	2390.44660	19	30.0	14.0	0.0
254	257	0.07887	0.06658	2340.27880	20	13.0	6.0	0.0
283	282	0.06631	0.05598	2291.52210	21	1.0	0.0	0.0
253	254	0.04586	0.03872	2282.16360	22	194.0	94.0	0.0
1	215	0.34759	0.23965	2208.33390	23	77.0	37.0	0.0
1	364	0.28509	0.19656	2206.43980	24	77.0	37.0	0.0
364	285	0.05848	0.04032	2165.72640	25	77.0	37.0	0.0
257	283	0.05375	0.04537	2148.47950	26	122.0	59.0	0.0
300	285	0.08114	0.05594	2143.59720	27	104.0	51.0	0.0
360	253	0.04971	0.03427	2139.46980	28	0.1	0.0	0.0
251	360	0.09869	0.06804	2133.77100	29	77.0	37.0	0.0
220	223	0.07098	0.05992	2122.69150	30	243.0	118.0	0.0
223	237	0.08179	0.06905	2072.96680	31	77.0	37.0	0.0
215	216	0.10600	0.07308	2048.19080	32	77.0	37.0	0.0
208	236	0.07676	0.05292	2034.51460	33	0.1	0.0	0.0
264	265	0.07237	0.04990	2013.12030	34	121.0	58.0	0.0
265	367	0.00877	0.00605	1974.68500	35	194.0	94.0	0.0
367	340	0.00110	0.00076	1974.17500	36	122.0	59.0	0.0
340	341	0.02741	0.01890	1964.28640	37	77.0	37.0	0.0
268	297	0.05044	0.03478	1933.00580	38	0.1	0.0	0.0
1	351	0.22661	0.15624	1915.90190	39	0.1	0.0	0.0
341	368	0.17910	0.12348	1915.32590	40	96.0	47.0	0.0

Table A.3: 415-Bus System Data (Continued)

Branch Data					Bus Data			
From	*To*	*Resistance* (Ω)	*Reactance* (Ω)	*Apparent Power* (kVA)	*Bus*	*Active Demand* (kW)	*Capacitive Demand* (kVAr)	*Inductive Demand* (kVAr)
216	218	0.06579	0.04536	1911.82240	41	122.0	59.0	0.0
218	219	0.00292	0.00202	1908.79460	42	70.0	34.0	0.0
351	379	0.02339	0.01613	1905.81120	43	58.0	28.0	0.0
379	380	0.10340	0.08730	1904.68940	44	0.1	0.0	0.0
380	229	0.04119	0.03477	1899.77660	45	122.0	59.0	0.0
368	345	0.11513	0.07938	1881.80950	46	122.0	59.0	0.0
297	296	0.05044	0.03478	1875.25340	47	122.0	59.0	0.0
219	220	0.08041	0.05544	1873.33550	48	86.0	42.0	0.0
1	350	0.22661	0.15624	1781.35660	49	77.0	37.0	0.0
229	228	0.06309	0.05327	1780.23320	50	0.1	0.0	0.0
345	346	0.05848	0.04032	1779.24160	51	122.0	59.0	0.0
350	203	0.02339	0.01613	1772.62740	52	122.0	59.0	0.0
383	251	0.01097	0.00756	1744.23860	53	122.0	59.0	0.0
94	119	0.05603	0.06609	1735.98550	54	0.1	0.0	0.0
129	346	0.26170	0.18043	1727.66010	55	42.0	20.0	0.0
237	372	0.05375	0.04537	1704.18730	56	122.0	59.0	0.0
372	239	0.02658	0.02244	1702.06350	57	13.0	6.0	0.0
239	243	0.08354	0.07053	1668.79650	58	77.0	37.0	0.0
235	236	0.04203	0.02898	1654.43050	59	50.0	24.0	0.0
159	182	0.05410	0.06381	1575.12520	60	0.1	0.0	0.0
208	277	0.06725	0.04637	1541.76570	61	60.0	29.0	0.0
160	129	0.22784	0.19235	1439.25790	62	71.0	34.0	0.0
70	382	0.03107	0.02142	1413.52540	63	122.0	59.0	0.0
281	282	0.05373	0.03704	1379.71170	64	77.0	37.0	0.0
203	206	0.10340	0.08730	1376.34500	65	95.0	46.0	0.0
59	70	0.05373	0.03704	1349.27610	66	121.0	58.0	0.0
159	161	0.08407	0.05796	1338.35300	67	77.0	37.0	0.0
228	371	0.04674	0.03946	1322.43270	68	103.0	50.0	0.0
371	374	0.03943	0.03329	1321.28340	69	52.0	25.0	0.0
277	279	0.04825	0.03326	1304.28580	70	57.0	27.0	0.0
374	226	0.00234	0.00197	1300.17650	71	171.0	83.0	0.0
267	268	0.15643	0.10786	1289.43000	72	121.0	58.0	0.0
206	207	0.05988	0.05055	1245.92150	73	39.0	19.0	0.0
73	77	0.07676	0.05292	1222.87700	74	119.0	58.0	0.0
363	381	0.26316	0.18144	1216.88460	75	49.0	24.0	0.0

Table A.3: 415-Bus System Data (Continued)

Branch Data					Bus Data			
From	*To*	*Resistance* (Ω)	*Reactance* (Ω)	*Apparent Power* (kVA)	*Bus*	*Active Demand* (kW)	*Capacitive Demand* (kVAr)	*Inductive Demand* (kVAr)
381	268	0.30958	0.21344	1212.17430	76	0.1	0.0	0.0
119	122	0.05117	0.03528	1199.21100	77	50.0	24.0	0.0
182	186	0.04830	0.05698	1167.33700	78	44.0	21.0	0.0
279	280	0.03436	0.02369	1163.41470	79	82.0	40.0	0.0
349	207	0.03213	0.02713	1113.16720	80	132.0	64.0	0.0
299	296	0.03801	0.02621	1083.35800	81	194.0	94.0	0.0
186	166	0.03774	0.03843	1076.52290	82	0.1	0.0	0.0
226	225	0.02741	0.01890	1075.60790	83	122.0	59.0	0.0
129	154	0.03505	0.02959	1058.24330	84	3.0	1.0	0.0
166	170	0.03774	0.03843	1035.47790	85	52.0	25.0	0.0
72	73	0.09869	0.06804	1031.99820	86	103.0	50.0	0.0
232	349	0.07595	0.06412	1023.13850	87	21.0	10.0	0.0
129	151	0.03290	0.02268	1013.29950	88	21.0	10.0	0.0
282	234	0.05550	0.04685	1010.09120	89	21.0	10.0	0.0
3	20	0.61039	0.42084	996.76800	90	5.0	3.0	0.0
129	141	0.03213	0.02713	976.52280	91	0.1	0.0	0.0
300	301	0.09320	0.06426	969.27380	92	0.1	0.0	0.0
296	260	0.04788	0.03301	963.71720	93	21.0	10.0	0.0
170	174	0.02921	0.02466	949.88840	94	18.0	9.0	0.0
280	281	0.06214	0.04284	938.59960	95	122.0	59.0	0.0
266	267	0.09942	0.06854	935.23070	96	116.0	56.0	0.0
225	224	0.06945	0.04788	935.22840	97	7.0	3.0	0.0
122	118	0.20103	0.13860	927.02710	98	64.0	31.0	0.0
118	84	0.04021	0.02772	924.71970	99	49.0	24.0	0.0
90	370	0.15790	0.10886	916.68310	100	16.0	8.0	0.0
98	94	0.04021	0.02772	910.01980	101	77.0	37.0	0.0
83	90	0.12098	0.08341	909.64940	102	119.0	58.0	0.0
382	383	0.15022	0.10357	908.47050	103	71.0	34.0	0.0
2	14	0.01645	0.01134	863.56390	104	77.0	37.0	0.0
321	299	0.07018	0.04838	858.22290	105	194.0	94.0	0.0
224	222	0.06945	0.04788	844.58110	106	122.0	59.0	0.0
116	98	0.06214	0.04284	838.42930	107	55.0	27.0	0.0
383	370	0.01828	0.01260	835.15800	108	38.0	18.0	0.0
174	180	0.06369	0.06485	817.62050	109	22.0	10.0	0.0
64	67	0.04496	0.03100	812.86620	110	0.1	0.0	0.0

Table A.3: 415-Bus System Data (Continued)

Branch Data					Bus Data			
From	*To*	*Resistance* (Ω)	*Reactance* (Ω)	*Apparent Power* (kVA)	*Bus*	*Active Demand* (kW)	*Capacitive Demand* (kVAr)	*Inductive Demand* (kVAr)
159	184	0.22661	0.15624	809.16560	111	77.0	37.0	0.0
281	235	0.04934	0.03402	794.39360	112	122.0	59.0	0.0
14	16	0.09869	0.06804	788.12640	113	38.0	18.0	0.0
16	19	0.15717	0.10836	787.27870	114	122.0	59.0	0.0
268	292	0.09869	0.06804	783.80950	115	27.0	13.0	0.0
2	13	0.03213	0.02713	774.26260	116	64.0	31.0	0.0
13	4	0.04528	0.03822	773.91790	117	0.1	0.0	0.0
4	12	0.06718	0.05672	773.46910	118	0.1	0.0	0.0
79	83	0.24123	0.16632	772.49870	119	0.1	0.0	0.0
97	116	0.04386	0.03024	767.08150	120	0.1	0.0	0.0
84	33	0.04203	0.02898	763.47250	121	79.0	38.0	0.0
117	97	0.04021	0.02772	759.20740	122	247.0	119.0	0.0
232	231	0.09686	0.06678	759.02280	123	0.1	0.0	0.0
96	117	0.07858	0.05418	758.53970	124	0.1	0.0	0.0
19	8	0.02193	0.01512	753.07840	125	0.1	0.0	0.0
294	292	0.09174	0.06325	747.08520	126	0.1	0.0	0.0
67	68	0.08626	0.05947	735.41780	127	0.1	0.0	0.0
20	51	0.08772	0.06048	735.40930	128	0.1	0.0	0.0
2	17	0.08772	0.06048	730.45420	129	77.0	37.0	0.0
17	18	0.11696	0.08064	729.78430	130	122.0	59.0	0.0
62	64	0.06031	0.04158	727.21940	131	62.0	30.0	0.0
184	187	0.03505	0.02959	724.95100	132	105.0	51.0	0.0
187	167	0.08471	0.07151	724.61590	133	122.0	59.0	0.0
322	321	0.09503	0.06552	717.64910	134	77.0	37.0	0.0
260	324	0.10782	0.07434	710.97080	135	77.0	37.0	0.0
179	160	0.06945	0.04788	689.75550	136	0.1	0.0	0.0
12	15	0.10516	0.08878	687.50960	137	85.0	41.0	0.0
1	373	0.02778	0.01915	681.62140	138	8.0	4.0	0.0
373	352	0.10417	0.07182	681.37650	139	122.0	59.0	0.0
78	79	0.02193	0.01512	681.31930	140	35.0	17.0	0.0
22	33	0.04386	0.03024	678.94570	141	55.0	27.0	0.0
243	356	0.00914	0.00630	676.22570	142	153.0	74.0	0.0
356	357	0.05117	0.03528	676.08180	143	316.0	153.0	0.0
8	9	0.09503	0.06552	661.25560	144	105.0	51.0	0.0
9	3	0.01462	0.01008	660.64970	145	20.0	10.0	0.0

Table A.3: 415-Bus System Data (Continued)

Branch Data					Bus Data			
From	*To*	*Resistance* (Ω)	*Reactance* (Ω)	*Apparent Power* (kVA)	*Bus*	*Active Demand* (kW)	*Capacitive Demand* (kVAr)	*Inductive Demand* (kVAr)
58	20	0.59211	0.40824	652.90850	146	95.0	46.0	0.0
58	62	0.12939	0.08921	648.02550	147	38.0	18.0	0.0
77	59	0.38743	0.26712	647.25390	148	83.0	40.0	0.0
59	69	0.02120	0.01462	644.85980	149	50.0	24.0	0.0
18	5	0.12244	0.08442	643.92050	150	77.0	37.0	0.0
161	172	0.08772	0.06048	643.91180	151	122.0	59.0	0.0
5	6	0.04934	0.03402	643.20080	152	102.0	49.0	0.0
307	300	0.07822	0.05393	637.57160	153	60.0	29.0	0.0
235	234	0.08333	0.05746	635.51820	154	77.0	37.0	0.0
161	185	0.13158	0.09072	634.86330	155	194.0	94.0	0.0
77	78	0.05117	0.03528	632.40350	156	56.0	27.0	0.0
101	96	0.10600	0.07308	629.43530	157	122.0	59.0	0.0
357	244	0.01279	0.00882	625.66590	158	0.1	0.0	0.0
352	414	0.07054	0.04864	621.57710	159	3.0	1.0	0.0
324	323	0.08772	0.06048	621.47190	160	1.0	0.0	0.0
222	221	0.08772	0.06048	619.45280	161	52.0	25.0	0.0
172	188	0.09138	0.06300	613.49040	162	194.0	94.0	0.0
384	243	0.22734	0.15674	612.41210	163	10.0	5.0	0.0
15	11	0.13291	0.11220	608.13060	164	128.0	62.0	0.0
295	294	0.02266	0.01562	607.09620	165	16.0	8.0	0.0
160	180	0.04386	0.03024	605.20790	166	37.0	18.0	0.0
85	244	0.13999	0.09652	604.87430	167	154.0	75.0	0.0
20	44	0.01462	0.01008	601.41840	168	0.1	0.0	0.0
376	230	0.02775	0.02343	601.12990	169	0.1	0.0	0.0
233	376	0.01168	0.00986	600.98620	170	78.0	38.0	0.0
301	302	0.05556	0.03830	593.52720	171	0.1	0.0	0.0
69	65	0.03107	0.02142	587.06570	172	27.0	13.0	0.0
230	231	0.04557	0.03847	564.94200	173	103.0	50.0	0.0
167	175	0.09055	0.07645	552.81670	174	122.0	59.0	0.0
21	57	0.21565	0.14868	548.89630	175	72.0	35.0	0.0
141	130	0.04674	0.03946	547.72570	176	0.1	0.0	0.0
68	85	0.02924	0.02016	547.13360	177	122.0	59.0	0.0
414	401	0.07273	0.05015	545.56990	178	194.0	94.0	0.0
100	101	0.05848	0.04032	544.02380	179	0.1	0.0	0.0
185	164	0.09138	0.06300	538.49840	180	77.0	37.0	0.0

Table A.3: 415-Bus System Data (Continued)

Branch Data					**Bus Data**			
From	*To*	*Resistance* (Ω)	*Reactance* (Ω)	*Apparent Power* (kVA)	*Bus*	*Active Demand* (kW)	*Capacitive Demand* (kVAr)	*Inductive Demand* (kVAr)
401	402	0.07091	0.04889	528.66770	181	82.0	40.0	0.0
102	100	0.05483	0.03780	525.97740	182	53.0	26.0	0.0
265	266	0.10782	0.07434	521.23910	183	122.0	59.0	0.0
6	7	0.04021	0.02772	517.09750	184	64.0	31.0	0.0
336	323	0.05483	0.03780	508.51760	185	86.0	42.0	0.0
382	66	0.03290	0.02268	506.49440	186	82.0	40.0	0.0
263	264	0.06871	0.04738	506.02040	187	0.1	0.0	0.0
21	72	0.19372	0.13356	498.90660	188	167.0	81.0	0.0
154	134	0.07887	0.06658	496.10020	189	0.1	0.0	0.0
322	329	0.03143	0.02167	486.59440	190	0.1	0.0	0.0
65	71	0.07127	0.04914	481.45320	191	131.0	64.0	0.0
154	156	0.03213	0.02713	476.39280	192	21.0	10.0	0.0
262	263	0.06309	0.05327	474.53340	193	21.0	10.0	0.0
261	262	0.03797	0.03206	474.33230	194	21.0	10.0	0.0
175	181	0.08471	0.07151	472.45400	195	21.0	10.0	0.0
402	403	0.05958	0.04108	466.16710	196	0.1	0.0	0.0
53	22	0.04021	0.02772	463.30990	197	0.1	0.0	0.0
7	3	0.05190	0.03578	460.67000	198	0.1	0.0	0.0
339	265	0.06798	0.04687	457.74010	199	0.1	0.0	0.0
155	151	0.06945	0.04788	457.54850	200	0.1	0.0	0.0
403	404	0.06835	0.04712	452.50530	201	52.0	25.0	0.0
200	119	0.07676	0.05292	447.15920	202	202.0	98.0	0.0
296	295	0.07420	0.05116	446.09100	203	202.0	98.0	0.0
221	220	0.08407	0.05796	428.95720	204	73.0	35.0	0.0
259	261	0.05112	0.04316	428.61020	205	81.0	39.0	0.0
257	259	0.06871	0.04738	428.36480	206	115.0	56.0	0.0
188	168	0.09138	0.06300	427.46790	207	118.0	57.0	0.0
168	176	0.11331	0.07812	427.16770	208	318.0	154.0	0.0
176	179	0.06579	0.04536	426.81720	209	161.0	78.0	0.0
309	307	0.09869	0.06804	423.35370	210	126.0	61.0	0.0
47	21	0.08407	0.05796	421.01870	211	59.0	29.0	0.0
151	152	0.05483	0.03780	419.63130	212	24.0	12.0	0.0
156	137	0.08407	0.05796	414.12600	213	24.0	12.0	0.0
130	131	0.05483	0.03780	412.02120	214	5.0	2.0	0.0
134	139	0.11976	0.10111	410.48110	215	126.0	61.0	0.0

Table A.3: 415-Bus System Data (Continued)

Branch Data					Bus Data			
From	*To*	*Resistance* (Ω)	*Reactance* (Ω)	*Apparent Power* (kVA)	*Bus*	*Active Demand* (kW)	*Capacitive Demand* (kVAr)	*Inductive Demand* (kVAr)
164	165	0.03290	0.02268	395.95130	216	56.0	27.0	0.0
99	102	0.05117	0.03528	394.01730	217	62.0	30.0	0.0
288	300	0.18677	0.12877	391.66300	218	0.1	0.0	0.0
158	200	0.02193	0.01512	390.21190	219	32.0	15.0	0.0
124	158	0.10234	0.07056	389.93090	220	158.0	77.0	0.0
127	124	0.02924	0.02016	389.71270	221	126.0	61.0	0.0
128	127	0.27047	0.18648	389.10300	222	202.0	98.0	0.0
125	128	0.02193	0.01512	388.97960	223	41.0	20.0	0.0
57	125	0.09138	0.06300	388.72050	224	81.0	39.0	0.0
21	50	0.03655	0.02520	380.60010	225	126.0	61.0	0.0
44	25	0.12793	0.08820	379.37530	226	202.0	98.0	0.0
165	173	0.13889	0.09576	378.00480	227	18.0	9.0	0.0
234	233	0.02775	0.02343	376.58050	228	202.0	98.0	0.0
251	252	0.18823	0.12978	375.31920	229	106.0	51.0	0.0
51	52	0.06945	0.04788	375.27000	230	175.0	85.0	0.0
153	141	0.07303	0.06165	366.98240	231	174.0	84.0	0.0
10	11	0.04674	0.03946	357.30430	232	113.0	55.0	0.0
66	252	0.19298	0.13306	354.57060	233	202.0	98.0	0.0
94	113	0.03290	0.02268	354.38350	234	0.1	0.0	0.0
183	182	0.03290	0.02268	351.23030	235	202.0	98.0	0.0
94	111	0.06579	0.04536	345.47730	236	403.0	195.0	0.0
131	157	0.03655	0.02520	343.02730	237	202.0	98.0	0.0
84	99	0.13158	0.09072	339.58120	238	126.0	61.0	0.0
33	55	0.04386	0.03024	336.38950	239	0.1	0.0	0.0
26	53	0.10051	0.06930	327.72040	240	29.0	14.0	0.0
384	68	0.03107	0.02142	327.01400	241	9.0	4.0	0.0
20	33	0.06579	0.04536	325.93030	242	5.0	2.0	0.0
137	144	0.09503	0.06552	319.57440	243	0.1	0.0	0.0
113	114	0.07676	0.05292	312.28470	244	18.0	9.0	0.0
152	135	0.07676	0.05292	306.36060	245	45.0	22.0	0.0
132	153	0.08772	0.06048	300.24350	246	32.0	16.0	0.0
25	35	0.12793	0.08820	293.71320	247	61.0	30.0	0.0
71	63	0.02266	0.01562	291.44580	248	81.0	39.0	0.0
338	339	0.04203	0.02898	290.28250	249	126.0	61.0	0.0
55	23	0.07676	0.05292	289.84950	250	23.0	11.0	0.0

Table A.3: 415-Bus System Data (Continued)

Branch Data					Bus Data			
From	*To*	*Resistance* (Ω)	*Reactance* (Ω)	*Apparent Power* (kVA)	*Bus*	*Active Demand* (kW)	*Capacitive Demand* (kVAr)	*Inductive Demand* (kVAr)
66	384	0.03472	0.02394	286.61940	251	14.0	7.0	0.0
289	288	0.04678	0.03226	277.22760	252	18.0	9.0	0.0
139	143	0.06214	0.04284	274.87380	253	126.0	61.0	0.0
329	333	0.05848	0.04032	272.28170	254	5.0	3.0	0.0
173	179	0.11331	0.07812	263.28370	255	26.0	13.0	0.0
268	327	0.03838	0.02646	262.14390	256	18.0	9.0	0.0
111	106	0.06579	0.04536	259.94960	257	126.0	61.0	0.0
138	155	0.10600	0.07308	241.94560	258	81.0	39.0	0.0
52	56	0.11696	0.08064	239.63140	259	0.1	0.0	0.0
21	49	0.13524	0.09324	232.17010	260	126.0	61.0	0.0
230	228	0.02629	0.02219	231.03600	261	41.0	20.0	0.0
275	209	0.13962	0.09626	228.85510	262	0.1	0.0	0.0
72	74	0.02193	0.01512	228.76760	263	28.0	14.0	0.0
51	54	0.05483	0.03780	224.02660	264	30.0	14.0	0.0
57	149	0.06945	0.04788	223.95350	265	81.0	39.0	0.0
54	24	0.07310	0.05040	223.90060	266	202.0	98.0	0.0
32	44	0.25585	0.17640	221.73520	267	318.0	154.0	0.0
48	50	0.07310	0.05040	217.79810	268	176.0	85.0	0.0
162	183	0.08407	0.05796	215.66370	269	126.0	61.0	0.0
181	178	0.05848	0.04032	215.60800	270	6.0	3.0	0.0
314	309	0.06981	0.04813	212.63860	271	31.0	15.0	0.0
10	88	0.10954	0.09248	210.46320	272	60.0	29.0	0.0
333	334	0.04167	0.02873	210.08630	273	56.0	27.0	0.0
149	138	0.12793	0.08820	209.68810	274	126.0	61.0	0.0
157	133	0.11331	0.07812	207.46420	275	118.0	57.0	0.0
404	407	0.08333	0.05746	207.37670	276	126.0	61.0	0.0
84	104	0.07310	0.05040	205.13400	277	202.0	98.0	0.0
23	28	0.06945	0.04788	204.44800	278	10.0	5.0	0.0
28	36	0.09138	0.06300	204.32310	279	126.0	61.0	0.0
40	47	0.09138	0.06300	204.18240	280	202.0	98.0	0.0
144	148	0.09503	0.06552	202.72440	281	318.0	154.0	0.0
407	408	0.04898	0.03377	201.87130	282	82.0	40.0	0.0
404	405	0.04021	0.02772	199.25100	283	126.0	61.0	0.0
135	145	0.14255	0.09828	197.60280	284	22.0	10.0	0.0
301	305	0.04386	0.03024	195.77320	285	13.0	6.0	0.0

Table A.3: 415-Bus System Data (Continued)

Branch Data					**Bus Data**			
From	*To*	*Resistance* (Ω)	*Reactance* (Ω)	*Apparent Power* (kVA)	*Bus*	*Active Demand* (kW)	*Capacitive Demand* (kVAr)	*Inductive Demand* (kVAr)
243	246	0.03651	0.03083	193.69390	286	71.0	34.0	0.0
30	26	0.05483	0.03780	192.33870	287	101.0	49.0	0.0
324	266	0.10380	0.07157	190.66960	288	113.0	54.0	0.0
304	378	0.05885	0.04057	190.58530	289	126.0	61.0	0.0
329	330	0.02668	0.01840	188.76740	290	0.1	0.0	0.0
88	89	0.08041	0.05544	187.34890	291	34.0	17.0	0.0
136	132	0.14986	0.10332	183.45580	292	83.0	40.0	0.0
142	136	0.08041	0.05544	183.33510	293	59.0	29.0	0.0
114	115	0.04752	0.03276	176.67230	294	126.0	61.0	0.0
145	146	0.03290	0.02268	175.20020	295	145.0	70.0	0.0
76	72	0.05483	0.03780	173.88920	296	202.0	98.0	0.0
81	76	0.05300	0.03654	173.77870	297	50.0	24.0	0.0
327	328	0.05483	0.03780	172.21170	298	41.0	20.0	0.0
203	204	0.05112	0.04316	170.88190	299	202.0	98.0	0.0
159	199	0.27047	0.18648	169.35470	300	77.0	37.0	0.0
290	289	0.06287	0.04334	169.25260	301	161.0	78.0	0.0
1	375	0.01097	0.00756	168.53120	302	477.0	231.0	0.0
375	202	0.14986	0.10332	168.43750	303	68.0	33.0	0.0
310	305	0.08260	0.05695	168.16220	304	14.0	7.0	0.0
243	249	0.04878	0.04118	167.41070	305	4.0	2.0	0.0
160	181	0.09138	0.06300	166.17000	306	0.1	0.0	0.0
89	67	0.10782	0.07434	164.32060	307	66.0	32.0	0.0
150	148	0.02193	0.01512	163.22510	308	0.1	0.0	0.0
46	50	0.03655	0.02520	162.59360	309	60.0	29.0	0.0
84	109	0.04752	0.03276	162.16000	310	95.0	46.0	0.0
247	248	0.07273	0.05015	89.90730	311	0.1	0.0	0.0
63	61	0.10965	0.07560	156.49320	312	19.0	9.0	0.0
330	331	0.04167	0.02873	154.31730	313	67.0	32.0	0.0
292	290	0.01681	0.01159	149.77570	314	18.0	9.0	0.0
73	80	0.07310	0.05040	146.80710	315	33.0	16.0	0.0
115	112	0.04021	0.02772	146.68680	316	21.0	10.0	0.0
199	197	0.06945	0.04788	145.90910	317	33.0	16.0	0.0
197	191	0.01097	0.00756	145.80070	318	42.0	20.0	0.0
309	313	0.07858	0.05418	144.03550	319	52.0	25.0	0.0
405	406	0.07164	0.04939	143.67880	320	43.0	21.0	0.0

Table A.3: 415-Bus System Data (Continued)

Branch Data					Bus Data			
From	*To*	*Resistance* (Ω)	*Reactance* (Ω)	*Apparent Power* (kVA)	*Bus*	*Active Demand* (kW)	*Capacitive Demand* (kVAr)	*Inductive Demand* (kVAr)
408	410	0.05519	0.03805	142.62970	321	126.0	61.0	0.0
312	307	0.07237	0.04990	140.63440	322	107.0	52.0	0.0
209	210	0.11696	0.08064	140.01710	323	202.0	98.0	0.0
237	238	0.06222	0.05253	140.00540	324	126.0	61.0	0.0
334	335	0.05592	0.03856	140.00290	325	24.0	12.0	0.0
232	293	0.07493	0.05166	138.44750	326	101.0	49.0	0.0
24	29	0.09503	0.06552	138.43750	327	81.0	39.0	0.0
109	108	0.04966	0.04192	137.98450	328	155.0	75.0	0.0
37	32	0.10600	0.07308	136.30530	329	23.0	11.0	0.0
180	177	0.05483	0.03780	135.53020	330	31.0	15.0	0.0
406	390	0.04532	0.03125	127.91910	331	126.0	61.0	0.0
106	95	0.08407	0.05796	124.37570	332	13.0	6.0	0.0
43	48	0.08041	0.05544	122.08680	333	56.0	27.0	0.0
410	411	0.06433	0.04435	121.50270	334	120.0	58.0	0.0
104	105	0.04966	0.04192	119.66630	335	126.0	61.0	0.0
316	312	0.10526	0.07258	119.59260	336	403.0	195.0	0.0
304	305	0.20834	0.14364	119.26560	337	81.0	39.0	0.0
11	86	0.03505	0.02959	114.59060	338	177.0	86.0	0.0
260	287	0.03582	0.02470	112.26420	339	151.0	73.0	0.0
324	326	0.00548	0.00378	112.25950	340	9.0	4.0	0.0
323	322	0.06762	0.04662	112.24680	341	29.0	14.0	0.0
411	412	0.06762	0.04662	110.22170	342	14.0	7.0	0.0
345	369	0.05300	0.03654	107.62280	343	23.0	11.0	0.0
56	27	0.09503	0.06552	104.04330	344	45.0	22.0	0.0
369	370	0.20834	0.14364	102.62570	345	0.1	0.0	0.0
31	40	0.10600	0.07308	97.29650	346	36.0	17.0	0.0
74	75	0.10600	0.07308	96.37090	347	5.0	2.0	0.0
308	316	0.22186	0.15296	96.30830	348	9.0	4.0	0.0
305	308	0.05044	0.03478	96.21260	349	80.0	39.0	0.0
105	108	0.06579	0.04536	95.91920	350	0.1	0.0	0.0
337	338	0.02924	0.02016	95.32500	351	0.1	0.0	0.0
378	377	0.11148	0.07686	95.28570	352	0.1	0.0	0.0
314	318	0.07237	0.04990	90.96820	353	0.1	0.0	0.0
61	60	0.04386	0.03024	90.75270	354	0.1	0.0	0.0
60	58	0.01097	0.00756	90.65100	355	0.1	0.0	0.0

Table A.3: 415-Bus System Data (Continued)

Branch Data					Bus Data			
From	*To*	*Resistance* (Ω)	*Reactance* (Ω)	*Apparent Power* (kVA)	*Bus*	*Active Demand* (kW)	*Capacitive Demand* (kVAr)	*Inductive Demand* (kVAr)
257	258	0.10600	0.07308	89.91060	356	0.1	0.0	0.0
246	247	0.05263	0.03629	157.90040	357	0.1	0.0	0.0
204	205	0.06214	0.04284	89.90600	358	0.1	0.0	0.0
119	121	0.01022	0.00863	87.66520	359	0.1	0.0	0.0
310	314	0.07237	0.04990	86.32270	360	0.1	0.0	0.0
84	107	0.06579	0.04536	83.94240	361	0.1	0.0	0.0
34	47	0.17361	0.11970	81.28270	362	0.1	0.0	0.0
49	39	0.08772	0.06048	79.18980	363	0.1	0.0	0.0
39	30	0.11696	0.08064	79.08740	364	0.1	0.0	0.0
143	150	0.09869	0.06804	78.77780	365	0.1	0.0	0.0
300	286	0.10965	0.07560	78.72940	366	0.1	0.0	0.0
35	38	0.08041	0.05544	78.04590	367	0.1	0.0	0.0
38	41	0.10417	0.07182	77.94800	368	0.1	0.0	0.0
412	413	0.08735	0.06023	75.68290	369	0.1	0.0	0.0
414	385	0.07200	0.04964	75.58930	370	0.1	0.0	0.0
293	236	0.06945	0.04788	72.69280	371	0.1	0.0	0.0
133	140	0.10600	0.07308	71.91570	372	0.1	0.0	0.0
146	149	0.05483	0.03780	69.78170	373	0.1	0.0	0.0
313	317	0.06835	0.04712	69.76660	374	0.1	0.0	0.0
36	45	0.13158	0.09072	69.43260	375	0.1	0.0	0.0
216	217	0.09931	0.08384	68.88280	376	0.1	0.0	0.0
49	45	0.04386	0.03024	68.15720	377	86.0	41.0	0.0
362	272	0.01645	0.01134	66.64170	378	86.0	41.0	0.0
334	336	0.07127	0.04914	63.70350	379	0.1	0.0	0.0
302	303	0.04532	0.03125	63.29640	380	0.1	0.0	0.0
402	387	0.05665	0.03906	62.17180	381	0.1	0.0	0.0
1	273	0.01425	0.00983	62.16980	382	0.1	0.0	0.0
408	409	0.06689	0.04612	59.12810	383	0.1	0.0	0.0
41	43	0.11696	0.08064	57.72140	384	0.1	0.0	0.0
200	201	0.00731	0.00504	57.69780	385	68.0	33.0	0.0
110	84	0.04386	0.03024	56.14650	386	15.0	7.0	0.0
202	1	0.48246	0.33264	56.13080	387	56.0	27.0	0.0
103	110	0.07676	0.05292	56.05330	388	12.0	6.0	0.0
306	310	0.12646	0.08719	55.97100	389	50.0	24.0	0.0
304	306	0.06945	0.04788	55.87820	390	115.0	56.0	0.0

Table A.3: 415-Bus System Data (Continued)

Branch Data					Bus Data			
From	*To*	*Resistance* (Ω)	*Reactance* (Ω)	*Apparent Power* (kVA)	*Bus*	*Active Demand* (kW)	*Capacitive Demand* (kVAr)	*Inductive Demand* (kVAr)
405	389	0.05885	0.04057	55.46390	391	14.0	7.0	0.0
148	57	0.14620	0.10080	53.96460	392	5.0	2.0	0.0
29	34	0.11513	0.07938	53.03740	393	19.0	9.0	0.0
42	37	0.06762	0.04662	50.97780	394	34.0	17.0	0.0
221	344	0.02924	0.02016	50.09080	395	10.0	5.0	0.0
357	245	0.00548	0.00378	50.09010	396	40.0	19.0	0.0
317	319	0.12354	0.08518	48.30660	397	28.0	14.0	0.0
310	320	0.01279	0.00882	47.85430	398	14.0	7.0	0.0
296	298	0.03765	0.02596	45.61890	399	17.0	8.0	0.0
400	404	0.04752	0.03276	45.61800	400	41.0	20.0	0.0
310	315	0.06140	0.04234	45.10480	401	0.1	0.0	0.0
413	396	0.06945	0.04788	44.28480	402	0.1	0.0	0.0
315	311	0.08333	0.05746	43.47580	403	0.1	0.0	0.0
311	304	0.10526	0.07258	43.38380	404	0.1	0.0	0.0
75	81	0.08407	0.05796	41.79700	405	0.1	0.0	0.0
365	366	0.02559	0.01764	41.23680	406	0.1	0.0	0.0
409	394	0.06908	0.04763	38.01440	407	0.1	0.0	0.0
290	291	0.00548	0.00378	38.01330	408	0.1	0.0	0.0
318	315	0.06945	0.04788	35.04830	409	0.1	0.0	0.0
366	271	0.01645	0.01134	34.43860	410	0.1	0.0	0.0
140	147	0.15351	0.10584	33.05390	411	0.1	0.0	0.0
352	353	0.21382	0.14742	32.29700	412	0.1	0.0	0.0
239	240	0.00584	0.00493	32.20260	413	0.1	0.0	0.0
249	358	0.04313	0.02974	31.89600	414	0.1	0.0	0.0
358	359	0.00548	0.00378	31.79660	415	19.0	9.0	0.0
413	397	0.07054	0.04864	31.30580				
254	255	0.02741	0.01890	29.06920				
46	42	0.02559	0.01764	27.36590				
353	213	0.20103	0.13860	26.83460				
352	212	0.11367	0.07837	26.83380				
324	325	0.04825	0.03326	26.83320				
3	10	0.10782	0.07434	26.50240				
359	250	0.02010	0.01386	25.49530				
368	343	0.00914	0.00630	25.49520				
364	284	0.10417	0.07182	24.16680				

Table A.3: 415-Bus System Data (Continued)

Branch Data					Bus Data			
From	*To*	*Resistance* (Ω)	*Reactance* (Ω)	*Apparent Power* (kVA)	*Bus*	*Active Demand* (kW)	*Capacitive Demand* (kVAr)	*Inductive Demand* (kVAr)
190	189	0.07310	0.05040	23.53130				
68	93	0.08407	0.05796	23.26000				
189	193	0.02339	0.01613	23.25960				
92	87	0.01285	0.01085	23.25950				
138	194	0.01279	0.00882	23.25950				
199	192	0.01462	0.01008	23.25950				
135	195	0.00914	0.00630	23.25950				
107	103	0.05483	0.03780	22.66900				
336	337	0.06469	0.04460	22.41900				
409	393	0.07383	0.05090	21.02420				
410	415	0.06579	0.04536	21.02410				
254	361	0.05885	0.04057	20.21460				
361	256	0.04021	0.02772	20.12480				
374	227	0.00366	0.00252	20.12460				
412	399	0.05665	0.03906	18.78850				
359	251	0.14072	0.09702	17.63050				
401	386	0.05921	0.04082	16.55310				
341	342	0.11331	0.07812	15.65280				
406	391	0.07310	0.05040	15.65270				
412	398	0.07164	0.04939	15.65270				
243	355	0.00548	0.00378	15.41610				
355	354	0.12793	0.08820	15.32400				
314	317	0.08151	0.05620	15.21910				
331	332	0.02741	0.01890	14.31790				
147	142	0.10600	0.07308	13.68000				
403	388	0.08333	0.05746	13.41660				
303	304	0.19518	0.13457	12.29550				
27	31	0.10234	0.07056	12.20930				
163	184	0.07595	0.06412	11.26990				
277	278	0.03290	0.02268	11.18040				
411	395	0.05958	0.04108	11.18040				
95	112	0.03290	0.02268	11.15830				
370	348	0.11879	0.08190	9.84900				
354	241	0.07310	0.05040	9.84890				
319	318	0.06652	0.04586	9.39460				

Table A.3: 415-Bus System Data (Continued)

Branch Data					**Bus Data**			
From	*To*	*Resistance* (Ω)	*Reactance* (Ω)	*Apparent Power* (kVA)	*Bus*	*Active Demand* (kW)	*Capacitive Demand* (kVAr)	*Inductive Demand* (kVAr)
57	147	0.15717	0.10836	7.33430				
366	270	0.10051	0.06930	6.70830				
369	347	0.13158	0.09072	5.38520				
353	214	0.05007	0.03452	5.38520				
407	392	0.07858	0.05418	5.38520				
354	242	0.01828	0.01260	5.38520				
189	198	0.10965	0.07560	0.20000				
82	80	0.07310	0.05040	0.10000				
86	91	0.09503	0.06552	0.10000				
126	124	0.02924	0.02016	0.10000				
169	162	0.07676	0.05292	0.10000				
171	163	0.06426	0.05425	0.10000				
198	196	0.03655	0.02520	0.10000				